Development of ELN/COL- LA/CA matrix for urea encapsulation and study of its nitrogen release kinetics

Agmasu Mekonnen Admasu

Thesis Paper Submitted to the Department of Chemical Engineering

School of Mechanical, Chemical, and Material Engineering

Presented in Partial Fulfillment of the Requirement for the Degree of Master's in Chemical Engineering (Specialization in Process Engineering)

Office of Graduate Studies

Adama Science and Technology University

Adama, Ethiopia

September, 2022

Development of ELN/COL- LA/CA matrix for urea encapsulation and study of its nitrogen release kinetics

Agmasu Mekonnen Admasu

Major-Advisor

Dr. Tatek Temesgen

Co-Advisor

Dr. Melakuu Tesfaye

Thesis Paper Submitted to the Department of Chemical Engineering

School of Mechanical, Chemical, and Material Engineering

Presented in Partial Fulfillment of the Requirement for the Degree of Master's in Chemical Engineering (Specialization in Process Engineering)

Office of Graduate Studies

Adama Science and Technology University

Adama, Ethiopia

September, 2022

Declaration

I hereby declare that this Master Thesis entitled "**Development of ELN/COL- LA/CA matrix for urea encapsulation and study of its nitrogen release kinetics"** is my original work. That is, it has not been submitted for the award of any academic degree, diploma, or certificate in any other university. All sources of materials that are used for this thesis have been duly acknowledged through citation.

Agmasu Mekonnen	_____	_____
Name of the student	Signature	Date

Recommendation

We, the advisor(s) of this thesis, hereby certify that we have read the revised version of the thesis entitled **"Development of ELN/COL- LA/CA matrix for urea encapsulation and study of its nitrogen release kinetics"** prepared under our guidance by Agmasu Mekonnen is submitted in partial fulfillment of the requirements for the degree of Mater's of Science in Chemical Engineering (Specialization Process Engineering). Therefore, we recommend the submission of a revised version of the thesis to the department following the applicable procedures.

Dr. Tatek Temesgen	_____	_____
Major-Advisor	Signature	Date
Dr. Melakuu Tesfaye	_____	_____
Co-Advisor	Signature	Date

Approval Page

We, the advisors of the thesis entitled **"Development of ELN/COL- LA/CA matrix for urea encapsulation and study of its nitrogen release kinetics"** and developed by Agmasu Mekonnen certify that the recommendation and suggestions made by the board of examiners are appropriately incorporated into the final version of the thesis.

Dr. Tatek Temesgen	_____	_____
Major-Advisor	Signature	Date
Dr. Melakuu Tesfaye	_____	_____
Co-Advisor	Signature	Date

We, the undersigned, members of the Board of Examiners of the thesis by _____have read and evaluated the thesis entitled **"Development of ELN/COL- LA/CA matrix for urea encapsulation and study of its nitrogen release kinetics"** and examined the candidate during the open defense. This is, therefore, to certify that the thesis is accepted for partial fulfillment of the requirement of the degree of Master of Science in Chemical Engineering (Specialization in process engineering).

_____	_____	_____
Chairperson	Signature	Date
_____	_____	_____
Internal Examiner	Signature	Date
_____	_____	_____
External Examiner	Signature	Date

Finally, approval and acceptance of the thesis are contingent upon the submission of its final copy to the Office of Postgraduate Studies (OPGS) through the Department Graduate Council (DGC) and School Graduate Committee (SGC).

_____	_____	_____
Department Head	Signature	Date
_____	_____	_____
School Dean	Signature	Date
_____	_____	_____
Office of Postgraduate Studies, Dean	Signature	Date

ACKNOWLEDGEMENT

First of all, I would like to praise my GOD and his mother St.Mary for the successful completion of my thesis research work.

I would like to express my gratitude to my advisors Dr. Tatek Temesgen and Dr. Melaku Tesfaye for their support, guidance, and valuable criticism. This thesis would not have been accomplished without their outstanding supervision, scientific knowledge, and experience.

I would like to thank, Hungnawe Bayle head of the department of Chemical Engineering, for his valuable comment and support.

With respect, honor, and appreciation I dually acknowledge all lab technicians at Chemical Engineering laboratory as well as Mr. Zeyede, lab technicians at Melkasa Agricultural Research Center for their generous aid on this thesis.

I wish to extend my warm thanks to all my best friends and classmates for always being there for me when I needed their support.

TABLE OF CONTENTS

LIST OF TABLES

LIST OF FIGURES

LIST OF SCHEME

LIST OF ABBREVIATION

CA	Citric acid
CALAOLG	Citric acid lactic acid oligomer
CSRUF	Coated type slow release urea fertilizer
CRF	Control release fertilizer
CDCl3	Deuterated chloroform
ELN/COL	Elastin/collagen
ELPs	Elastin-like polypeptides
FTIR	Fourier Transform Infrared spectroscopy
Gly	Glycine
Hypro	Hydroxyproline
HPMC	Hydroxypropyl methylcellulose
LA	Lactic acid
LA/CA	Lactic acid/citric acid
LA/OLL-g-BC	Lactic acid oligomer- grafted- untreated bacterial cellulose
LB	Liquefied bagasse
MSRUF	Matrix-type slow-release urea fertilizer
NPK	Nitrogen, phosphorous, and potassium
NPs	Nanoparticles
NR	Natural rubber
NMR	Nuclear magnetic resonance
NUE	Nitrogen use efficiency
PLA	Poly-lactic acid
PU	Polyurethane
Pro (X)	Proline
SNCs	Silk nanocrystals
SRFs	Slow-release fertilizers
SRUF	Slow-release urea fertilizers
Val	Valine

ABSTRACTS

Direct administration of chemical fertilizers on soil was shown to have low utilization efficiency of the nutrients absorbed. The high solubility of chemicals like urea as a fertilizer has higher chances of leaching resulting in losses of nutrients. In this research, a new type of least water soluble ELN/COL-LA/CA matrix was synthesized to reduce the release of nutrients from urea fertilizer. ELN/COL-mixture was extracted from waste broiler skin and modified with lactic and citric acids for urea encapsulation. The urea powder was also dispersed on LA/CA modified ELN/COL matrix with a matrix to urea ratio of 1:1.5,1:1,1:2,and 1:3. The effect of reaction time, temperature, and lactic acid to citric acid ratio on the water solubility of the ELN/COL-LA/CA matrix was studied. The extracted ELN/COL from broiler skin was characterized by FTIR. ^{1}H-NMR and ^{13}C-NMR were also applied to further characterize the ELN/COL-LA/CA matrixes for the reaction mechanism and the type of bonds formed during the condensation reaction between ELN/COL and LA/CA. The solubility test for the synthesized ELN/COL-LA/CA matrix was investigated following the Kjeldahl method for its release kinetics. The FTIR and NMR results show that the ELN/COL-LA/CA matrix synthesized was formed due to the reaction between the primary structure of ELN/COL and that of LA/CA with a formation of amide as well as ester bonds. Further results from the solubility test, as well as the FTIR analysis, shows that the matrix which was synthesized at a reaction time of 4 hours, reaction temperature of 70 ^{o}C, and lactic acid to citric acid ratio of 1:1.5 was found to be the least water soluble matrix. The nitrogen release data were fitted and compared with two empirical models namely Higuchi and the Korsmeyer-Peppas to evaluate the release kinetics. The nitrogen release kinetics for urea dispersed ELN/COL–LA/CA matrix was found to have a good Korsmeyer-Peppas model fitting at an R^2 value of more than 0.98. The diffusion exponent (n) for the three samples (1:0.5, 1:1, and 1:2) matrix to urea ratio was ($n \geq 0.85$) showing a non-Fickian diffusion, Case II transport mechanism. But for the fourth sample which is a (1:3) ratio the value of the diffusion exponent was (n=0.75) representing anomalous transport.

Keywords: *Elastin,Collagen ,citric acid,lactic acid,matrix, diffusion exponent*

GRAPHICAL ABSTRACT

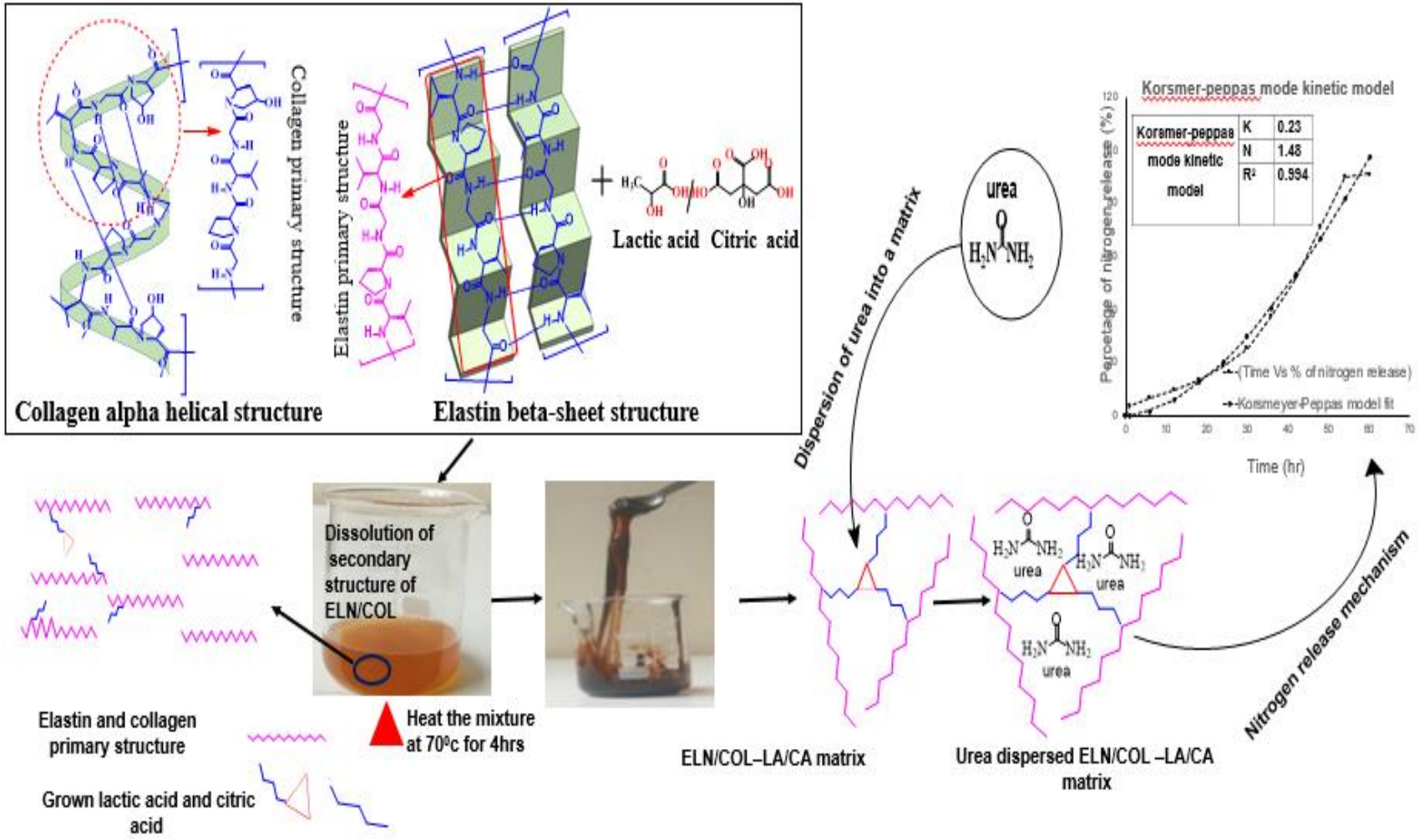

1 INTRODUCTION

1.1 Background of the study

Agriculture in the 21 st century is facing a great challenge. The world population is steadily increasing and is projected to reach around 9.8 billion people by 2050 (UN, 2017). Meanwhile, land available for agriculture is not expanding because of the limited area, soil quality, water availability, and cost. Farmers attempted to address this by using more fertilizer, which temporarily increased yields per hectare of soil, but in the long run, it markedly degraded the quality of the land and resulted in significant environmental problems (Lateef et al., 2016). Plants get most of the nutrients they need for growth from the soil. Nitrogen, phosphorus, and potassium are present in the soil, but they need to be periodically replenished by fertilizers.

For crops, nitrogen is necessary for the synthesis of proteins, chlorophyll, and protein-carrying molecules (Trenkel, 1997). Urea has the highest nitrogen content (46%), making it the most popular solid nitrogenous fertilizer for supplying nutrients to crops for enhanced growth. But when used in a stream of moving water, urea is very soluble, which could lead to leaching and impact the boundaries of planets. Crops will only absorb 35–50% of applied nitrogen due to its high solubility (increased likelihood of leaching and other losses), whereas 50–65% of applied nitrogen is lost and contributes to numerous environmental pollutions (Souri et al., 2019). Farmers must therefore apply an additional dose of this fertilizer, which costs money and has an impact on farm economics. Leaching immediately impacts water reserves, which disrupts flora and wildlife as well as aquatic life (Beig, Niazi, Jahan, Hussain, et al., 2020).

An effective method of mitigating the problem is to develop slow-release urea. Slow release urea fertilizers can release nutrients slowly, matching nutrient release behavior with crop absorption behavior, and has the advantages of a slow release rate, increasing the release period, reducing solubility, and improving nutrient utilization (Reyes-Escobar et al., 2015).

An effort to enhance the effectiveness and efficiency of urea based-fertilizer could be performed by modifying the urea fertilizer into 1) coated type slow-release urea fertilizer that achieves slow nutrient release through the physical barrier of the membrane material (Mann et al., 2019). These slow-release urea fertilizers have the characteristics of a long release period and high nutrient content and are currently the most widely used slow-release urea fertilizer (Zhang et al., 2021). However, coated slow-release urea fertilizers are generally recalcitrant in the environment,

require complicated technology for production, and present other issues (Beig, Niazi, Jahan, Pervaiz, et al., 2020); 2) Matrix-type slow-release urea fertilizers have dispersed nutrients in a carrier, and nutrients are released through the pores of the carrier (Qi et al., 2022).

Among these slow-release urea fertilizers, chemical controlled release fertilizers contain nutrients and materials in polymers, and their slow-release behavior follows the degradation behavior of the matrix. For example, urea-formaldehyde slow-release urea fertilizer has a relatively high degree of polymerization and a long slow-release period. However, this high degree of polymerization makes this slow-release urea fertilizer difficult to degrade (Liu et al., 2021). In addition, there is some functional slow-release urea fertilizer. For example, hydrogel slow-release urea fertilizer can maintain soil moisture while providing nutrients for plants (Zhou et al., 2018), but resistance to degradation still exists. In general, most slow-release urea fertilizer currently uses polymer materials, but they are not easily degraded, which limits their application. Finding an environmentally friendly and easily degradable material has become a key technology for preparing slow-release urea fertilizer.

This research was trying to develop matrix-type slow-release urea fertilizer from environmentally friendly degradable protein wastes from broiler skin (ELN/COL) which is also one of the sources of nitrogen, ELN/COL mixture synthesized from broiler skin contains 15 % of nitrogen within it. To produce a hydrophobic ELN/COL-LA/CA matrix in which urea fertilizer was dispersed on it to restrict the dissolution rate, ELN/COL mixture was reacted with a mixture of lactic and citric acid.

Collagen is the most common protein, making up around 30% of the total protein in both human and animal bodies. It is largely found in connective tissues, such as animal hair, bones, cartilages, tendons, and blood vessels (Cheng et al., 2009). There are many types of collagen, which are from collagen I to collagen XIX. Animal skin or hide contains collagen type I, mostly with approximately 90% of its dry weight (Kurt, 2015). Collagen possesses a greater amount of swelling properties in aqueous, acid, and alkaline systems in absence of salt concentration (Kanagaraj et al., 2006). Two types of covalent cross-linking, intramolecular and intermolecular, reinforce together collagen molecules to produce fibers with a specified internal and structural orientation (Brown et al., 1995). The formation of macromolecular fibers and, subsequently, their mechanical stability and other physical properties depend on intermolecular cross-linking (Exposito et al., 2002). Collagen-based biomaterials provide several benefits, including being

biocompatible, non-toxic, and having well-established structural characteristics. Such unique properties of collagen attract the interest of many researchers to use it as a natural polymer for controlled drug delivery (Ruszczak & Friess, 2003).

Elastin is a fibrous protein that is histologically found in the grain and dermis layer of the skin structure (Kanagaraj et al., 2006) and it is the principal constitutes of the connective tissue, particularly those tissues that contain elastomeric properties such as walls of arteries, the alveoli of the lungs, skins, tendons and elastic ligaments (Kanagaraj et al., 2006). The tunable phase behavior of elastin-mimetic polypeptides presents an interesting opportunity for encapsulation and con-trolled release application, this controlled release application could be achieved through covalent linkage, physical entrapment, or columbic attraction of substances that have been retained within the elastin deriva-tive to an elastin carrier (Cappello et al., 1998).

Lactic acid is considered one of the main well-known organic acids with a wide range of industrial applications. One of the most important organic acids with several industrial applications is this one. Lactic acid is primarily used in the culinary, chemical, cosmetic, and pharmaceutical industries. Because it has two interactive practical collections, hydroxyl, and carboxylic groups, lactic acid is regarded as the generality possible feedstock monomer for chemical conversions in the chemical industry. Sometimes, various chemical transformations of lactic acid result in potentially valuable compounds, including the production of propylene oxide by hydrogenation, propionic acid through reduction, acrylic acid through dehydration, 2, 3-pentanedione through condensation, and acetaldehyde through decarboxylation (via self-esterification) (Zhan et al., 2003). This important characteristic leads to lactic acid being useful in the modification of polymers like protein to have hydrophobic (water heating) for matrix preparation to produce a slow release of urea fertilizer(Chen et al., 2008).

Citric acid (CA) is an organic acid with the formula $C_6H_8O_7$. Because various protic groups on CA can form intramolecular hydrogen bonds to stabilize the anion, CA is a somewhat more potent acid than normal carboxylic acids. (Lee et al., 2020). CA is widely used as a pharmaceutically active substance in pharmaceuticals, personal care, and cosmetic products, as an acidulant and pH stabilizer in beverages, blood anticoagulants, as well as diuretic and flavoring agents (Ciriminna et al., 2017). In recent years, many emerging uses of CA have also been identified, e.g., chelating agent, binder, cross-linker, disinfectant, environmental remediation, and extracting agent (Ciriminna et al., 2017). All these properties were accounted for in the formation of an

organized network upon crosslinking, leading to the aggregation of particles which is an important characteristic in the formation of slow-release fertilizer (Mesias et al., 2019).

1.2 Statement of the problem

Urea is the most widely used nitrogen fertilizer which has a high nitrogen content. However, urea is released rapidly in a short time in soil (Xie et al., 2019). Volatilization, leaching, and runoff of nutrients caused waste of fertilizers and contamination of water (Xie et al., 2019). Due to the high solubility of urea fertilizer (thus higher chances of leaching and other losses), crops will only take up nitrogen in the range of 35–50%, while 50–65% of applied nitrogen is lost and contributes to various environmental pollutions (Souri et al., 2019). To decrease those limitations of urea fertilizer, many scholars were trying to synthesize slow-release fertilizers (SRFs). These fertilizers can be fabricated using many techniques with several modifications of the conventional urea fertilizers, but those techniques had still drawback since, high cost, non-biodegradability, and harmfulness to the environment (Saleh, Steinmetz, and Hemati2003). Therefore, it was very important to establish a reasonable fertilizer system by synthesizing urea dispersed ELN/COL-LA/CA matrix with a reduced water solubility to minimize the above drawbacks of urea fertilizer. Moreover, this ELN/COL matrix was prepared from broiler skin which was a waste product for the poultry processing industry. So valorizing this waste into a valuable product also reduces the negative environmental impact that results from the disposal of this waste into the environment.

1.3. Research question, hypothesis, and choice of system

- Is it possible to extract elastin/collagen mixture from broiler skin?
- Is it possible to synthesize, and develop an ELN/COL-LA/CA matrix with a reduced water solubility by reacting ELN/COL with citric and lactic acid?
- Can it be possible to disperse urea within the formulated ELN/COL-LA/CA matrix?
- Is it possible to reduce the nitrogen release of urea through the formation of urea dispersed ELN/COL–LA/CA matrix?

Based on the above research questions the ELN/COL-LA/CA matrix is assumed to be one of the promising biomaterials which have reduced water solubility and also has the capability of encapsulating urea fertilizer within it as a result it releases its nutrient(nitrogen) gradually.

Hypothesis: if it is possible to develop the least water soluble ELN/COL-LA/CA matrix from broiler skin and that of citric and lactic acid, and disperse urea within the synthesized ELN/COL-

LA/CA matrix, it may be possible to develop urea dispersed ELN/COL-LA/CA matrix with reduced water solubility.

1.4 Objectives of the study

1.4.1 General Objectives

Development of ELN/COL-LA/CA matrix for urea encapsulation and study of its nitrogen release kinetics.

1.4.2 Specific objectives

The following specific objectives are addressed to achieve the general objective.

- To extract and characterize ELN/COL from Broiler's skin.
- Synthesis, characterization, and study the solubility of ELN/COL –LA/CA matrix through the reaction between extracted ELN/COL, citric acid, and lactic acid.
- Dispersion of urea into the synthesized ELN/COL- LA/CA matrix and study its solubility in water.
- Study the nitrogen release kinetics of the urea dispersed ELN/COL- LA/CA matrix.

1.5 Significance of the study

This thesis has great significance in terms of adding knowledge to the production of slow-release urea fertilizer. It also introduces the application of wasted protein (i.e. broiler's skin) as a feedstock for the application in the agricultural sector. Moreover, it enhances the habits of valorizing different organic waste for agricultural uses. As it is a pioneer in terms of synthesis and development of a completely bio-based, green, and compatible formulation for slow-release urea fertilizer (SRUF), it will also motivate researchers and other professionals to study and apply slow-release urea fertilizer (SRUF). The other major significance of this study is that it reduces volatilization, leaching, and runoff of nutrients from urea fertilizer as a result it minimizes waste of urea fertilizers and also environmental waste results from continuous use of normal urea fertilizer.

2 LITERATURE REVIEW

2.1 What are Fertilizers?

Fertilizers: Fertilizers are natural or synthetic substances produced to supply nutrients to plants. It is used to increase the productivity of crops in agricultural fields. Farmers involved in agricultural practices or farming use fertilizer in their day-to-day life to increase the yield of crops. Fertilizers are products that are required for the enhancement of soil and retention of water for the growth of plants. It supplies nutrients such as nitrogen, potassium, and phosphorus to the plants for their effective growth (; Shaviv, 2001). Generally, these fertilizers are of two types: (i) organic and (Feng & Wang) inorganic.

2.2 Types of Fertilizers

There are different types of fertilizers used in agricultural fields. They are as follows:

2.2.1 Organic Fertilizers

They are prepared from plant and animal waste materials. They include wastes from poultry and chicken meat processing industry, agricultural, livestock, vegetable waste, etc. Organic fertilizers help in enriching the soil by promoting the reproduction of microorganisms and changing the physical and chemical properties of the soil for high productivity.

2.2.2 Inorganic Fertilizers

Inorganic fertilizers are chemical substances that consist of nutrients used for plant growth. They are as follows:

Types of Inorganic Fertilizers

1. **Nitrogenous Fertilizers**: They are a source of nitrogen for the crops. Nitrogen promotes leaf area and leaf area index. It intensifies the green color of the leaves and is a constituent of essential cellular components such as amino acids, proteins, and nucleic acids. It is also the controller of P, K, and other nutrients, and improves the succulence of many crops (Sedano-Castro et al., 2011), promoting photosynthesis because the nitrogen increases the amount of chlorophyll (Torres-Olivar et al., 2014). As a result, it increases the yield and promotes the growth of plants, Figure 2.1 illustrates the role of nitrogen in crop production. Urea, ammonium sulfate, calcium ammonium nitrate, etc. are some examples of nitrogenous fertilizers.

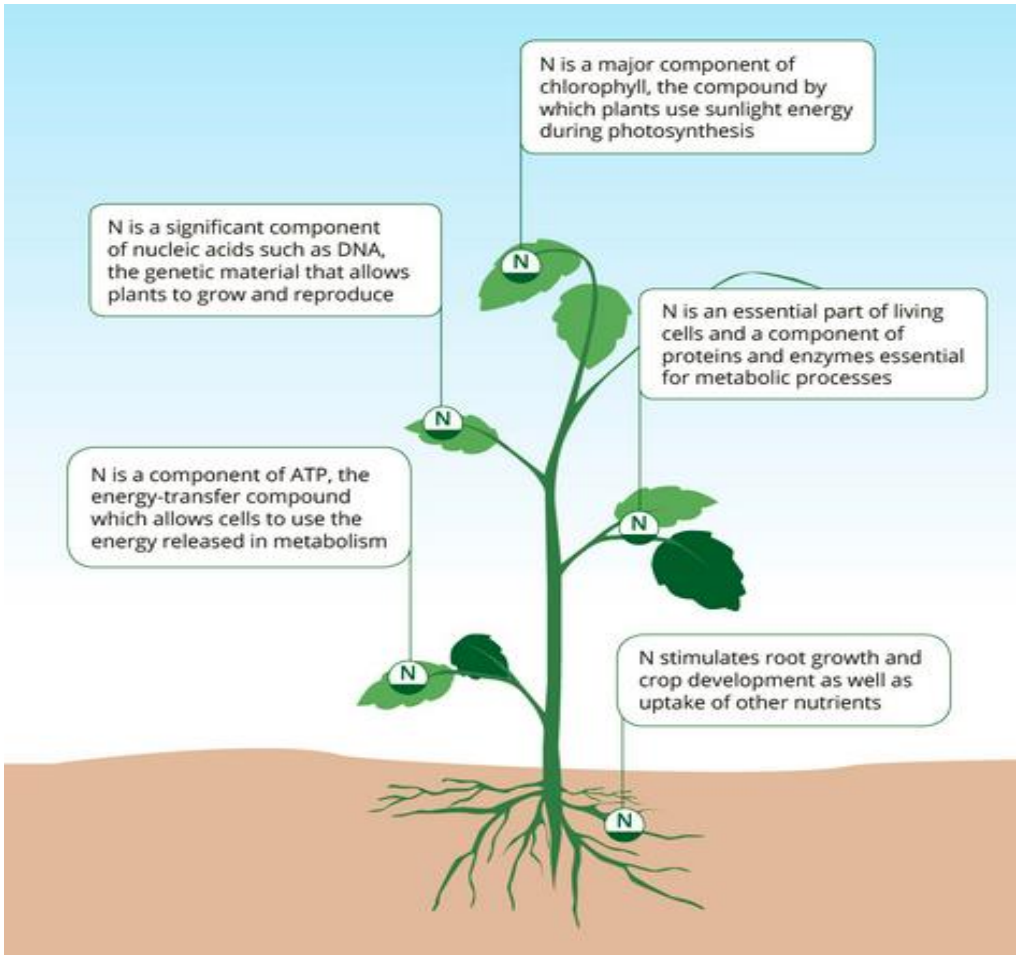

Figure 2.1 The role of nitrogen in crop production (Torres-Olivar et al., 2014)

2. **Phosphorus Fertilizers:** The ones that are used as the main source of phosphorus are called phosphorus fertilizers. Phosphorus promotes healthy root growth, and early shoot growth speeds ground cover for erosion protection, enhances the quality of fruit, vegetable, and grain crops, and is vital to seed formation (Hoshide, 2005). Few of the commercially available phosphorus fertilizers are single superphosphate, triple super phosphate, di-calcium phosphate, diammonium phosphate, etc.
3. **Potassium Fertilizers**: Potassium stimulates early crop growth, and improves protein production and water-use efficiency (Rawat et al., 2016). Potassium-enriched fertilizer includes muriate of potash (KCl) and potassium sulfate.

2.3 Urea Fertilizer

Urea ($CO(NH_2)2$) fertilizer is used as the main source of nitrogen (N), which is one of the major nutrients that is used on a large scale in fertilizers manufacture. About 48% of the world population today is alive by means of nitrogen-based fertilizers (Leghari et al., 2016). Urea fertilizer contains the highest nitrogen content (46% N) of all the solid nitrogenous fertilizers. It also shows the highest water solubility. Because of its high nitrogen content, urea provides a greater quantity of nitrogen to plants and soil in comparison with other nitrogenous fertilizers (Beig, Niazi, Jahan, Hussain, et al., 2020). The amount of nitrogen taken up by a crop determines the effectiveness of urea fertilizer over a specified time. When applied to soil, urea reacts with water to form ammonia, which makes the nitrogen within the fertilizer available to plants.

2.4 Limitation of urea fertilizer

It has been demonstrated that plants that receive chemical fertilizers directly do not efficiently use the nutrients they take in. The most widely used N-fertilizer, urea, was estimated to have NUE levels of just 30 to 50%, with 2 to 30% lost through volatilization, 15 to 25% lost through soil organic compound reactions, and 1 to 10% lost through leaching into water systems, raising serious environmental issues (Versino et al., 2019). Figure (2.2) shows the simplified nitrogen (urea) cycle in the soil and how urea nitrogen in the soil change from one form to another.

Urease enzymes in the soil change the nitrogen in urea to ammonium through mineralization, which is then changed to nitrite and nitrate through the nitrification process. Due to irrigation runoff or high rainfall, the soil is unable to retain the urea fertilizer; as a result, nitrate will leach into groundwater and surface water bodies. Consequently, high concentrations of nitrate in plants and drinking water could pose high risks to human health (Savci, 2012).

Besides water pollution, nitrogen is also lost through volatilization as N_2 and N_2O, through complete and incomplete denitrification processes respectively (Savci, 2012). Ammonium could also be lost as NH_3 through volatilization. Nitrogen-based fertilizers have also been reported to be the source of N_2O, which is the primary substance for worldwide ozone depletion in the 21st century (Ravishankara et al., 2009).

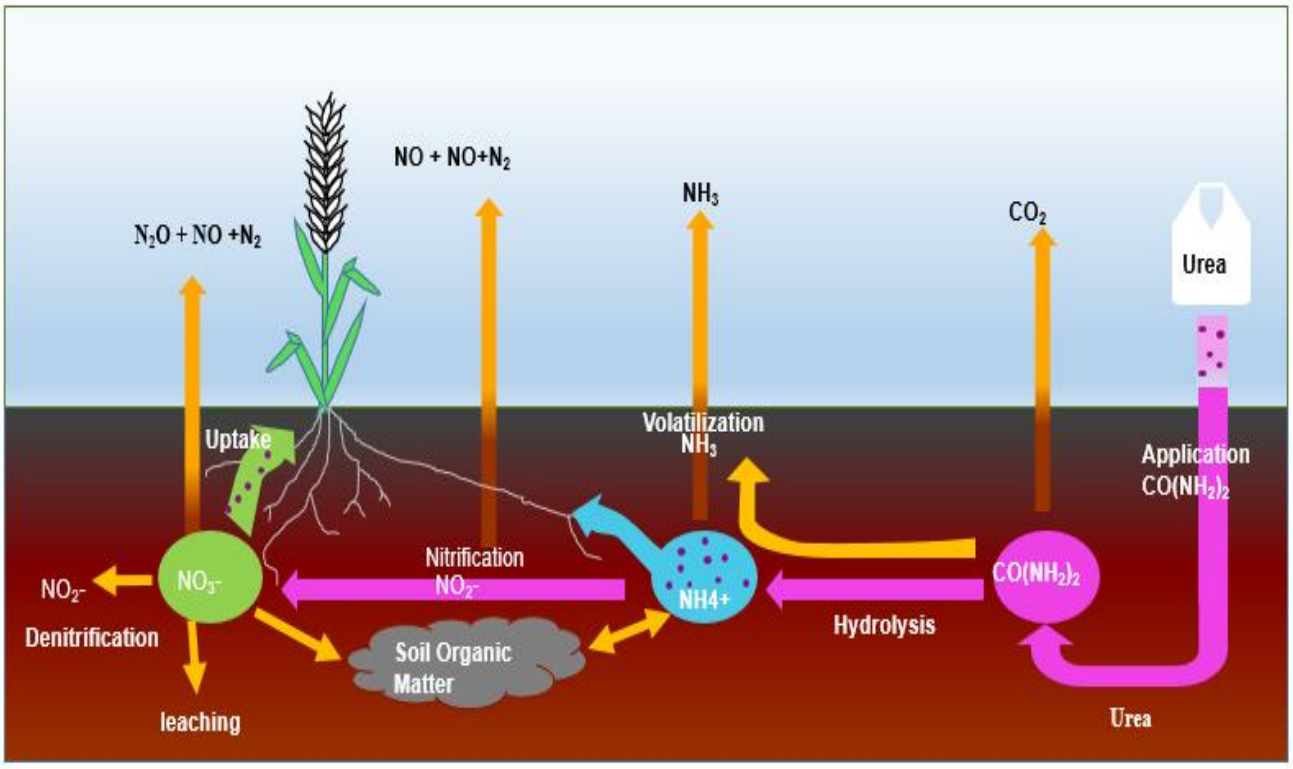

Figure 2.2 Simplified nitrogen (urea) cycle (Sánchez-García et al., 2014)

2.5 Methods/mechanisms for reducing limitation of urea fertilizer

To decrease those limitations of urea fertilizer, many scholars were trying to synthesize slow-release fertilizers (SRFs). These fertilizers can be fabricated using many techniques with several modifications of the conventional urea fertilizers, one of these modifications is done to increase the time of nutrient availability for the plant by increasing the release time in comparison to conventional urea fertilizers (Lubkowski, 2016). This slow release fertilizer was synthesized through; **Coated type slow release urea fertilizer (CSRUF)** achieves slow nutrient release through the physical barrier of the membrane material (Mann et al., 2019) and **Matrix-type slow release urea fertilizer(MSRUF)** has dispersed nutrients in a carrier, and nutrients are released through the pores of the carrier, dissolution/relaxation of the matrix, (Qi et al., 2022).

The European Standardization Committee Task Force has made some recommendations on the criteria of SRFs such that the rate of nutrient release must be slower than conventional fertilizer.

2.5.1 Coated type slow release urea fertilizer (CSRUF)

Hydrophobic substances, normally polymers, are used for coating urea fertilizer (normally shaped in one of three forms, i.e., prills, granules, or tablets) to control its release rate in soil. The

materials used for coating are normally segregated into two types: organic polymeric substances or inorganic mineral compounds (Wang et al.2013). Polymeric resins and thermoplastic polymers are classified as organic substances, while gypsum, sulfur, bentonite, and other inorganic mineral-based substances come under the category of inorganic coatings.

Up until now, many polymer and non-polymer substances have been tested during trials as possible coating materials for the slow release of urea. Widely used coating substances include sulfur, Zeolite, Bentonite, Polyether sulfone, Latex, and polymeric resins along with some artificial man-made polymeric substances (Babadi et al., 2015); (Hermida et al., 2019); (Yang et al., 2017). Additions to the above coating materials could be cement; cement/elastomeric blend; amine; amine/polymeric wax blend and mineral oil mixtures. But the major drawback of using the above materials for coating is their high cost, non-biodegradability, and harmfulness to the environment (Saleh, Steinmetz, and Hemati2003). Moreover; the coated type slow-release urea fertilizer uses neem oil as a coating material which has nitrification inhibitor characteristics and enhanced nitrogen use efficiency of the crop and yield. The neem oil consists of de-acetyl, azadirachtin, epinimbin, melicians, and salanin components which presented a treatment-based nitrification inhibition method (Khandey et al., 2017). But the major drawback of using neem oil as a coating material was its hydrophilicity property makes it easily soluble in water.

2.5.2 Matrix-type slow release urea fertilizer (MSRUF)

(Zhang et al., 2021). However, coated slow-release urea fertilizers are generally recalcitrant in the environment, require complicated technology for production, and present other issues (Beig, Niazi, Jahan, Pervaiz, et al., 2020); Matrix-type slow-release urea fertilizers have dispersed nutrients in a carrier, and nutrients are released through the pores of the carrier, and dissolution/relaxation of the matrix (Qi et al., 2022). Among these slow-release urea fertilizers, chemical controlled release fertilizers contain nutrients and materials in polymers, and their slow-release behavior follows the degradation behavior of the matrix. For example, urea-formaldehyde slow-release urea fertilizer has a relatively high degree of polymerization and a long slow-release period. However, this high degree of polymerization makes this slow-release urea fertilizer difficult to degrade (Liu et al., 2021). In addition, there is some functional slow-release urea fertilizer. For example, hydrogel slow release urea fertilizer can maintain soil moisture while providing nutrients for plants (Zhou et al., 2018), but hydrogel is hydrophilic and the dissolution of fertilizer dispersed through hydrogel material is impeded by its ability to retain high amounts

of water (swelling), resistance to degradation still exists. In general, most slow release urea fertilizer currently uses polymer materials, but they are not easily degraded, which limits their application. Finding an environmentally friendly and easily degradable material like protein, polysaccharide has become a key technology for preparing slow release urea fertilizer.

Table 2.1 Summarizes both coated and matrix-type slow-release urea fertilizer (SRFs).

No	Coating /Matrix material	Modifier	Research Findings	References
1	Gypsum & Sulfur	Sulfur/paraffin; ground magnesium lime//polyol	Addition of hydrophobic sealant slows down release but is still faster than commercial CRF.	(Babadi et al., 2015)
2	Phospho-gypsum	Paraffin wax/Span™ 80	The addition of emulsifier significantly reduces the release rate due to enhanced paraffin adhesion.	(Yu & Li, 2019)
3	Zeolite	Corn and potato starch, bentonite, white cement, acrylic polymer	A suitable binder type can slow down the release rate.	(Dubey et al., 2019)
4	Bentonite	Starch, hydroxypropyl methylcellulose (HPMC); hydrophilic polymer (polyacrylamide); hydrophobic polymer	Nanocomposite provides a superior controlled release. The urea release rate is affected by binder type and slowed down due to adsorption by bentonite.	(Hermida et al., 2019)

		(polycaprolactone)		
5	Polystyrene	Wax; Polyurethane	Wax is brittle and cannot prevent water penetration into the coating. Increasing size slows down the release and reduces the coating material required.	(Yang et al., 2012)
6	Polyether sulfone	Fe_2O_3 nanoparticles (NPs)	A new class of SRF. Fe_2O_3 NP increases coating thickness and reduces release rate. It also allows the carrier to be recovered and recycled.	(Emami et al., 2017)
7	Aliphatic Polyester	-	The increasing size of SRF but using smaller urea crystals slow down degradability and release rate.	(Ye et al., 2020) (Bi et al., 2020)
8	Bio-based Epoxy	Different ratios of liquified bagasse (LB) to bisphenol-A diglycidyl ether (Abdel-Basset et al.)	Increases compactness and hydrophobicity and retards release rate.	(Li et al., 2018)

9	Biobased Polyurethane (PU)	Isocyanate, acrylonitrile modification, superabsorbent from chicken feather meal; nano fumed silica	Double layer polymer coating significantly retards the release rate. Castor oil-based PU has better adherence as the coating material. Nano-fumed silica reduces porosity and pore size. Isocyanate affects the structure of PU which affects the release rate.	(Bortoletto-Santos et al., 2020)
10	urea/urea–formaldehyde		Extruded fertilizer nanocomposites presented good mechanical resistance, and that the urea release was noticeably controlled by the extent of polymerization	(Yamamoto et al., 2016)
11	Latex	-	Urea content affects the swelling degree which greatly affects the release rate.	(Yang et al., 2017)
12	Starch	Borate as a cross-linker and catalyst, *l*ignin for hydrophobicity improvement	lignin retards the urea release and the starch-urea-borate film is stable and stayed intact for one month after	(Ariyanti et al., 2013)

			immersing in water which shows high potential as a biopolymer for slow release fertilizer	
13	Natural rubber	Cassava starch; attapulgite/NR and NR-g-Polyacrylic acid	Hydrophobic NR can retard release rate with enhanced hydrophilicity through grafting. Multicoated SRF with NR and hydrogel shows great controlled release.	(Cui et al., 2020)
14	Starch-based matrix	vinyl acetate through in situ graft-copolymerization	Vinyl acetate reduced the swellability of the starch matrix; the urea nitrogen was slowly-release in water than normal urea with time.	(Niu et al., 2012)
15	Sawdust cellulose hydrogel	Potassium persulfate (KPS) and N, N'-methylene bis acrylamide (MBA) were used as the initiator and cross-linker, respectively	The largest water absorbency of the sample was reached. In addition, it had a good nitrogen release property.	(X. Zhang et al., 2020)

2.6 General structure and properties of proteins

Proteins are essential biological macromolecules, capable of performing vital functions in the body as enzymes, hormones, and regulatory, transport, and structural molecules involved in key

immune, circulatory, and homeostatic processes. They are the most predominant macromolecules present in living cells, representing over 50% of the dry weight of a cell (Cozzone & Ltd, 2002) and accounting for roughly 20% of the total body mass (Di Lullo et al., 2002)**.** It is a polymer of amino acids, arranged in a linear sequence and connected by covalent bonds.

2.6.1 Amino Acid

Amino acids are the building block of proteins. Amino acids are important organic compounds that contain amine (-NH_2) and Carboxyl (-COOH) functional groups, along with a side-chain (R group) that is specific for each amino acid Figure 2.3. Twenty different amino acids are commonly found in proteins. All of these 20 common amino acids are α-amino acids except proline and their general structure is shown below. They have a carboxyl group and amino group which is covalently bonded to an α-carbon atom. They differ from each other in their side chain R groups. Since the remaining structure is the same therefore properties of these amino acids are primarily determined by the side chain groups. The nature of these side chains may be polar, nonpolar (aliphatic), hydrophilic, hydrophobic, acidic, basic, and aromatic(Cheon).

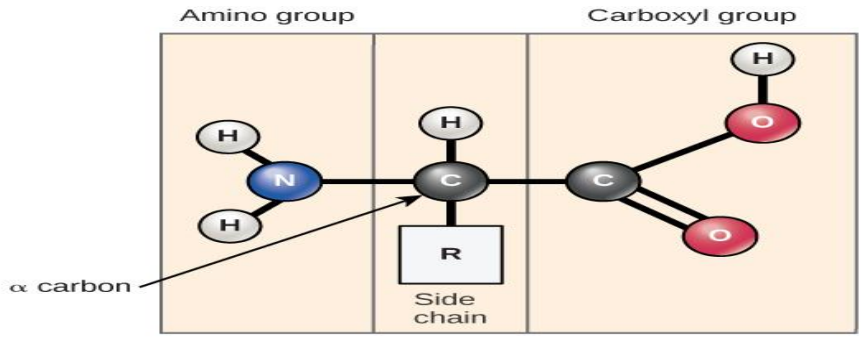

Figure 2.3 Structure of amino acid containing R side chain (Cheon)

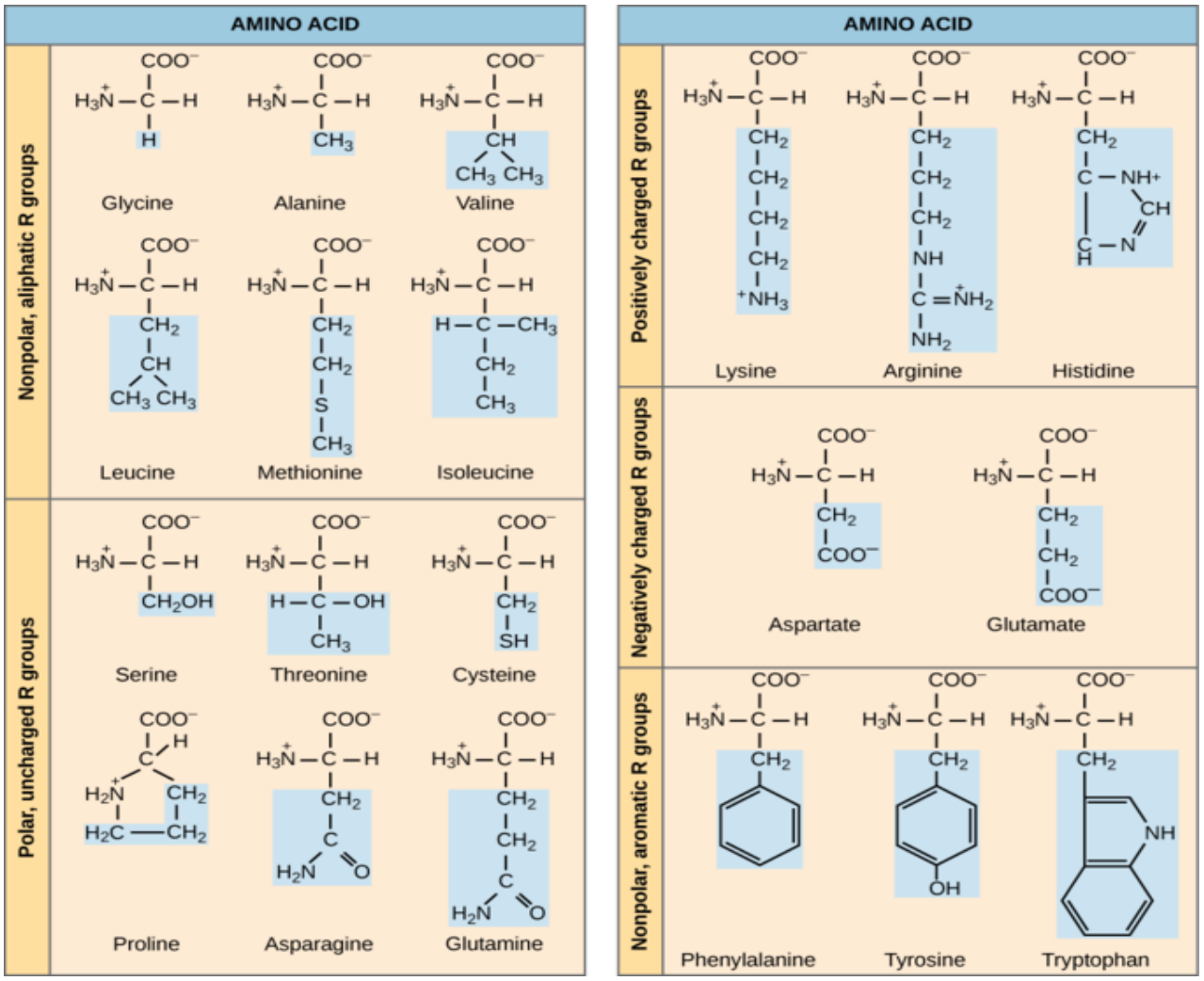

Figure 2.4 Types of amino acids (Cheon)

2.7 Protein Structure

Proteins are macromolecules and have four different levels of structure – primary, secondary, tertiary, and quaternary (Bailey, 2018).

2.7.1 The primary structure

The primary structure of a protein is produced from condensation reactions between amino acids, with each reaction resulting in the formation of a peptide bond (Dugas & Penney, 2013). Amino acids, as their name indicates, contain both a basic amino group and an acidic carboxyl group. This di-functionality allows the individual amino acids to join in long chains by forming peptide bonds: amide bonds between the $-NH_2$ of one amino acid and the -COOH of another. Sequences with fewer than 50 amino acids are generally referred to as peptides, while the terms, protein, and

polypeptide, are used for longer sequences. A protein can be made up of one or more polypeptide molecules. The end of the peptide or protein sequence with a free carboxyl group is called the carboxy-terminus or C-terminus. The terms, amino-terminus, and N-terminus, describe the end of the sequence with a free α-amino group (Bailey, 2018).

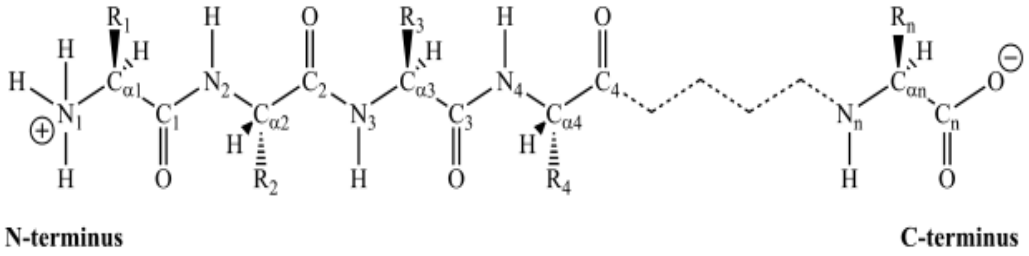

Figure 2.5 Stereochemistry of protein primary structure *(Murray et al., 2017)*

2.7.2 Secondary Structure

A protein's secondary structure is whatever regular structures arise from interactions between neighboring or nearby amino acids as the polypeptide starts to fold into its functional three-dimensional form. Secondary structures arise as H-bonds form between local groups of amino acids in a region of the polypeptide chain. Rarely does a single secondary structure extend throughout the polypeptide chain. It is usually just in a section of the chain. The most common forms of secondary structure are the α-helix and β-pleated sheet structures and they play an important structural role in most globular and fibrous proteins (Andersen, 2001).

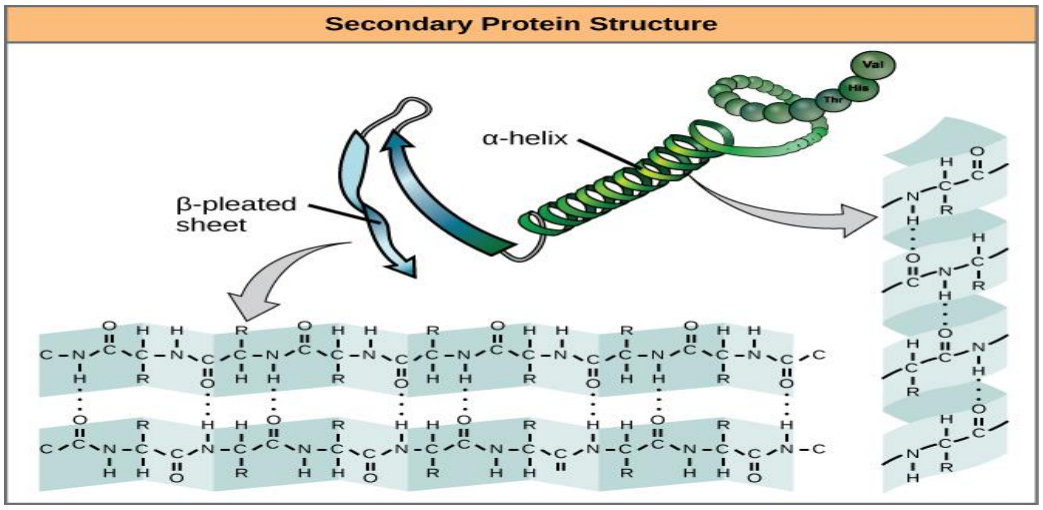

Figure 2.6 Secondary structure α-helix and a β-pleated sheet of protein *(Tayyab & Boyce, 2006)*.

In the α-helix chain, the hydrogen bond forms between the oxygen atom in the polypeptide backbone carbonyl group in one amino acid and the hydrogen atom in the polypeptide backbone amino group of another amino acid that is four amino acids farther along the chain. This holds the stretch of amino acids in a right-handed coil. Every helical turn in an alpha helix has 3.6 amino acid residues. The R groups (the side chains) of the polypeptide protrude out from the α-helix chain and are not involved in the H bonds that maintain the α-helix structure.

In β-pleated sheets, stretches of amino acids are held in an almost fully-extended conformation that "pleats" or zig-zags due to the non-linear nature of single C-C and C-N covalent bonds. β-pleated sheets never occur alone. They have to be held in place by other β-pleated sheets. The stretches of amino acids in β-pleated sheets are held in their pleated sheet structure because hydrogen bonds form between the oxygen atom in a polypeptide backbone carbonyl group of one β-pleated sheet and the hydrogen atom in a polypeptide backbone amino group of another β-pleated sheet. The β-pleated sheets which hold each other together align parallel or antiparallel to each other. The R groups of the amino acids in a β-pleated sheet point out perpendicular to the hydrogen bonds holding the β-pleated sheets together and are not involved in maintaining the β-pleated sheet structure.

2.7.3 Tertiary Structure

The three-dimensional structure that a polypeptide chain adopts is called the tertiary structure. The tertiary structure may be formed by folded secondary structures as a result of interactions among side chains of amino acids. The resulting structure of a polypeptide can be globular or fibrous. Protein folding typically resulted from one or more intramolecular attractions which may be a hydrogen bond, electrostatic interaction, hydrophobic interaction, or a disulfide bond due to Cysteines and Van der Waals interaction. The secondary structure appears from a hydrogen bond between peptide bonds (C=O - HN) but the tertiary structure appears due to the formation of hydrogen bonds among side chains (Rn-Rm). A functional unit called the domain made by folding is the main characteristic of tertiary structure (Levitt & Chothia, 1976).

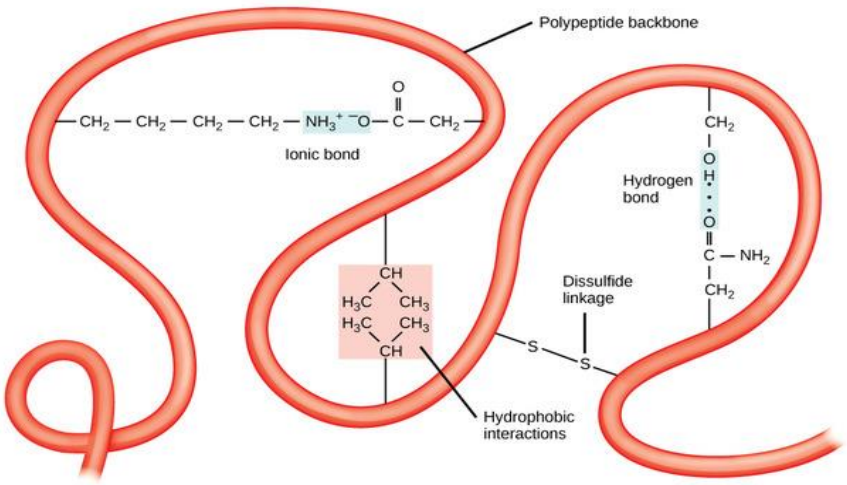

Figure 2.7 Tertiary structure of a protein (Hepler & Gilman, 1992).

2.7.4 Quaternary Structure

Quaternary Structure Some proteins contain two or more separate polypeptide chains or subunits that may be identical or different. The arrangement of these protein subunits in three dimensions is known as a quaternary structure which is biologically functional. These subunits or polypeptide chains may be similar or different thus producing homogeneous and heterogeneous quaternary structures respectively. The hemoglobin proteins possess a heterogeneous quaternary structure because it is made up of 2 α-chains and two β-chains (Figure 5) (Fermi et al., 1984). Similarly, aspartate transcarbamylase possesses twelve polypeptide chains or subunits (six catalytic and six regulatory) that are arranged in the form of two catalytic trimers and three regulatory dimers. Based on a higher level of structure, proteins are classified as fibrous and globular. Fibrous proteins contain a single type of secondary structure such as strands or sheets and their tertiary structure is relatively simple where as in globular proteins, the polypeptide chains are arranged into spherical or globular shape and it often contain several types of secondary structures (Cheon).

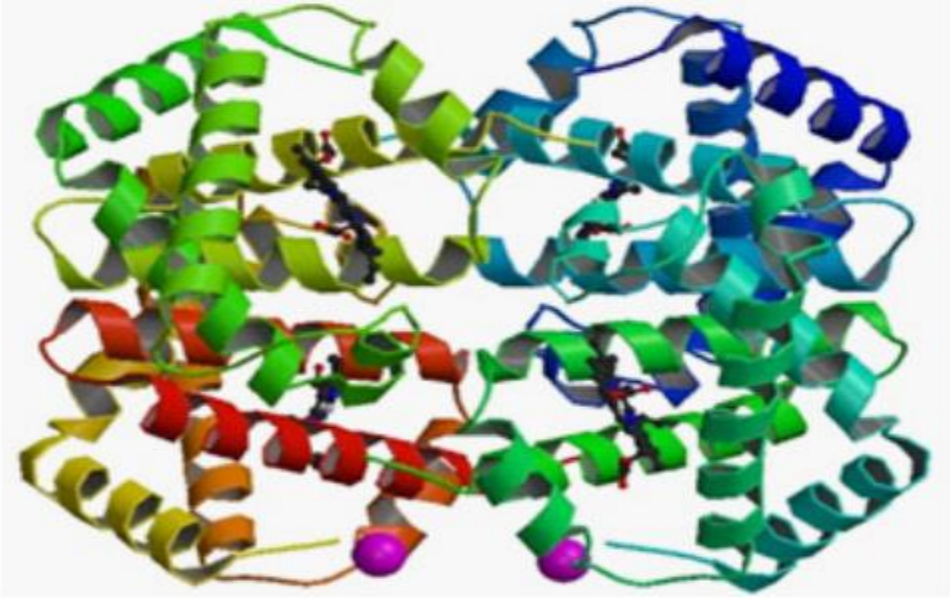

Figure 2.8 Quaternary structure protein of human deoxyhemoglobin *(Fermi et al., 1984)*

2.8 Elastin and its derivatives

Elastin is an extracellular matrix protein polymer and it is the major abundant protein in our body next to collagen and provides resilience and elasticity to organs and tissue. It is composed of elastic fibers (a yellowish fiber composed chiefly of elastin and occurring in networks or sheets) which give elasticity to tissues in the body found primarily in connective tissue in combination with collagen and polysaccharides.

Elastin is a biopolymer of amino acid chains with high elasticity, and it is found in the body where this property is important, particularly in arteries where it aids blood flow. Elastin is also important in the lungs, elastic ligaments, skin, and bladder. Deficiencies in the elastin gene may lead to diseases such as cutilaxa, Williams–Beuren syndrome, and supra-valvular aortic stenosis (SVAS). The loss of elastin in the skin decreases the flexibility of the skin and reduces wound healing ability (Faury, 2001). The formation of elastin has been discovered through its major components, such as imitators in elastin-like polypeptides and the natural precursor tropoelastin. Tropoelastin‟s sequence primarily consists of non-polar residues including alanine, valine, glycine, and proline.

Depending on their physical and functional characteristics, Tropoelastin contains two main classes of domains, which are broadly termed hydrophobic or hydrophilic classes (Abdulkhani et al., 2014). Through interactions principally between their hydrophobic (water-hating) sequences,

it involves a remarkable process of ordered self-assembly at physiological temperatures. These properties will give elastin to the best applicants for incorporation into biomaterials for a range of applications in hydrophobic matrix preparation for slow delivery application.

2.8.1 Biochemistry and Synthesis of Elastin

Elastin is encoded by a single-copy gene, ELN, and is synthesized by various cells, including fibroblasts, smooth muscle cells, and endothelial cells, as a soluble precursor protein that on secretion matures to give 60–70 kDa tropoelastin. In the skin, the dermal fibroblast cell is the primary producer of tropoelastin. Tropoelastin consists of predominantly alternating hydrophobic and hydrophilic domains (Wen et al., 2020). After tropoelastin is synthesized, it is extensively crosslinked in the matrix to produce insoluble elastin fibers. The crosslinking process can be described in two parts: the coacervation of tropoelastin, accompanied by lysyl oxidase family oxidation of lysine side-chains with ensuing crosslinking of compared tropoelastin molecules (Wen et al., 2020). Elastin is insoluble due to the cross-linking of amino acid chains. Tropoelastin is a precursor protein of elastin and is composed of hydrophilic (lysine, valine, and proline) and hydrophobic (glycine, valine, and proline) domains. The hydrophobic domains are involved in coacervation and the hydrophilic domains are used for cross-linking. Coacervation involves the agglomeration of protein molecules, which is an important step in the formation of elastin fibers as it enables the tropoelastin monomers to align and form cross-links. Elastin can be applied in biomaterials in several forms, including insoluble elastin fibers, hydrolyzed soluble elastin, recombinant tropoelastin (fragments), repeats of synthetic peptide sequences, block copolymers of elastin, or used in combination with other biopolymers Elastin is the dominant protein in extensible tissues and is primarily present in the lungs, aorta, and skin (Faury, 2001). Elastin-like polypeptides (ELPs) are a class of polypeptides, inspired by the amino acid sequence of natural elastin, which are composed of oligomeric repeats of the pentapeptide sequence Val-Pro-Gly-X-Gly (VPGXG) (X is any amino acid except Pro) (Trabbic-Carlson et al., 2003).

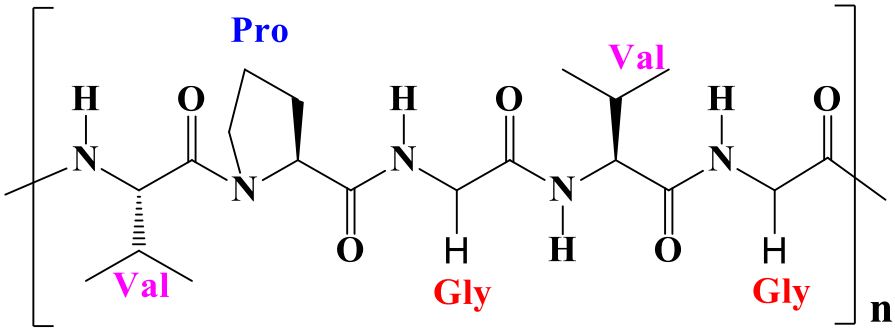

Figure 2.9 Amino acid repeating units (VPGVG) of Elastin *(Bravo-Anaya et al., 2019)*.

2.9 Collagen and Its Derivatives

Collagen is the main constituent of connective tissue and is the most abundant protein in animals, composing 30% of total protein mass. It is found in the extracellular matrix and fibrous tissue. The first reported collagen biomaterial was biodegradable sutures, termed "catgut," which is a collagen biomaterial derived from the intestines of sheep. The term collagen does not refer to a single protein, but a family of proteins. There are currently 29 types of collagen that have been identified (Chattopadhyay & Raines, 2014). Collagen is the most abundant protein in animals. This fibrous, structural protein comprises a right-handed bundle of three parallel, left-handed polyproline II-type helices. Much progress has been made in elucidating the structure of collagen triple helices and the physicochemical basis for their stability (Shoulders & Raines, 2009b). Pro, Hyp, and Gly are the most common triplet (10.5%) in collagen (Ramshaw et al., 1998). In animals, individual collagen triple helices, known as tropocollagen (Bailey), assemble in a complex, hierarchical manner that ultimately leads to the macroscopic fibers and networks observed in tissue, bone, and basement membranes. Production of collagen and the other components of the extracellular matrix (elastin and proteoglycans) is high when there is a sufficient level of mechanical tension on fibroblasts. When this tension is reduced, for example with aging, the production of the matrix proteins falls and there is an expression increase of matrix-degrading enzymes (Varani et al., 2006). Both collagen and elastin are important structural proteins widely expressed in skin tissues. Skin relaxation during photo-aging is manifested by a reduction in the content of collagen and elastin in the skin. Collagen accounts for 75% of the dermal composition and is the main component of the dermis. Although elastin only accounts for 2% of the dermal composition, it has an important function to promote the homeostasis of the skin(Abdulkhani et al., 2014), so the content of collagen and elastin in the skin plays an important

role in skin health. With the aging of the body, collagen and elastin fibers may show signs of aging, like cross-linking and breakage. And also, the production of collagen and elastin may decrease, resulting in increased stiffness and decreasing elasticity in the skin, and more frequent formation of wrinkles which are typical symptoms of skin aging (Z. Zhang et al., 2020).

2.9.2 Structure of Collagen

Collagen is an abundant structural protein in all animals. In humans, collagen comprises one-third of the total protein, accounts for three-quarters of the dry weight of skin, and is the most prevalent component of the extracellular matrix (ECM). Collagen is a major structural protein, forming molecular cables that strengthen the tendons and resilient sheets that support the skin and internal organs. Bones and teeth are made by adding mineral crystals to collagen. Collagen provides structure to our bodies, protecting and supporting the softer tissues, and connecting them with the skeleton (Shoulders & Raines, 2009a). Collagen consists of a protein with three polypeptide chains, each of which contains a repeat Gly-X-Y amino acid sequence, where X and Y are usually proline and hydroxyproline, respectively. The 29 types of collagen are similar in that they all contain three polypeptide chains in a characteristic triple-helix structure. The variation is related to their structure, where the differences are restricted to the length of the helix and the number and nature of the carbohydrates attached to the triple-helix. Collagen types I, II, III, V, and XI have fibrillar quaternary structures (Abdel-Basset et al., 2020). Their structure is organized as follows: amino acids form the primary structure; the secondary structure is the local chain configuration of the Gly-X-Y peptide; the tertiary structure is the triple-helix molecule, and the quaternary structure is the arrangement of triple-helix molecules to form microfibrils. Type I collagen occurs mainly in the skin, vessels, and tendons and type II is the predominant collagen in cartilage, and type III collagen is found in the walls of blood vessels. Conversely, type IV collagen is a constituent of the membrane which separates the epithelial tissue of mesodermal tissues. It is also non-helical and does not form fibrils. Type I collagen is the most abundant type in animals and is the most commonly used in medicine (Abdel-Basset et al., 2020).

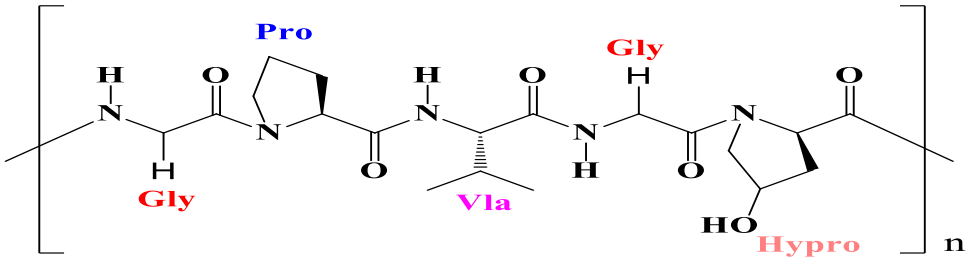

Figure 2.10 Repeating amino acid (GPVGVHYP) unit of Collagen (Kibret et al.).

(Goldberga et al., 2018).,study collagen Structure and Function Relationships from Solid-State NMR Spectroscopy. Detailed NMR and molecular modeling work have shown that the abundant Gly-Pro-Hyp (Hyp = hydroxyproline) triplets in collagen triple helices confer well-defined flexibility because the proline is conformationally metastable, in contrast to the expectation that these triplets confer structural rigidity. The alignment of the Gly-Pro-Hyp triplets within the fibril structure means that the Gly-Pro-Hyp molecular flexibility generates fibril flexibility. The fibrillar bands of Gly-Pro-Hyp are highly correlated with collagen ligand binding sites, leading to the hypothesis that the fibril alignment of Gly-ProHyp triplets is essential to protect collagen−ligand binding against external stresses on the tissue (Goldberga et al., 2018).

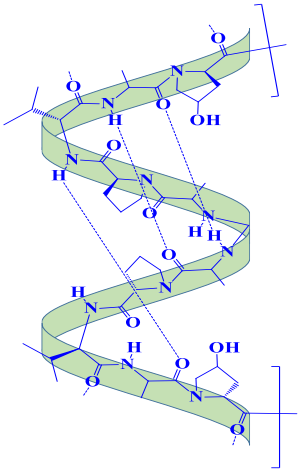

Figure 2.11 Collagen alpha-helix Structure (*(Shoulders & Raines, 2009a)*

2.10 Industrial Application of Lactic acid and its use in surface modification of polymers

Lactic acid (LA) is a biomolecule that offers several industrial and biomedical applications, some with high-value products. Lactic acid (2-hydroxy propionic acid) is one of the large-scale chemicals that is produced via fermentation. The commonly used feedstocks are carbohydrates obtained from different sources like corn starch, sugarcane, or tapioca starch depending on local availability. The carbohydrates are hydrolyzed into monosaccharides and then fermented under the absence of oxygen by microorganisms into lactic acid. Lactic acid is the building block for poly lactic acid, but it is also used in surface modification of many polymers' for medical applications like encapsulation and drug delivery systems (Bhattarai et al., 2006). Bio-based lactic acid is optically active, and the production of either L- (+)- or D- (–)-lactic acid can be directed with bioengineered microorganisms.

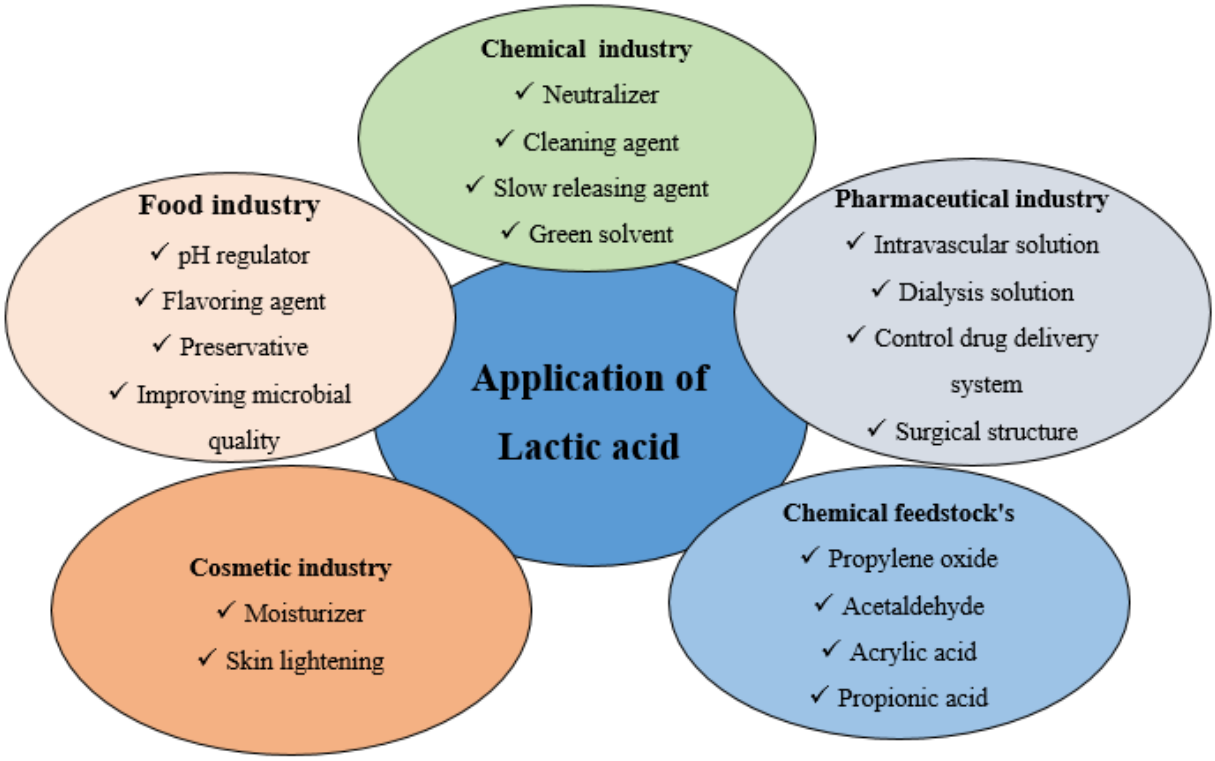

Figure 2.12 Industrial application of Lactic acid(Ahmad et al., 2020)

2.10.1. Lactic acid Oligomer Grafted Biopolymers

Lactic acid oligomer grafted chitosan: Growing of lactic acid oligomer on chitosan backbone takes place due to the presence of free amino function and the hydroxyl group of chitosan and the hydroxyl group of lactic acid without a catalyst. (Bhattarai et al., 2006), were developed lactic acid-grafted chitosan for high drug loading and prolonged drug release. By using bovine serum protein, a drug encapsulation efficiency is 92% and a release rate of 28% from chitosan nanoparticles over 4 weeks were confirmed and The lactic acid-grafted chitosan nanoparticles demonstrated a drug encapsulation efficiency of 96% and a protein release rate of 15% over 4 weeks (Bhattarai et al., 2006). The drug release rate increased and drug encapsulation efficiency decreased because of the increased protein concentration. The chitosan is amended with lactic acid oligomer prepared from solutions of neutral pH, proposing an additional advantage of allowing drugs or drugs to be uniformly incorporated in the matrix structure with insignificant or no denaturation that is not the behavior of chitosan which is generally soluble only in acid solution (Bhattarai et al., 2006).

Lactic acid oligomer grafted cellulose: Lactic acid oligomer- grafted- untreated bacterial cellulose (PLA/OLLA-g-BC) bio-nano composites were successfully prepared by Rahul Patwa et al., using the solvent casting technique and they tried to demonstrate the synthesis of (OLLA-g- BC) by in situ condensation polymerization. During the synthesis of OLLA-g-BC, hydrophilic BC was converted into hydrophobic due to structural grafting of OLLA chains with BC molecules increased and compatibilization between hydrophobic poly (lactic acid) (PLA) and hydrophilic BC, thus enhancing various properties of PLA based bio nanocomposites (Patwa et al., 2019).

Lactic acid grafted silk: Growing of lactic acid oligomer on silk backbone takes place due to the presence of free amino function of silk and hydroxyl group of lactic acid. Melakuu Tesfaye et al., demonstrate novel manufacture by reactive extrusion method of branched cum cross-linked poly (lactic acid) (PLA) with graft chain topology nano silk fibroin. The grafting of silk nanocrystals (SNCs) on PLA macromolecules provides a remarkable improvement in the rheological and thermal properties. Melakuu Tesfaye et al., demonstrate the novel manufacture of branched cum cross-linking poly (lactic acid) (PLA) with graft chain topology of nano silk fibroin by reactive extrusion process. This result gave the fundamental information to predict the formation of radicals on the SNC macromolecular structure that promotes grafting on PLA

backbone chains (Tesfaye et al., 2017). Melakuu Tesfaye et al., observed that the gel percentage of SNC (silk) −PLA increases from 10% to 60% and there is also a significant interaction between SNC and PLA macromolecules apart from the polymer-to-polymer cross-linking interaction, which leads to the long-chain branching. This result gave the fundamental information to predict the formation of radicals on the SNC macromolecular structure that promotes grafting on PLA backbone chains (Tesfaye et al., 2017).

Melakuu Tesfaye et al., report the growth of lactic acid in silk which is a type of protein that has an active amide group similar to elastin and collagen. Lactic acid may also use to produce a biopolymer by creating an interaction between the ELN/COL amide group and the carboxyl group of lactic acid.

2.11 Industrial application of citric acid and its use as a cross-linking agent

The citric acid (CA) is widely used in the food and drug industry and is an excellent candidate as a crosslinking agent. CA is widespread (lemon juice contains approximately 5% of CA) and is prepared commercially by fungal fermentation of glucose. CA and its salts, with a good affinity for metal ions, are used in a wide variety of applications: in soft drinks and effervescent salts, as an antioxidant in food, as a sequestering agent for metal ions, as a cleaning and polishing agent for metals, as a mordant in dyeing. Moreover, CA and its salts have fundamental biological functions. For example, CA is involved as an intermediate in the 'Krebs cycle in all living cells, also known as the 'citric acid cycle, for the production of usable energy (Glusker, 1980). Recently, CA was used as a crosslinking agent in various cellulose derivative systems (Glusker, 1980), (Wang & Chen, 2005), (Coma et al., 2003), (Xie et al., 2006), (Yang & Wang, 1998) and different mechanisms have been proposed in the literature to explain the crosslinking reaction of cellulose polymers with CA. (Xie et al., 2006), for example, studied the optimum conditions for corn starch and CA reaction to produce resistant starch and studied the thermal stability of citrate starch products. The authors reported that when CA is heated it will dehydrate to yield the cyclic anhydride that reacts with starch; successively another cyclic anhydride function can be achieved into CA structure through the other two non-reacted carboxylic groups, allowing then the attachment of another hydroxylic starch group (Fig. 2.5).

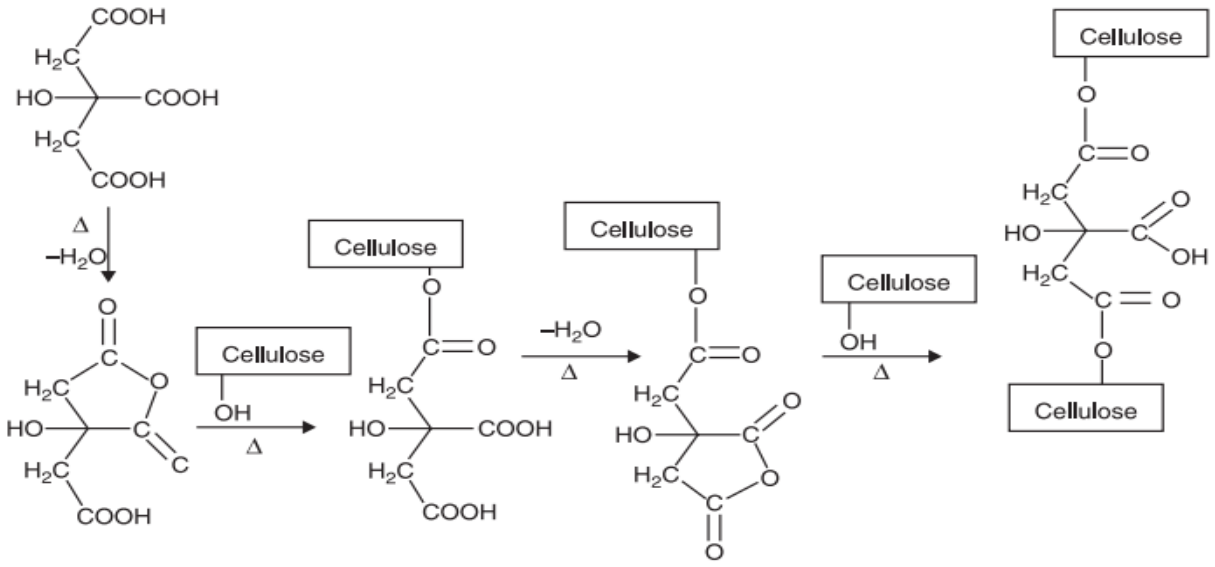

Figure 2.13 Crosslinking reaction mechanism of citric acid with cellulose (Salam, 2015).

Coma et al. (2003) carried out the crosslinking of hydroxyl propyl methyl cellulose with CA, simply heating the reagents and determining the rate of crosslinking. According to (Zhou et al., 1995) the two main stages of the reaction of poly-functional carboxylic acids with cellulose are firstly due to the attachment of the poly-functional carboxylic acids via esterification with a cellulosic hydroxyl group and its further reaction – via esterification – with another cellulosic hydroxyl group producing a crosslink between cellulose chains. This mechanism is based on an anhydride intermediate formation. Attachment of the carboxylic acid moiety to cellulose's hydroxyl group via esterification reaction of the first cyclic anhydride would expose a new carboxylic acid unit in citric acid, which has the proper chemical connectivity to form a new intramolecular anhydride moiety with the adjacent carboxylic acid unit. Further reaction with a cellulose hydroxyl of another chain can then lead to cross-linking. According to (Poerwono et al., 2001) studies, a combination of citric acid and glycine was used to improve the dissolution stability of hard gelatin capsules by preventing pellicle formation or cross-linking of the capsule gelatin.

3 MATERIALS AND METHODOLOGIES

3.1 Materials and chemicals

3.1.1 Equipment/Materials

The raw materials and equipment used for the present study were broiler skin from Adama city at Keble 17(chicken traders), urea, beaker, cutter, measuring cylinder, water bath, balance, separator funnel, temperature-controlled oven, hotplate, manual pelletizer, fluidized mixer, round bottom flask, spatula, sample holder, petri dish and glove. For the characterization of the final product, Fourier Transform Infrared spectroscopy (FTIR), Nuclear magnetic resonance (NMR), and Nitrogen content analyzer (Kjeldahl setup) were used.

3.1.2 Chemicals and reagents

All the chemicals that were used in this research are sodium chloride (NaCl), Acetone, sodium hydroxide (NaOH), citric acid, lactic acid, and distilled water.

3.2 Methodology

3.2.1 Extraction of elastin/collagen mixture

The raw Broiler's skin sample was taken from Adama city around Keble 17(chicken traders). The sample was cut into small pieces and then soaked with 10 %vol of 1M NaCl solution for 24 hours. After 24 hrs extraction, the pellets were washed with demineralized water multiple times and defatted with 10 % vol acetone for 1 hour three times. Then dry the pellets in the atmosphere for one hour. The dry skin was dissolved in 10 %vol of 0.1 N NaOH and heated for 15 min in a boiling water bath with constant shaking. After cooling, it was further extracted again for 45min in a boiling water bath at 100°C (Nadalian et al., 2013). Then after separating the fat contents using a separating funnel and finally the separated product was dried in the oven at 80°C to get an elastin and collagen mixture (Elavarasan et al., 2016).

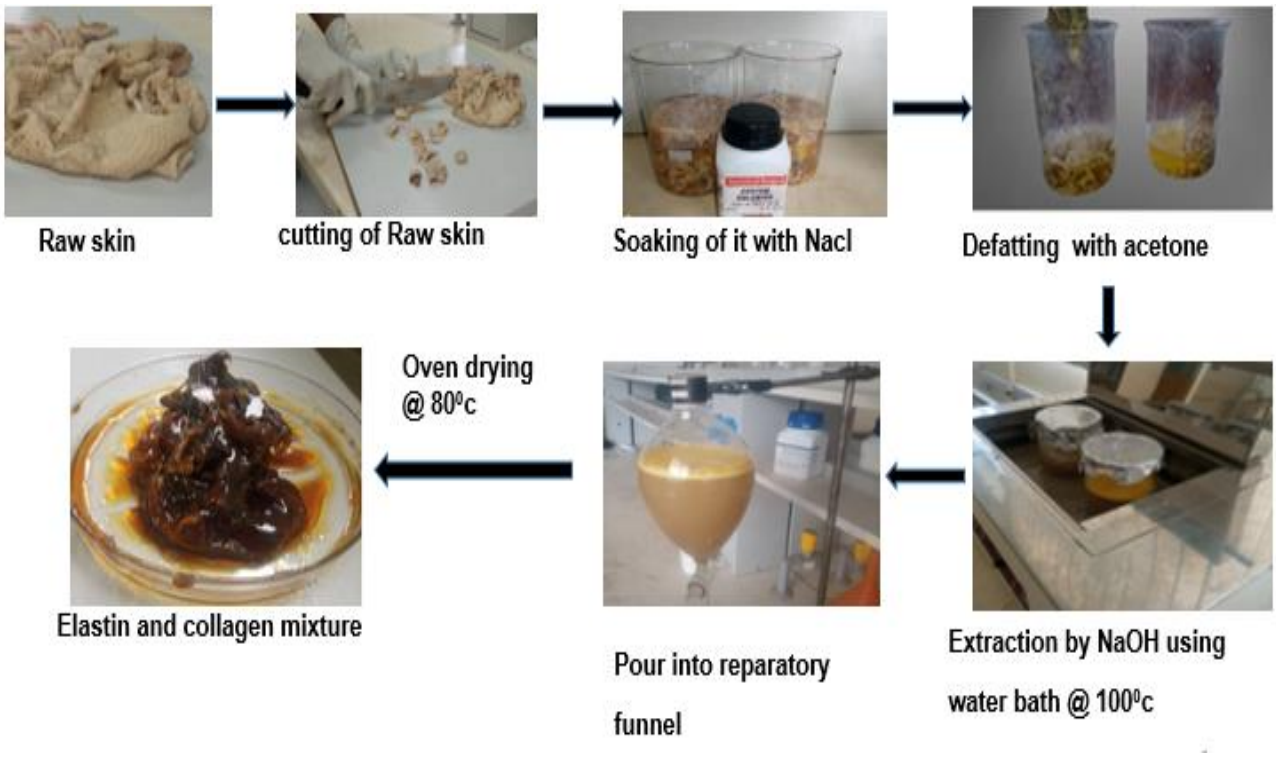

Figure 3.1 Extraction of Elastin and Collagen from broiler skin.

3.2.2 Synthesize ELN/COL-LA/CA matrix from the extracted ELN/COL mixture.

ELN/COL mixture was dissolved and reacted with lactic and citric acid in the hot plate by varying temperature, reaction time, and lactic acid to a citric acid ratio to get ELN/COL-LA/CA matrix with a reduced water solubility according to the following experimental matrix.

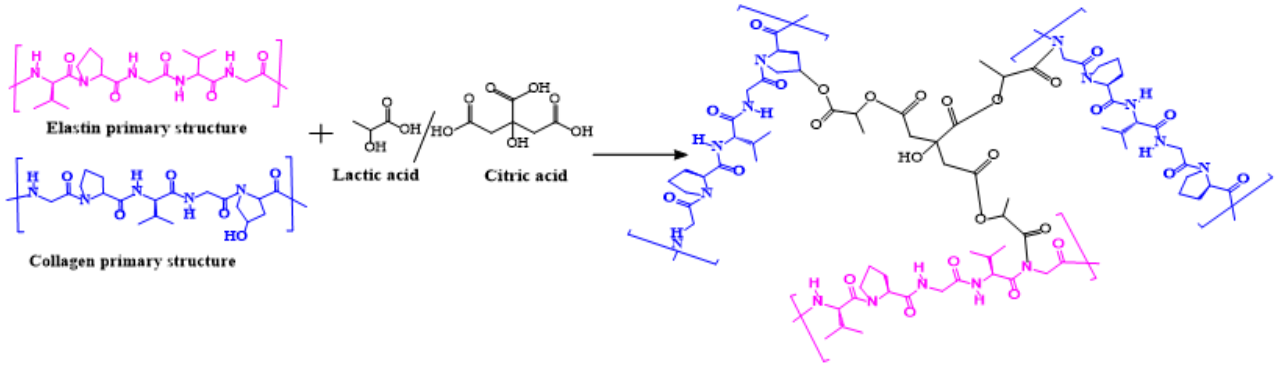

Figure 3.2 Reaction of ELL/COL with LA/CA

Table 3.1 Effect of Time on the Solubility of ELN/COL- LA/CA matrix

Exp. run	ELN/COL (gram)	Lactic acid (LA) to citric acid (CA) ratio	Temperature (ºC)	Reaction time (hour)	Response solubility in water (%TN release)
1	3	1:1.5	70	2.0	
3	3	1:1.5	70	3.0	
5	3	1:1.5	70	4.0	

Table 3.2 Effect of Temperature on the Solubility of ELN/COL-LA/CA matrix

Exp. Run	ELN/COL (gram)	Lactic acid (LA) to citric acid (CA) ratio	Temperature (ºC)	Reaction time (hour)	Response solubility in water (%TN release)
1	3	1:1.5	90	Optimized	
3	3	1:1.5	70	Optimized	
5	3	1:1.5	50	Optimized	

Table 3.3 Effect of Lactic acid (LA) to citric acid (CA) ratio on the Solubility of ELN/COL-LA/CA matrix

Exp. Run	ELN/COL (gram)	Lactic acid (LA) to citric acid (CA) ratio	Temperature (ºC)	Reaction time (hour)	Response solubility in water(%TN release)
1	3	1:0.5	Optimized	Optimized	
2	3	1:1	Optimized	Optimized	
4	3	1:2	Optimized	Optimized	

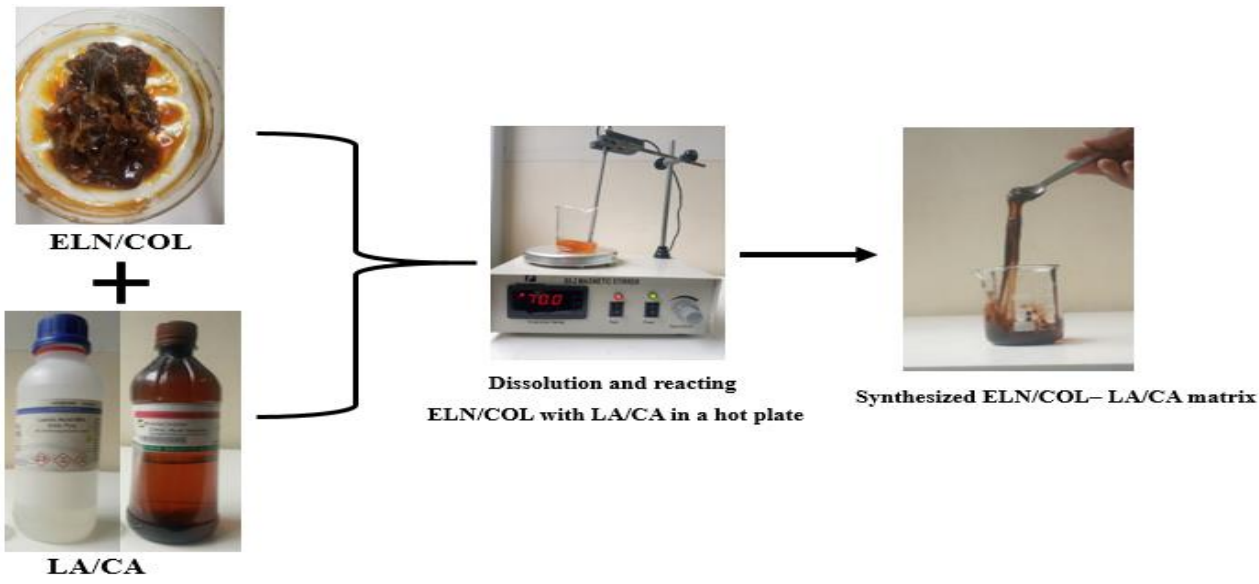

Figure 3.3 Synthesize ELN/COL-LA/CA matrix from the extracted ELN/COL mixture.

3.2. Dispersion of urea within the synthesized ELN/COL-LA/CA matrix.

The urea dispersed ELN/COL-LA/CA matrix samples were prepared by adding particular amounts of nutrient (urea) into the synthesized ELN/COL-LA/CA matrix and mixed with a fluid mixer. And finally, the urea dispersed ELN/COL-LA/CA matrix was pelletized with a manual pelletizer. The urea dispersed ELN/COL– LA/CA matrix was prepared according to the following matrix to urea ratio.

Table 3.4 Amount/ratio of urea that was dispersed in the extracted ELN/COL – LA/CA matrix

Samples	ELN/COL-LA/CA matrix (gram)	Urea (gram)	Matrix to urea ratio
S_1	2	1	1:0.5
S_2	2	2	1:1
S_3	2	4	1:2
S_4	2	6	1:3

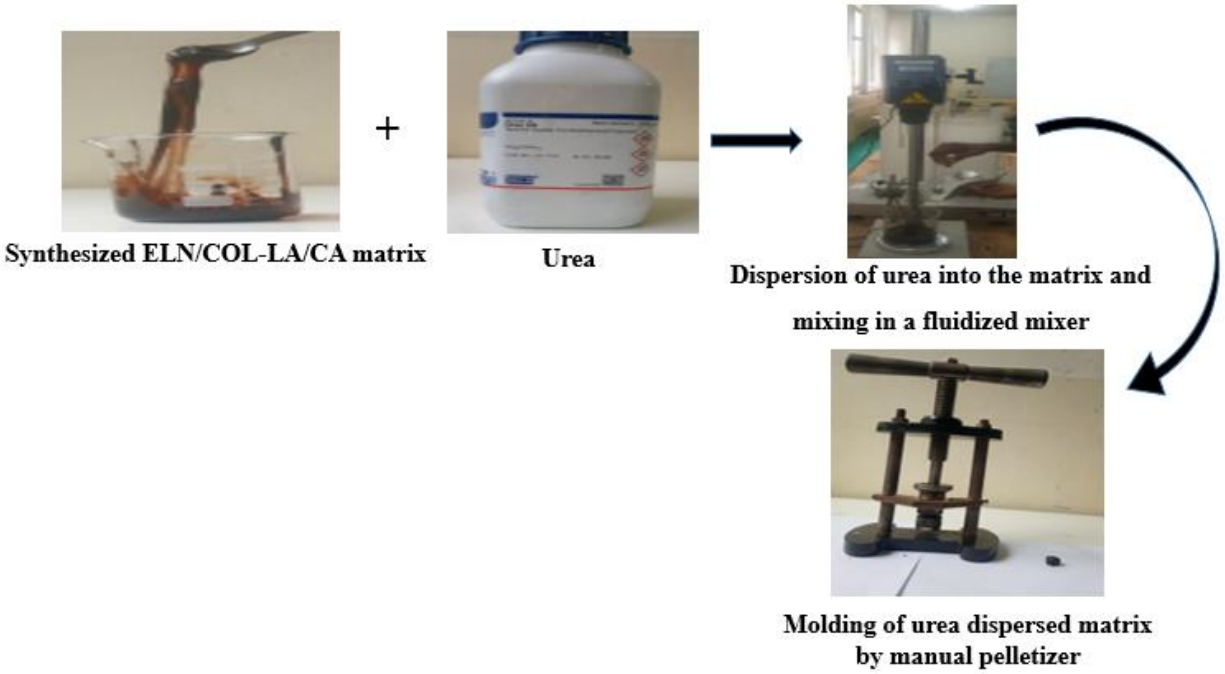

Figure 3.4 Dispersion of urea within the synthesized ELN/COL-LA/CA matrix

3.3 Characterizations

3.3.1 Fourier Transform Infrared Spectroscopy (FTIR)

The functional group analysis of extracted elastin/collagen mixture and ELN/COL-LA/CA matrix and also further identification or selection of the least water soluble ELN/COL-LA/CA matrix was done using Fourier transform infrared spectroscopy (Model: FTIR-6600 type A and Serial number A013861790) attenuated with total reflectance (ATR) mode in the range of 4000 to 500 $cm^{-1}$with 4 cm^{-1} resolution and 64 scan rates by comparing the intensity of the hydroxyl (O-H) group as well as the amide and ester groups (C=O).

3.3.2 Nuclear magnetic resonance analysis (NMR) for the synthesized ELN/COL- LA/CA matrix, and CALAOLG

The idealized chemical structure and the reaction mechanism of ELN/COL with a mixture of citric and lactic acid were investigated by ^{1}H NMR and ^{13}C-NMR characterizations (Yao et al., 2004). The samples were dissolved in deuterated chloroform ($CDCl_3$), filtered with a 0.25 μm filter, and transferred to a 5 mm diameter NMR tube. For this case, the samples were completely dissolved in chloroform before the analysis.

3.3.3 Solubility test for the extracted ELN/COL-LA /CA matrix

To test the solubility of the ELN/COL-LA/CA matrix one gram of ELN/COL-LA/CA matrix was measured and immersed in a 500 ml beaker that contains 200ml distilled water and the sample was taken from the beaker with a time interval of 1,12,24,36,48,60, and 72 hours and its water solubility with time were performed by measuring the percentage of nitrogen release from the matrix to the water by Kjeldahl method (S. Nielsen, 2010). This test was performed to select a least soluble matrix (minimum percentage of nitrogen released from the matrix to water) for urea dispersion.

3.3.4 Analysis of the release kinetics/mechanism of urea dispersed ELN/COL-LA/CA matrix in water

The kinetics of nitrogen release in water at room temperature and natural pH for urea dispersed ELN/COL-LA/CA matrix was determined by the Kjeldahl method (S. Nielsen, 2010). Briefly, 1 gram of samples was soaked into a beaker containing 200 ml of distilled water. 5 ml of the solution was withdrawn from the beaker at preset time intervals (Wei et al., 2019). Profiles of the percentage of nitrogen release as a function of time were then obtained by the Kjeldahl method (S. Nielsen, 2010). The measurements were replicated two times under identical laboratory conditions. The mechanism of the nitrogen release from the urea dispersed ELN/COL–LA/CA matrix was investigated by fitting the most suggested release kinetic models on nitrogen release % versus time data. A non-regression analysis using Microsoft® Excel 2016 Solver Add-in was performed. Two classic empirical diffusion models were selected (Eq (1) - (Nadalian et al.)): The Higuchi, and Korsmeyer-Peppas models to analyze the nitrogen release kinetic (Phang et al., 2020). The Higuchi model assumes that Fickian diffusion is the predominant release mechanism, as shown:

$$\frac{M_t}{M_\infty} = Kt^{0.5} \dots\dots\dots\dots\dots\dots\dots\dots\dots (1)$$

Where t is time, Mt/M∞ is the fraction of active agent (nitrogen) released at time t, and K is the release rate kinetic constant for the Higuchi model. Higuchi model empirical equation was developed based on a few hypotheses (Paul, 2011) i. the solubility in the matrix is much lower than the initial solute concentration in the matrix; ii. the diffusion process or pathway is one-

dimensional; iii. The polymer swelling and dissolution are negligible and iv. the diffusivity is constant (Phang et al., 2020).

Korsmeyer-Peppas's kinetic model was Eq. (Nadalian et al.).

$$\frac{M_t}{M_\infty} = Kt^n \ldots\ldots\ldots\ldots\ldots\ldots\ldots\ldots\ldots\ldots (2)$$

Where $\frac{M_t}{M_\infty}$ is the fraction of active agent (nitrogen) released at time t, K is the release rate kinetic constant for Korsmeyer-Peppas, and n is the diffusion exponent, indicative of the transport mechanism. The nitrogen release mechanism from the matrix is classified according to n values. If $n < 0.5$, it is the Fickian diffusion mechanism; if $0.45 < n < 0.85$, it belongs to the non-Fickian (anomalous) transport model, the mechanism of nitrogen release is governed by diffusion and swelling; if $n > 0.85$ it is a Case II model, its mechanism was similar to that of anomalous transport model, the main difference is the velocity of solvent diffusion. In Case II, the velocity of solvent diffusion is less than the polymeric relaxation process. In Anomalous transport, the velocity of solvent diffusion and the polymeric relaxation possess similar magnitudes (Bruschi, 2015).

4 RESULT AND DISCUSSION

4.1 FTIR analysis of the extracted elastin and collagen mixture

The FTIR spectra of the extracted elastin and collagen mixture were presented in Figure (4.1) below. The typical bands characteristic for elastin and collagen proteins are observed, Amide A which arises from the N–H stretching vibrations were observed at the wave number (3200-3600) cm-1 and the O-H stretching was also visible in this range, and overlap to amide A. The Amide B band is related to the asymmetrical stretch of CH_3 stretching vibration, which is observed at 2955 cm^{-1} (Skopinska-Wisniewska et al., 2017).

The amide I peak which is associated with C=O stretching vibration or possibly hydrogen bonding coupled with COO^- was observed in the wave number of (1610-1665) cm^{-1}. Because both the C = O and the N—H bonds are involved in the hydrogen bonding that takes place between the different elements of the secondary structure, the locations of the Amide I bands are sensitive to the secondary structure content of a protein.

Collagen and elastin are well known for their distinguished secondary structures of α-helical and β-sheet respectively. The peak observed at a wave number of (1100-950) cm^{-1} designates the collagen α-helical secondary structure while the β-sheet structure of elastin is indicated in the wave number (1610-1665) cm^{-1} in the position of the amide I bond with a similar result was reported by (Kibret et al.). The amide II band, which was associated with N-H bending vibration coupled with C-N stretch, was observed at (1540–1560) cm^{-1}, indicative of the N-H group being involved in hydrogen bonding. Amide III is associated with C-N stretching vibration with N-H bend and C-O stretching was also observed in the range of (1266–1360) cm^{-1}. The bands in the region between (1430-1480) cm^{-1} displayed the C-H bending (scissoring) vibrations of $-CH_2$ and $-CH_3$ groups from the glycine, valine, proline, and hydroxyproline side chains of the ELN/COL mixture, and also the bands in the region (1440-1395) cm^{-1} displayed the O-H bending of the proteins respectively (Wang et al., 2017).

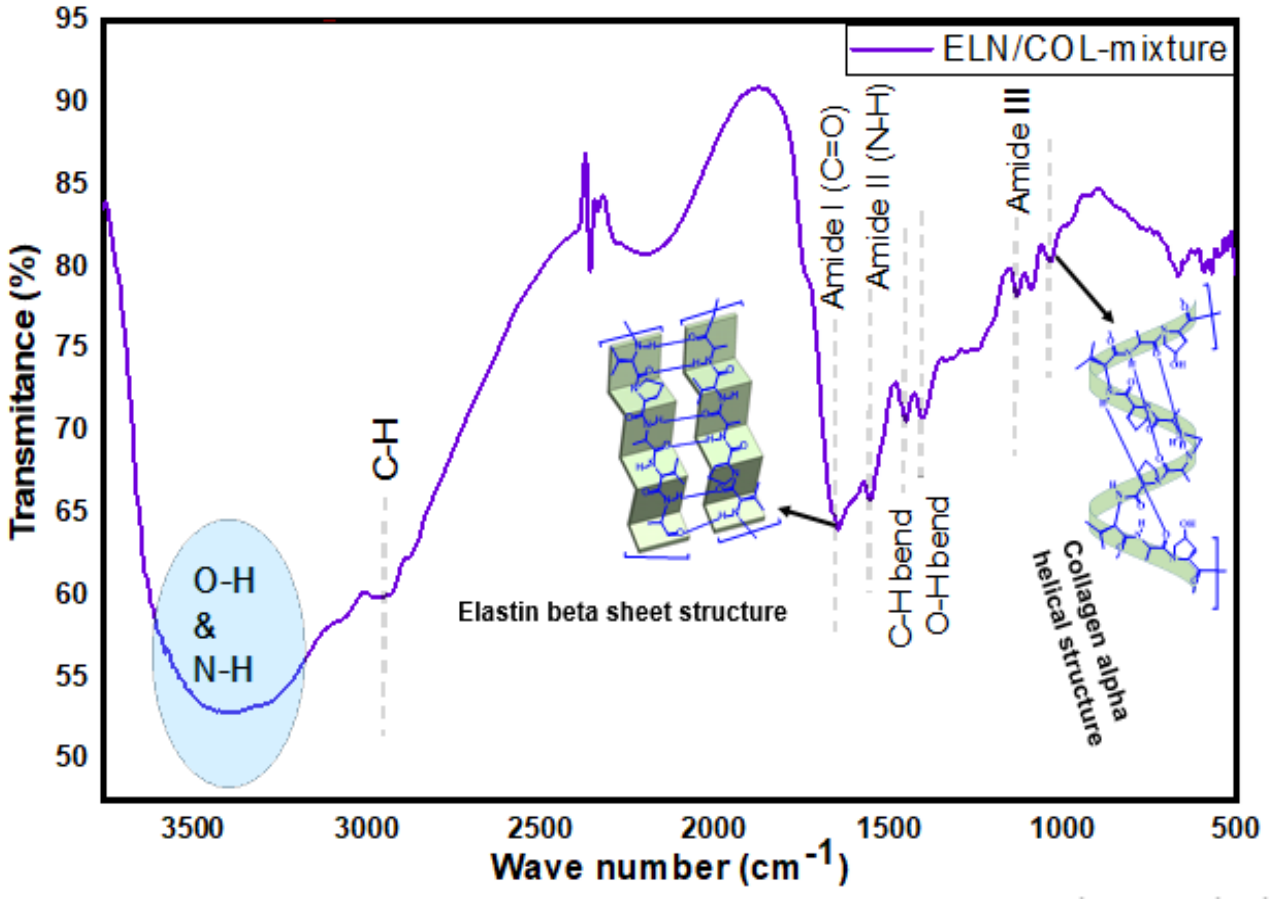

Figure 4.1 FTIR spectra for ELN/COL mixture

Table 4.1 FTIR peak for ELN/COL mixture

FTIR peak for the extracted ELN/COL-mixture	**Functional group**
(3200-3600) cm^{-1}	O-H & N–H stretching
2955 cm^{-1}	C-H stretching
(1610-1665) cm^{-1}	**Amide I** (stretching vibrations of the C=O bond of the amide)
(1540-1560) cm^{-1}	**Amide II** (bending vibrations of the N—H bond of the amide)
(1430-1480) cm^{-1}	C-H bending (scissoring) vibrations of $-CH_2$ and $-CH_3$ groups of ELN/COL
(1440-1395) cm^{-1}	O - H bending

(1266–1360)	Amide III (C-N stretching vibration with N-H bend and C-O stretching)
(1100-950) cm^{-1}	Designates the collagen α-helical secondary structure

4.2 Dissolution and reaction mechanism of ELN/COL mixture with lactic acid and citric acid

Scheme (4.1) shows that the extracted protein from broiler skin (ELN/COL) has been completely dissolved in a mixture of lactic acid and citric acid (weak organic acid). Solubilization of the extracted protein within a mixture of lactic acid and citric acid might reduce the secondary macromolecular interaction formed by NH and C=O groups of the consecutive chains of the peptide bonds, which is responsible for the formation of α-helix and β-sheet stacks of collagen and elastin, respectively. ELN/COL dissolution in a mixture of lactic acid and citric acid was conducted in a hot plate before the temperature reached 70 °C. During the dissolution step, the weakening of protein secondary structure results in the delamination of α-helix and β-sheet stacks, leading to the interaction of the primary structure of ELN/COL by lactic acid and citric acid oligomers rather than hydrogen bonding.

After successfully solubilizing the ELN/COL mixture within lactic acid and citric acid, condensation reactions were carried out at 70 ^{o}c for four hours. So at the start of the reaction, the lactic acid monomer was grown on the hydroxyproline side chain of collagen and the amino groups of ELN/COL mixture with their primary amino acid sequence. And also citric acid was grown on the lactic acid monomers which were grown on the hydroxyproline side chain of collagen. As the reaction time proceeds, the hydroxyl ends of the grown lactic on ELN/COL mixture and the carboxyl ends of the grown citric acid were condensed with a formation of an ester bond within it, and as a result, a cross-linked ELN/COL – LA/CA matrix was formed.

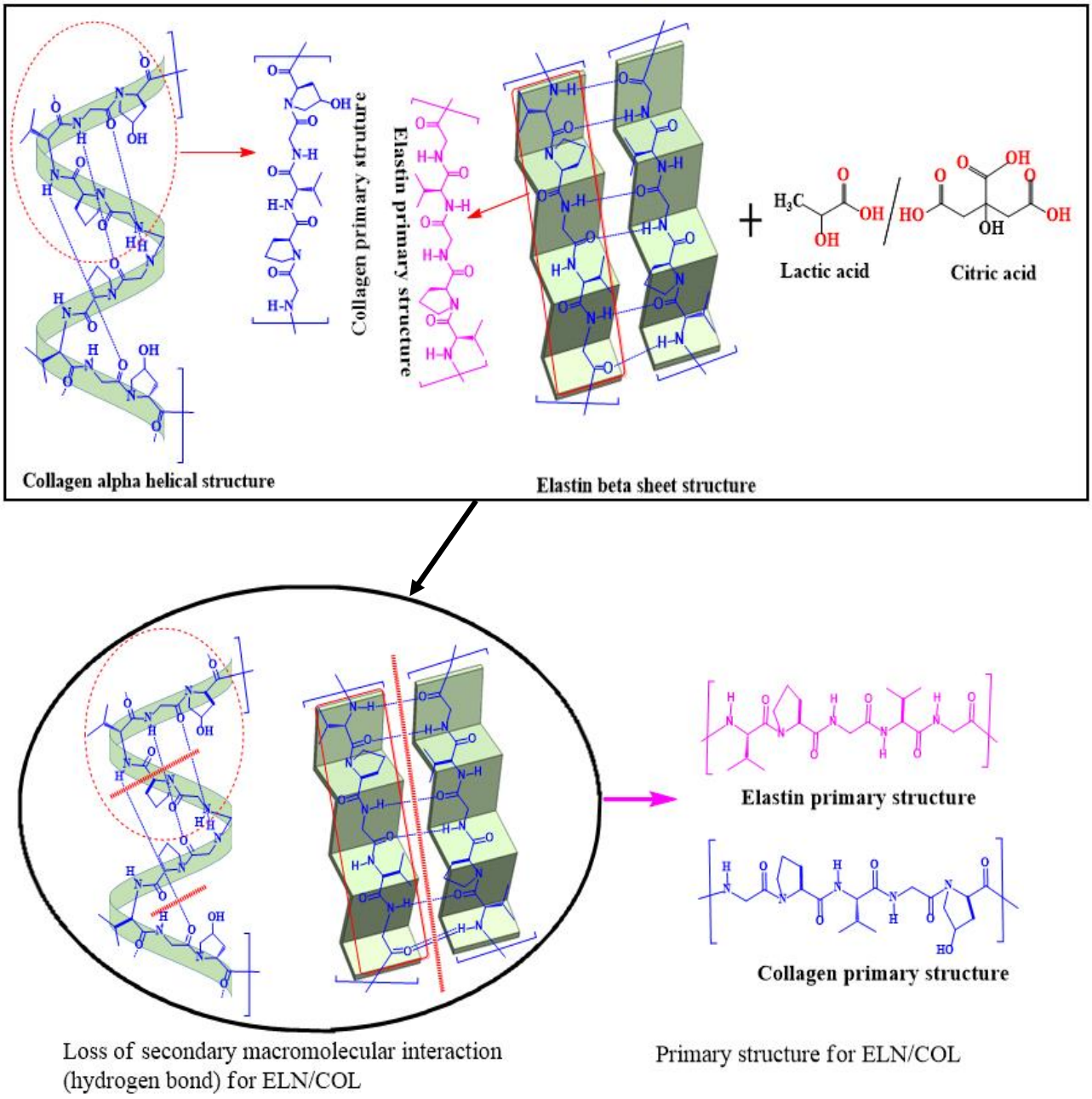

Scheme 4. 1 Dissolution of ELN/COL in a mixture of lactic acid and citric acid

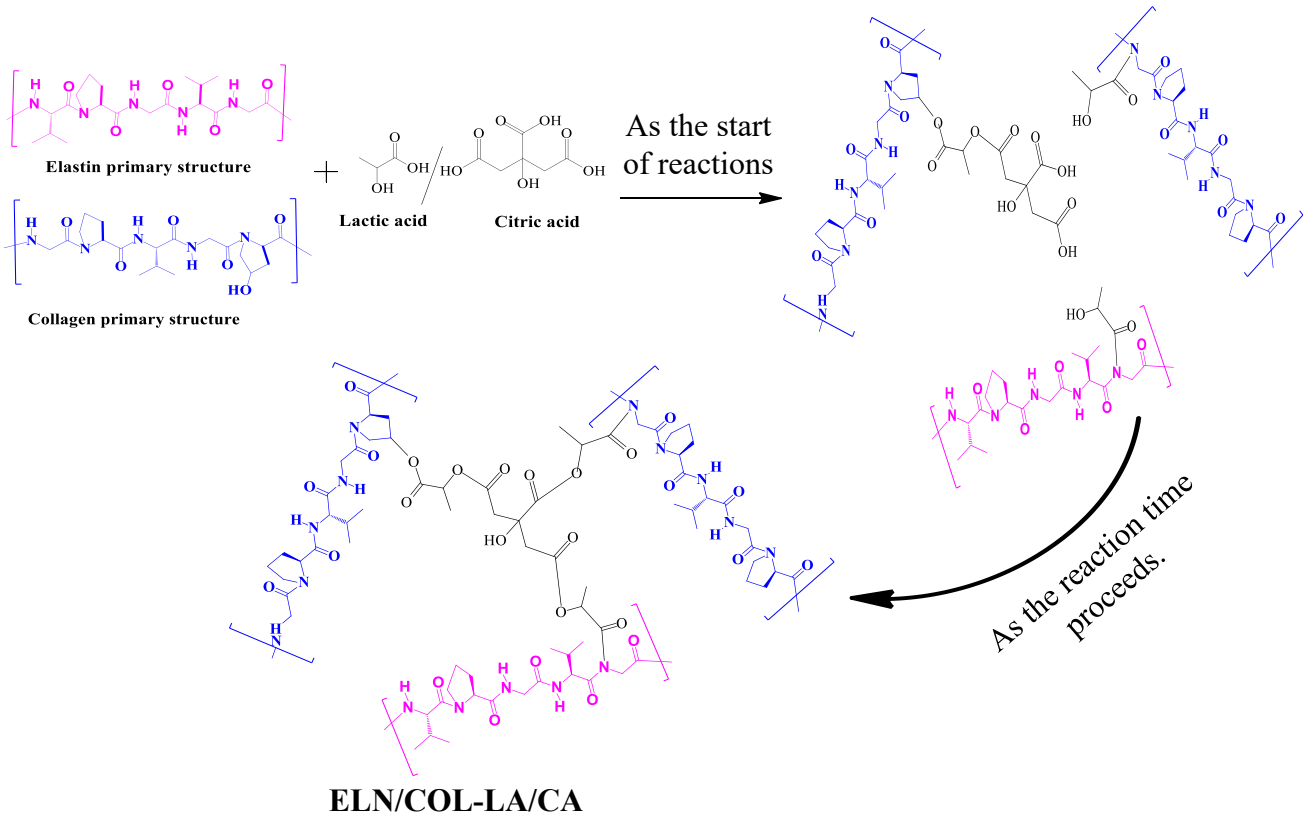

Scheme 4. 2 Reaction Scheme (a mechanism) for ELN/COL- mixture with lactic acid and citric acid

4.3 Chemical structure analysis (H-NMR and C-NMR) for citric acid and lactic acid oligomer (CALAOLG)

Citric acid-lactic acid oligomer (CALAOLG): As indicated in Scheme (4.3) and further confirmed by the H-NMR spectra of **CALAOLG** (Figure 4.2), there are two distinct positions of the methine and methyl groups from the citric acid-lactic acid oligomer; one is near the core citric acid (CA) and the other is far from it.

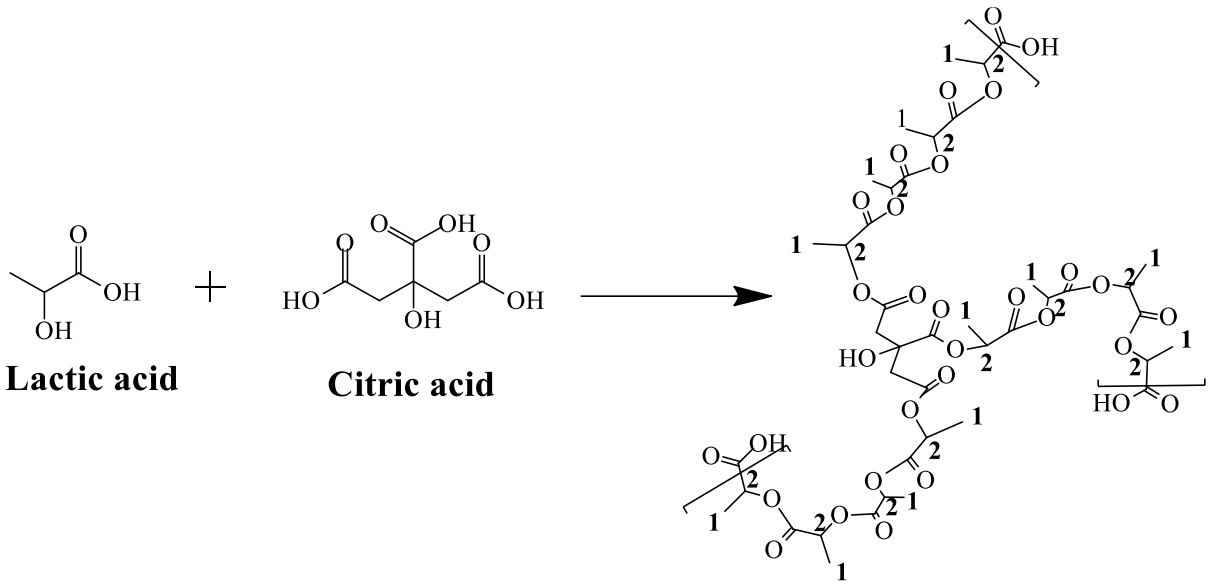

Scheme 4. 3 Reaction Scheme for citric acid-lactic acid Oligomer (CALAOLG)

The methyl group in the CALAOLG has a doublet peak (-CH neighboring proton) which was shown at a chemical shift of 1.53,1.55 and 1.57 ppm resulting from the esterification reaction of OH and COOH groups of lactic acid. Another additional peak was shown at a chemical shift of 1.52 ppm this was formed due to the esterification reaction between citric acid and lactic acid. On the other hand, the methine (CH) group of CALAOLG shows a quartet peak (-CH_3 neighboring proton) at a chemical shift of 5.13, 5.15, and 5.17 ppm resulting from the esterification reaction of OH and COOH groups of lactic acid, and also another additional peak at a chemical shift of 5.12 ppm was shown. This is due to the esterification reaction between citric acid and lactic acid. As the chain length of the oligomerization of lactic acid on citric acid increases, the chemical shifting of the chemicals becomes greater or moves to the left for all hydrogen types. (Espartero et al., 1996). And from the NMR result, there is no methyl ((-CH_3) and methine (CH) peak at a chemical shift of 1.3 and 4.33 ppm, respectively. This shows there is no free lactic acid in the CALAOLG (Espartero et al., 1996), and also no (-OH) peak from the carboxylic group was shown at a chemical shift of 11 ppm. This also shows that there is no free citric acid in CALAOLG. From the C-NMR results as shown in Figure (4.3) for CALAOLG, the 1) methyl carbon (-R-CH_3) group was shown at a chemical shift of around 16 ppm, and also the 2) methine carbon group (-CH-O-) was also shown at a chemical shift of 68.99 ppm, 3) the carbonyl bond (C=O) adjacent to the core molecule (-O-CH) was also observed at a chemical shift of 169.58 ppm.

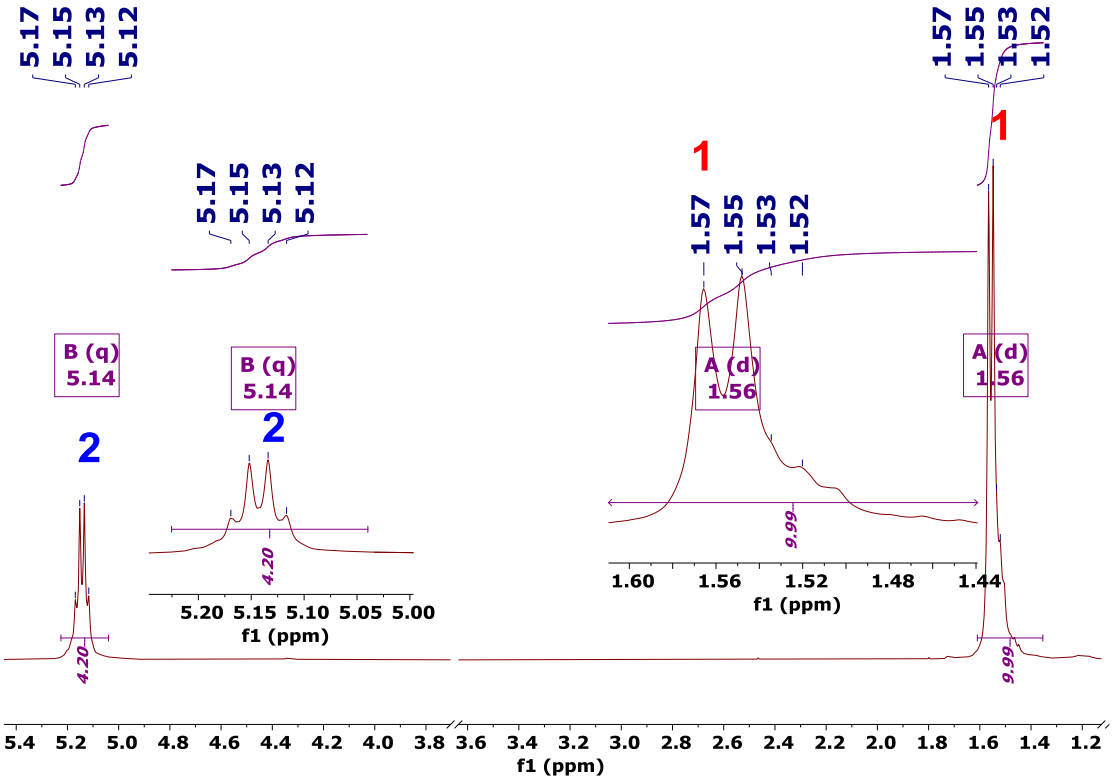

Figure 4.2 [1]H-NMR Spectra for CALAOLG

Table 4.2 [1]H - NMR Chemical Shifts (in ppm) of citric acid – lactic acid oligomer

Peak label	**Chemical shift (ppm)** **H-NMR**	**Assignment**
1	~ 1.56	Hydrogen from the methyl (-CH_3-) in the chain
2	~ 5.14	--CH in the chain

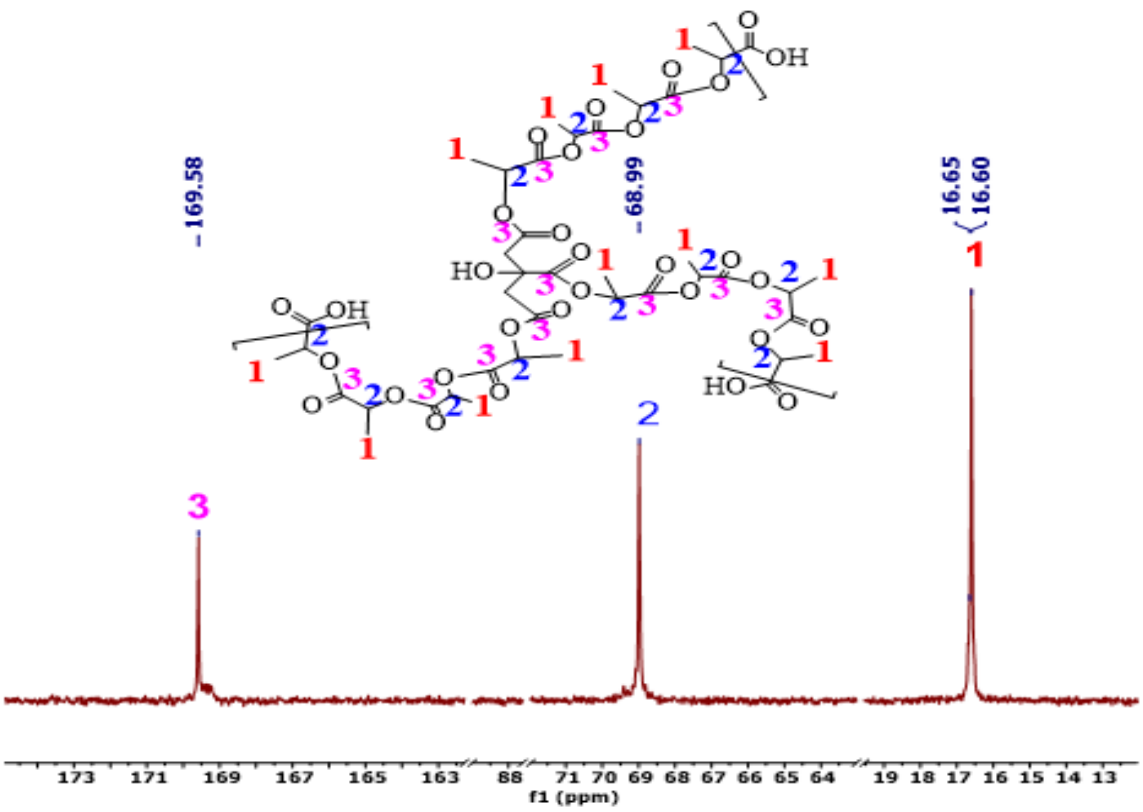

Figure 4.3 ^{13}C-NMR Spectra for CALAOLG

Table 4.3 ^{13}C - NMR Chemical Shifts (in ppm) of citric acid – lactic acid oligomer

Peak label	**Chemical shift (ppm) C-NMR**	**Assignment**
1	~ 16.65	C-H_3 (methyl carbon)
2	~ 68.99	C-H (adjacent to ester oxygen and CH_3)
3	~ 169.58	C=O Adjacent to (-O-CH (ester oxygen))

4.4 Chemical structure analysis (H-NMR and C-NMR) for ELN/COL – LA/CA matrix

As indicated in Scheme (4.4) and further confirmed by H-NMR spectra of the ELN/COL-LA/CA matrix (Figure 4.4), there are three distinct positions of the methine and two distinct positions of methyl, and also one amine group was observed in the synthesized matrix.

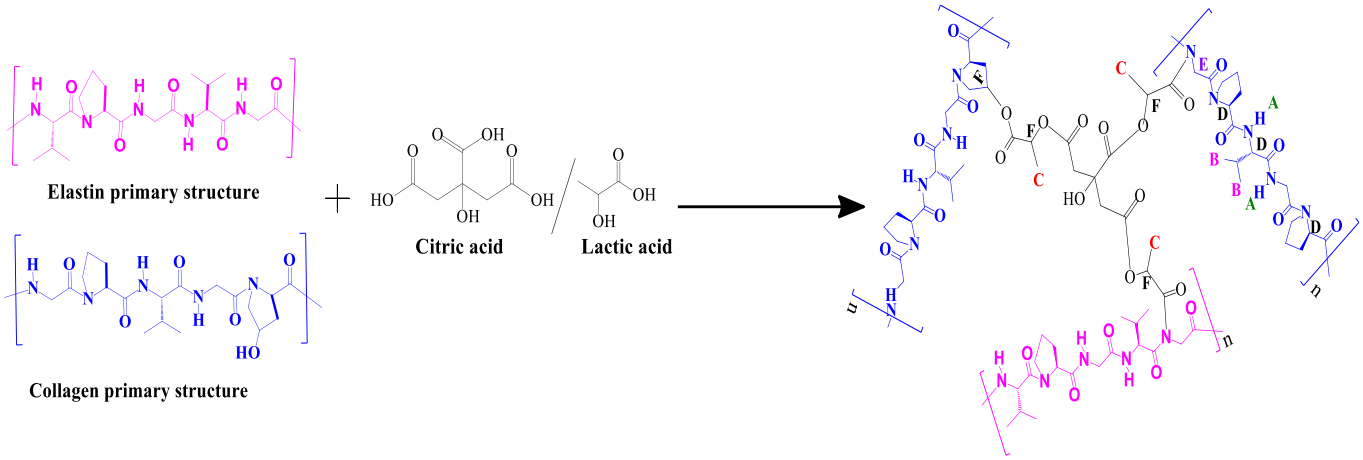

Scheme 4. 4 Reaction Scheme for the synthesis of ELN/COL-LA/CA matrix

The methyl group of the ELN/COL-LA/CA matrix as shown in Figure (4.4) has two different doublet peaks, the first peak was shown at a chemical shift of around 1.43 ppm and 1.44 ppm and the second was observed at a chemical shift of 1.51 ppm, 1.53 ppm, and 1.54 ppm. There are also new singlet peaks at a chemical shift of 1.22 ppm, which results from the amine group (-NH-) of the ELN/COL mixture located by the letter (A). Additional peaks are also observed at a chemical shift of 4.34 ppm and 4.97 ppm, which were not observed in CALAOLG. There is also another intense and broad peak observed at a chemical shift of 5.13 ppm. The presence of doublet peaks at a chemical shift of 1.43 ppm and 1.44 ppm is responsible for the methyl group from the valine side chain of the ELN/COL mixture as indicated by a letter (B). In addition, the broad doublet peaks found between the 1.51,1.53, and 1.54 ppm stand for the methyl (CH_3) groups from the chain of lactic acid which was grown on ELN/COL-mixture as indicated by (C). The formation of a new peak at a chemical shift of 4.34 and 4.97 ppm is due to the presence of methine (-CH-) neighboring the amide bond in the primary amino acid sequence of the ELN/COL mixture and the methylene (-CH_2-) from the glycine side chain of ELN/COL mixture neighboring the nitrogen, which has two amide bonds, one is within the sequence of their amino acid and the other is the newly formed amide bond with that of the grown lactic acid as indicated by (D & E) respectively. There is also another broad and intense peak at a chemical shift of 5.13, which is the peak for methine (-CH-) in the chain of the grown lactic acid within the ELN/COL- LA/CA matrix neighboring ester bond when we compare it to the H-NMR of CALAOLG, it has a broader peak. This was due to the formation of an additional ester bond between the hydroxyproline side chain of collagen and that of lactic acid, indicated by (F). From the C-NMR results for ELN/COL- LA/

CA matrix as shown in Figure (4.5), the 1) methyl carbon (-R-CH_3) group was shown at a chemical shift of around 16 ppm. Its peak was more intense and broad than the methyl peak in CALAOLG. This is due to the additional methyl group from the valine side chain of ELN/COL. And also the 2) methylene carbon group (-CH_2) was also observed at a chemical shift of around 20.02 and 20.4 ppm. this results from the carbon at the proline and hydroxyproline side chain of the ELN/COL mixture, this peak was not observed in the C-NMR of CALAOLG, the 3) Methine (CH) carbon group (-CH-N-) of ELN/COL-mixture which was neighboring with amide bond within their primary amino acid sequence was also shown at a chemical shift of 66.58 ppm, 4) methine carbon group (-CH-O-) neighboring with ester bond was also shown at a chemical shift 68.97 ppm, this peak was also observed in CALAOLG but the methine peak in ELN/COL-LA&CA matrix was more broad than the methine peak in CALAOLG this is due to additional ester bond formation between ELN/COL and that of lactic acid 5) the carbonyl bond (C=O) adjacent to the core molecule (-O-CH) and (-N-) were also observed at a chemical shift of 169.37 and 169.54 ppm respectively.

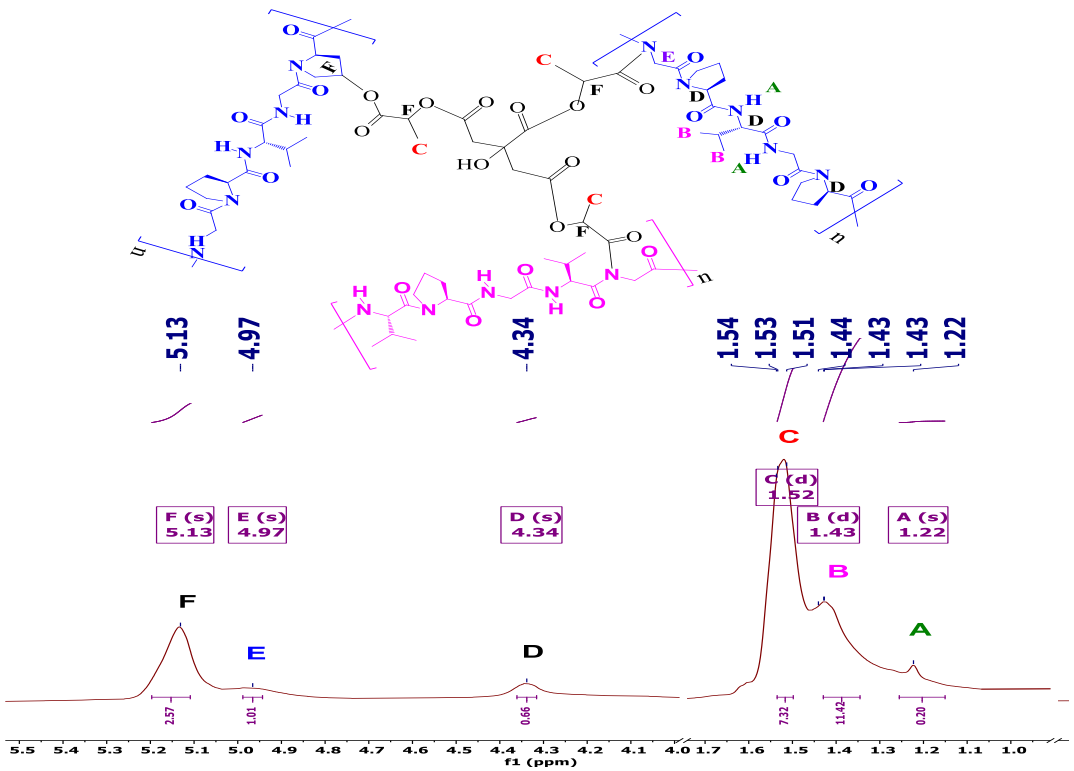

Figure 4.4 ^{1}H-NMR Spectra for ELN/COL-LA/CA matrix

Table 4.4 ^{1}H- NMR Chemical Shifts (in ppm) of ELN/COL – LA/CA matrix

Peak label	**Chemical shift (ppm) H-NMR**	**Assignment**
A	~ 1.22	Amine group (-NH-) of ELN/COL mixture
B	~ 1.43	Methyl group from the valine side chain of ELN/COL mixture
C	~ 1.52	Methyl (CH_3) groups from lactic acid which was grown on ELN/COL.
D	~ 4.34	Methine (-CH-) peak of the matrix neighboring the one amide bond 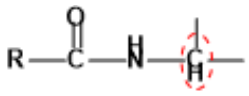
E	~ 4.97	Methylene ($-CH_2-$) neighboring the two amide bond 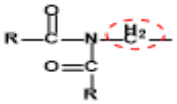
F	~ 5.1	Methine (-CH-) in the chain of grown LA and ELN/COL mixture neighboring ester bond 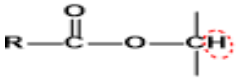

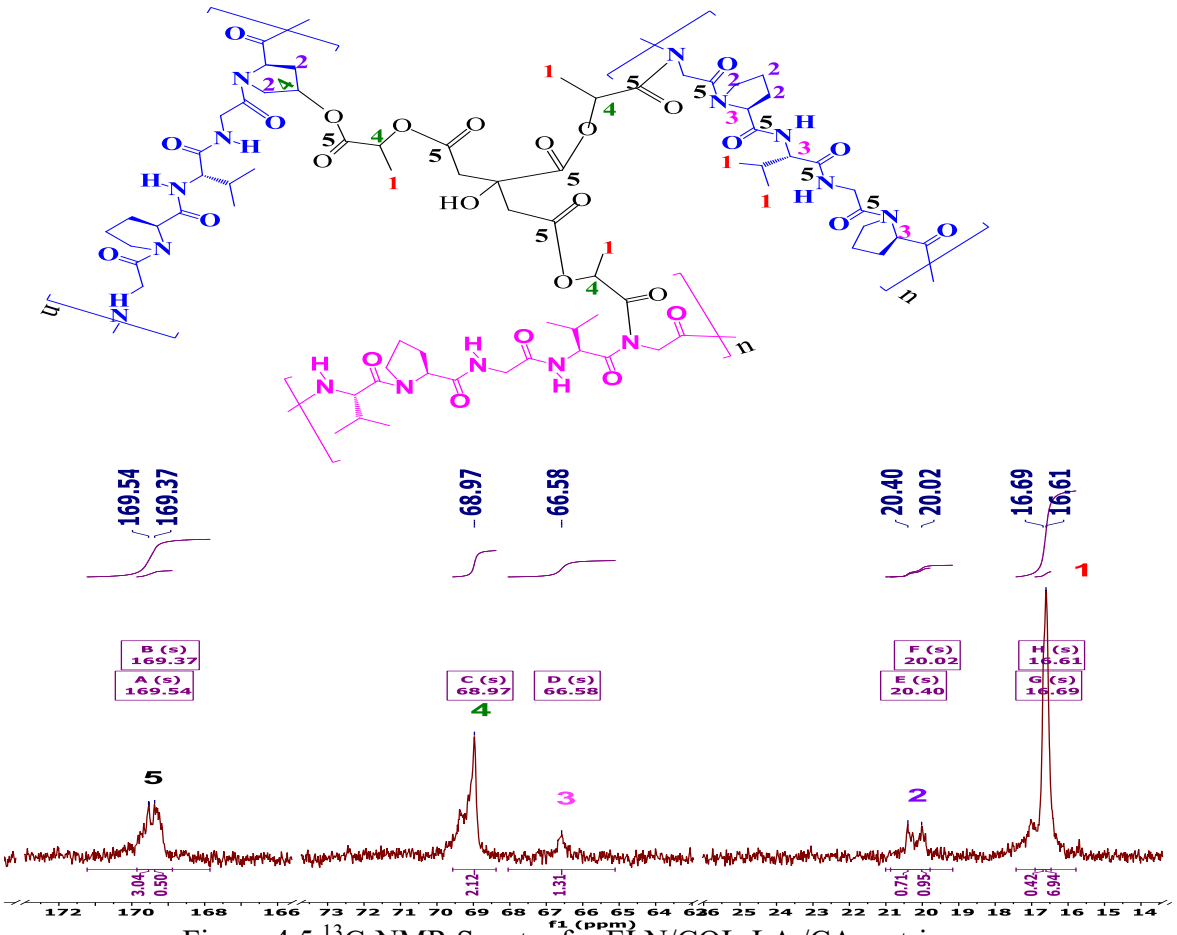

Figure 4.5 ^{13}C-NMR Spectra for ELN/COL-LA /CA matrix

Table 4.5 ^{13}C- NMR Chemical Shifts (in ppm) of ELN/COL – LA/CA matrix

Peak label	Chemical shift (ppm) H-NMR	Assignment
1	~ 16.61 & 16.69	Methyl carbon (-R-CH_3) from the valine side chain of ELN/COL mixture and in the chain of grown LA
2	~ 20.02 & 20.02	Methylene carbon group (-CH_2-) from the carbon at the glycine, proline, and hydroxyproline side chain of ELN/COL mixture
3	~ 66.58	Methine (CH) carbon group (-CH-N-) of ELN/COL-mixture which was neighboring with amide bond within their primary amino acid sequence
4	~ 66.97	Methine carbon group (-CH-O-) neighboring with ester bond was also shown at a chemical shift of 68.97 ppm

		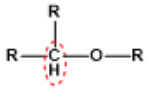
5	~ 169.37 & 169.54	Carbonyl bond (C=O) adjacent to the core molecule (-O-CH) and (-N-) 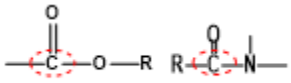

4.5 Total nitrogen content (Percentage) analysis for the extracted ELN/COL-LA/CA matrix

The percentage of total nitrogen content for the extracted ELN/COL– LA/CA matrix, which was conducted under different conditions, was analyzed by the Kjeldahl method. This analysis was conducted for the purpose of the solubility test of the matrix since the solubility test for the synthesized matrix was measured in terms of the percentage of nitrogen released from the matrix to water. So, from Figure (4.6), as shown below, the percentage of total nitrogen for the synthesized ELN/COL-LA/CA matrix increased as the time of reaction between the ELN/COL mixture and that of lactic acid and citric acid was increased. Since increasing the reaction time means increasing the contacting time for the reactant, as a result, it favors condensation reaction between them with the removal of water. The graph also shows that as the reaction temperature between ELN/COL and LA/CA increases, its percentage of total nitrogen also increases. Since increasing temperature can also increase the collusion between the reactants, as a result, it favors condensation reactions between them. Even if further temperature increases can lead to the breakage of bonds, their total nitrogen content is not affected by this breakage. Furthermore, the ratio of lactic acid to citric acid also has a role in the percentage of total nitrogen for the synthesized ELN/COL-LA/CA matrix, so from the Figure (4.6) shown below (the rainbow color), as the ratio of LA: CA was increased, its percentage of total nitrogen for the synthesized matrix decreased since increasing the ratio of lactic acid to citric acid means increasing the amount of citric acid, which does not have any nitrogen-containing functional group in its structure.

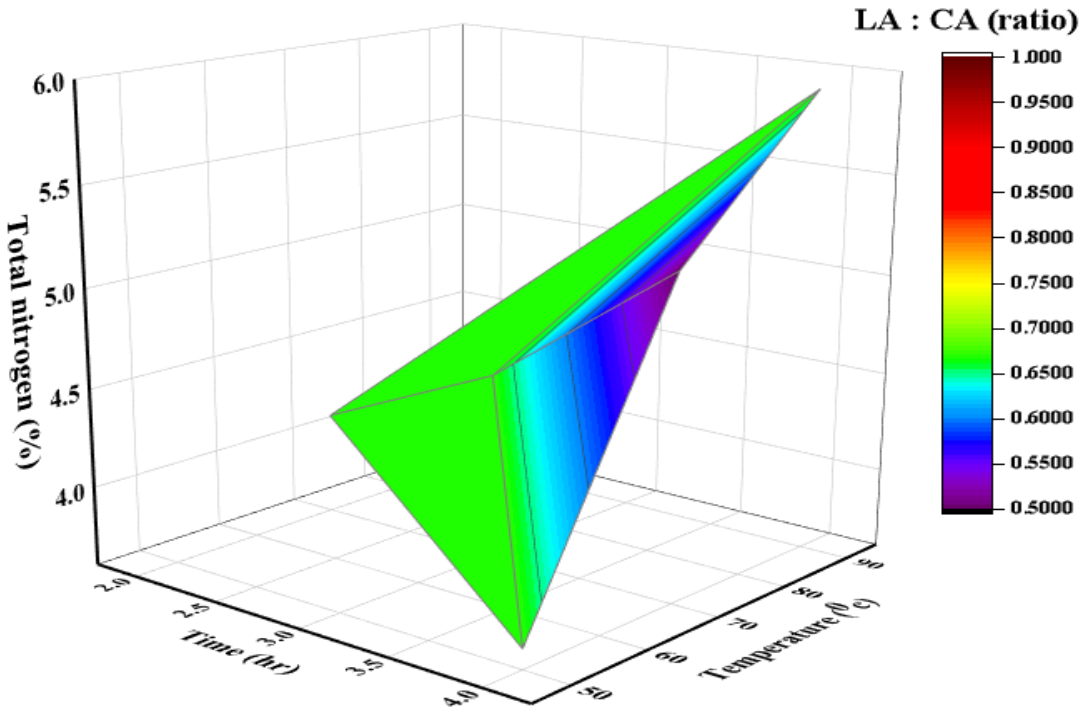

Figure 4.6 Percentage of total nitrogen for ELN/COL – LA/CA matrix which was synthesized under various conditions

Table 4.6 Percentage of total nitrogen for ELN/COL-LA/CA matrix which was synthesized under various conditions

No	Extracted ELN/COL-LA/CA matrix at various conditions	Content of total nitrogen (%)
1	ELN/COL-LA/CA matrix @ 2-hour reaction time	4.12
2	ELN/COL-LA/CA matrix @ 3-hour reaction time	4.53
3	ELN/COL-LA/CA matrix @ 4-hour reaction time	5.32
4	ELN/COL-LA/CA matrix @ 50^{o}c reaction temperature	3.7
5	ELN/COL-LA/CA matrix @ 70^{o}c reaction temperature	5.32
6	ELN/COL-LA/CA matrix @ 90^{o}c reaction temperature	5.92
7	ELN/COL-LA/CA matrix with LA: CA ratio of 1:1	5.54
8	ELN/COL-LA/CA matrix with LA: CA ratio of 1:1.5	5.32
9	ELN/COL-LA/CA matrix with LA: CA ratio of 1:2	4.59

4.6 Effect of reaction time, temperature, and lactic acid to citric acid ratio on the Solubility of the synthesized ELN/COL-LA/CA matrix in water

The solubility test was performed to select the least soluble ELN/COL-LA/CA matrix for urea encapsulation. This test was indirectly performed by measuring the percentage of nitrogen released from the extracted matrix into the water by the Kjeldahl method.

4.6.1 Effect of reaction time on the solubility of the synthesized ELN/COL-LA/CA matrix in water

Three different experiments were conducted to select the best reaction time for the reaction between the ELN/COL mixture and that of lactic and citric acid, which gives the least soluble matrix. The experiment was conducted by varying the reaction time (2, 3, and 4) hours at a fixed temperature of 70 ^{o}c and lactic acid to citric acid ratio of 1:1.5 and that of ELN/COL 3 gram. So to select the matrix which is least soluble in water, a solubility test was conducted by immersing a gram of the synthesized matrix into the distilled water and a sample was taken by syringe at different time intervals of (1,12,24,36,48,60, and 72) hours, so the amount/percentage of nitrogen released from the matrix to water was determined by the Kjeldahl method (S. S. J. F. A. Nielsen, 2010).

From the results, as shown in Figure (4.7) below, the percentage of nitrogen released from the matrix to water was greater for the matrix which was synthesized at a 2-hour reaction time than for 3 and 4-hour reaction times throughout the whole time interval, it released around 34% of its nitrogen within 72 hours from the matrix to water. But the matrix which was conducted for a 4-hour reaction time shows the least percentage of nitrogen released from the matrix to the water it releases around 10.5 % of nitrogen within 72 hours.

As a result, the matrix that had the least percentage of nitrogen released from the matrix to the water had the least soluble matrix and the matrix that had a high percentage of nitrogen released from the matrix to the water was highly soluble in the water. From this, a 4-hour reaction time matrix was least soluble than the other matrixes since as the reaction time between ELN/COL and that of LA/CA increased, the contact time between the carboxylic group of LA/CA and the amine group as well as the hydroxyl group of ELN/COL mixture also increased. As a result, its hydrophobic property was enhanced through ester linkage as well as amide bond formation through a condensation reaction with the removal of water.

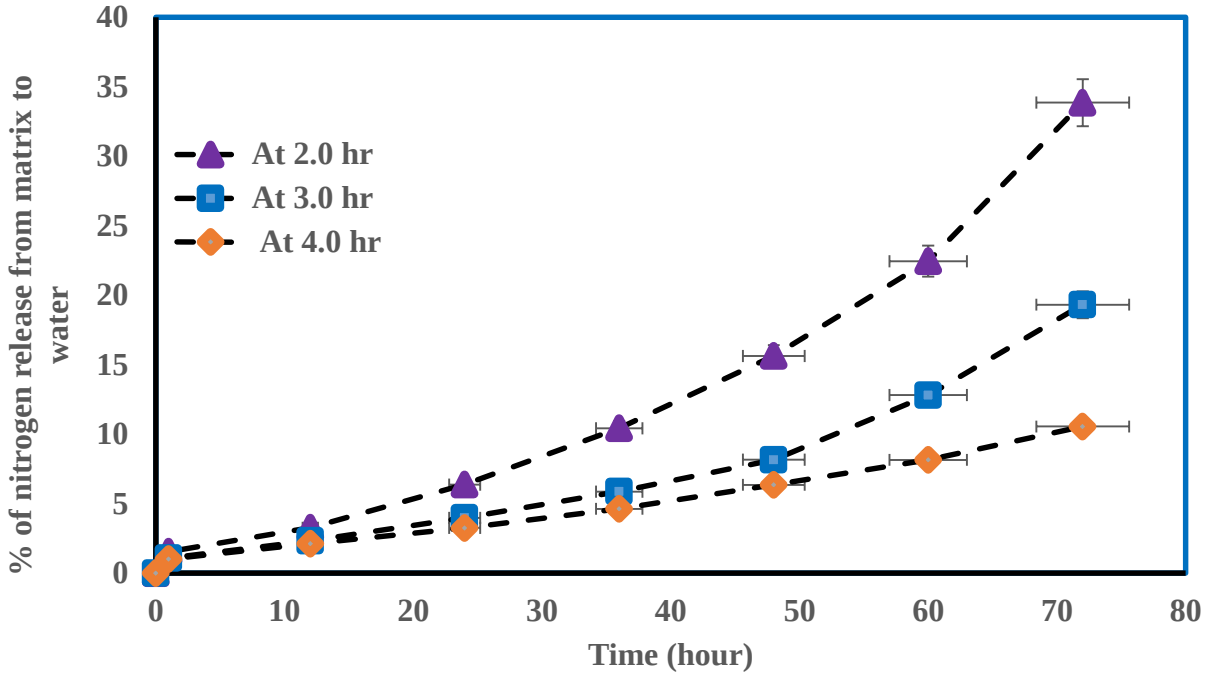

Figure 4.7 Effect of reaction time on the percentage of nitrogen released from ELN/COL-LA/CA matrix to water with different time intervals

4.6.2 Effect of temperature on the solubility of the synthesized ELN/COL-LA/CA matrix in water

Three different experiments were conducted to select the best reaction temperature for the reaction between ELN/COL and that of lactic acid and citric acid, which gives the least soluble matrix. The experiment was conducted by varying the reaction temperature (50, 70, and 90 ^{o}c) at a fixed reaction time of 4 hours since this was taken according to section 4.6.1 (least soluble matrix was formed at a 4-hour reaction time), and the lactic acid to citric acid ratio of 1:1.5 and that of ELN/COL to 3 grams. So to select the matrix which was least soluble in water, a solubility test was conducted by immersing a gram of the extracted matrix into the distilled water and a sample was taken by syringe with different time intervals of (1,12,24,36,48,60 and 72) hours so the amount/percentage of nitrogen release from the matrix to water was determined/measured by Kjeldahl method (S. S. J. F. A. Nielsen, 2010).

From the results as shown in Figure (4.8) below the percentage of nitrogen releases from the matrix to water was greater at a reaction temperature of 50 ^{o}c than 70 ^{o}c and 90 ^{o}c throughout the whole time interval, it releases 46 % of its nitrogen within 72 hours from the matrix to water. But

the matrix which is conducted at a reaction temperature of 70 ^{o}c shows the least percentage of nitrogen release from the matrix to the water, it releases around 10.5 % of nitrogen within 72 hours.

As a result, the matrix that had the least percentage of nitrogen released from the matrix to the water had the least soluble matrix, and the matrix that had a high percentage of nitrogen released from the matrix to the water was highly soluble in the water. From this, a matrix that was synthesized at a temperature of 70 ^{o}c was least soluble than other matrices since as the reaction temperature between ELN/COL and that of LA/CA increased from (50-70) ^{o}c the collusion for the active (reacting) site of a carboxylic group of LA/CA and the amine and hydroxyl group of ELN/COL mixture also increase as a result its hydrophobic property was enhanced with a formation of ester and amide bond through a condensation reaction with the removal of water.

But a further increase in the reaction temperature to 90 ^{o}c was increasing its solubility in water as shown in Figure (4.8) this is due to the denaturation of the ELN/COL mixture, which displayed a higher number of primary amine groups Such an increase in the primary amine groups would increase the hydrophilicity of the ELN/COL-LA/CA matrix as well as lead to bond breakage and degradation (Patel et al., 2013).

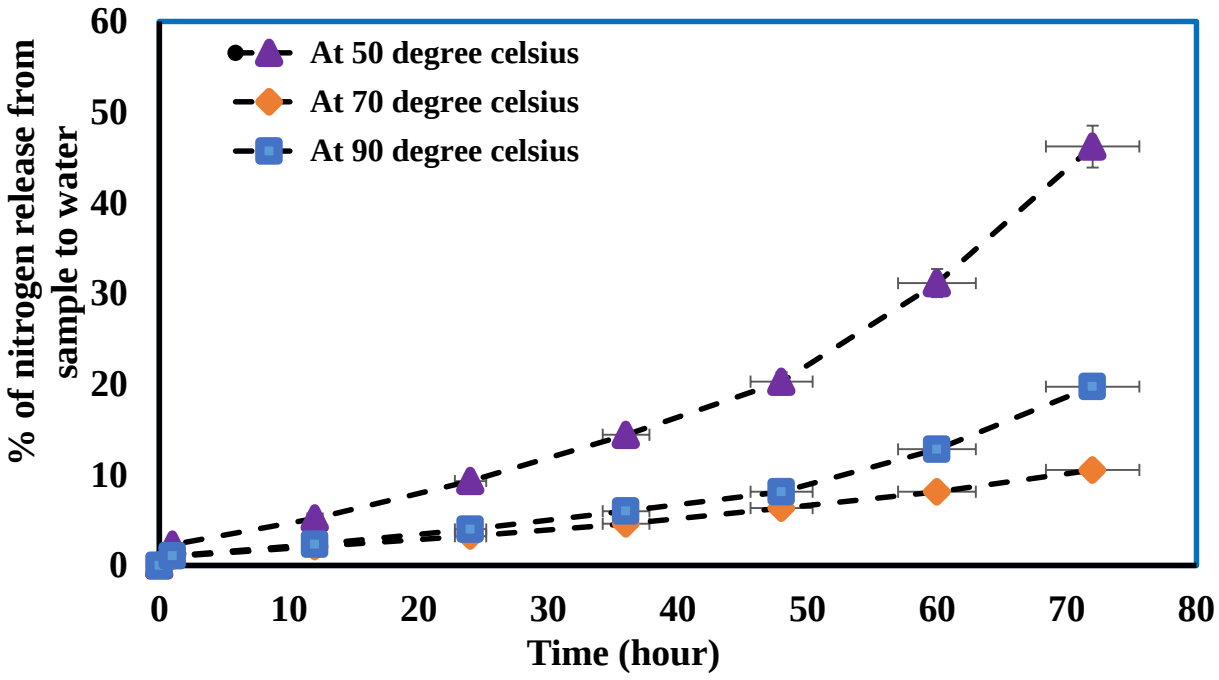

Figure 4.8 Effect of reaction temperature on the percentage of nitrogen released from ELN/COL-LA/CA matrix to water with different time intervals

4.6.3 Effect of lactic acid (LA) to citric acid (CA) ratio on the Solubility of the synthesized ELN/COL-LA/CA matrix in water

From sections 4.6.1 and 4.6.2, the reaction time and temperature which give the least soluble matrix were selected at 4 hours and 70 ^{o}c respectively. To select the lactic acid (LA) to citric acid (CA) ratio for the reaction between the ELN/COL mixture and that of lactic acid and citric acid which gives the least soluble matrix, three different experiments were conducted to select the best lactic acid (LA) to citric acid (CA) ratio.

The experiment was conducted by varying the LA: CA (1:1, 1:1.5, and 1:2) at a fixed reaction time and temperature of 4 hours and 70 ^{o}c respectively, since this was taken according to sections 4.6.1 & 4.6.2 (least soluble matrix were formed at a 4-hour reaction time and 70 ^{o}C). So to select the matrix, which is least soluble in water, a solubility test was conducted by immersing a gram of ELN/COL-LA/CA matrix into the distilled water and a sample was taken by syringe with a different time interval of (1,12,24,36,48,60, and 72) hours, so the amount/percentage of nitrogen released from the matrix to water was determined/measured by the Kjeldahl method (S. S. J. F. A. Nielsen, 2010).

From the results as shown in Figure (4.9) below the percentage of nitrogen released from the matrix to water was greater when LA: CA ratio was 1:1 than 1:1.5 and 1:2 throughout the whole time interval, it releases around 31 % of its nitrogen within 72 hours. But the matrix which was conducted at a LA: CA ratio of 1:1.5 shows the least percentage of nitrogen release from the matrix to the water, it releases around 10.5 % of nitrogen within 72 hours. As a result, the matrix which has the least percentage of nitrogen release from the matrix to the water has the least soluble matrix and which has the high percentage of nitrogen release from the matrix to the water was highly soluble in the water, so the matrix which was conducted at a LA: CA ratio of 1:1.5 was least soluble than other matrix's. From the Figure shown below as the amount of citric acid increased from (1:1 to 1:1.5) ratio, its insolubility also increased. Since increasing the ratio of lactic acid to citric acid means increasing the active functional groups (carboxylic and hydroxyl) which is important in the formation of a highly cross-linked ELN/COL-LA/CA matrix with an enhanced macromolecule network, and hydrophobicity (Miskeen et al., 2021).

But further increasing the lactic acid to citric acid ratio may lead to the presence of unreacted citric acid within it. This leads the matrix to have a high unreacted hydroxyl group as a result it is easily soluble in water (this was supported by the FTIR result in the next section (4.7.3)). To

sum up the solubility test of the ELN/COL-LA/CA matrix, the matrix, which was conducted at a temperature of 70 ^{o}c, a reaction time of 4 hours, and a LA: CA ratio of 1:1.5, was the matrix that was least soluble in the water and this was also supported by FTIR results in the next section (4.7).

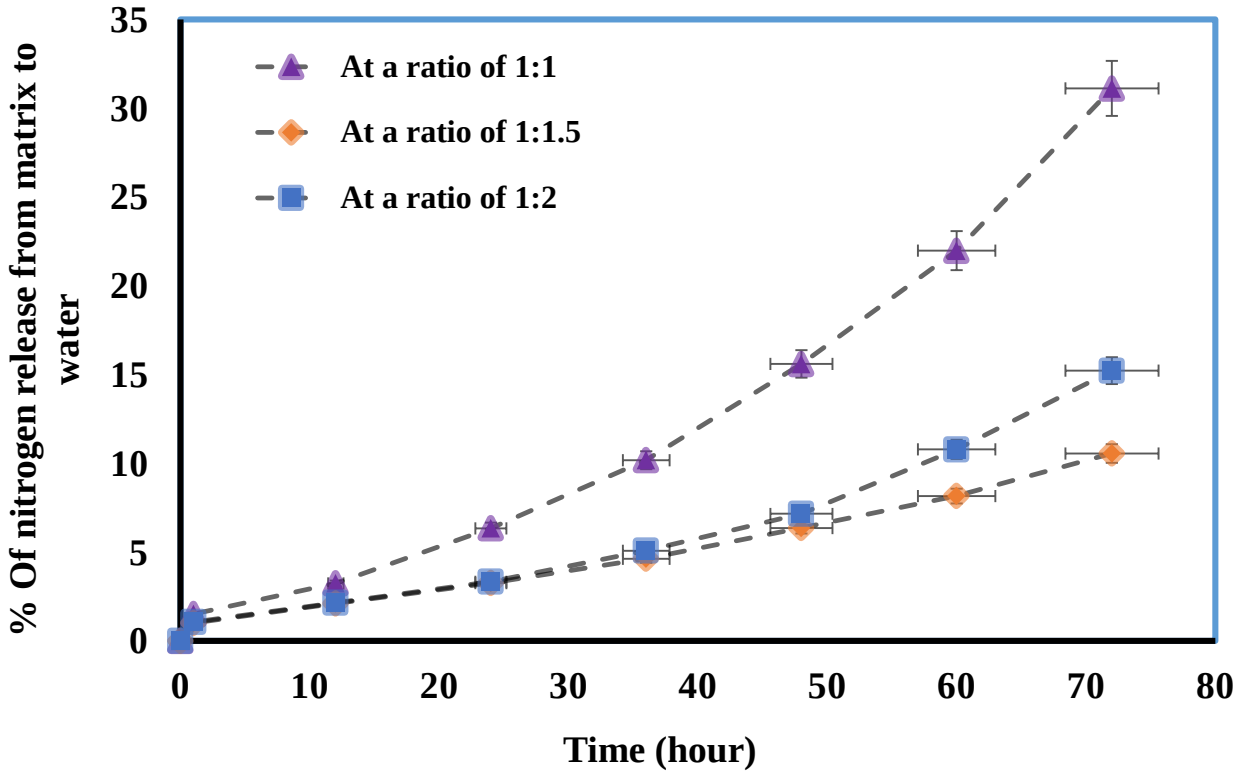

Figure 4.9 Effect of lactic acid to citric acid ratio on the percentage of nitrogen released from ELN/COL-LA/CA matrix to water with different time intervals

4.7 FTIR analysis of ELN/COL-LA/CA matrix which was synthesized under different conditions.

4.7.1 Effect of reaction time on ELN/COL-LA/CA matrix

From the FTIR results, as shown in Figure (4.10) below, there is an O-H stretching within the range of (3500–3300 cm^{-1} peaks) and C=O (ester bond, amide bond) at a wave number of (1740–1750 cm^{-1}) and (1645–1660 cm^{-1}) respectively.

It shows that as the reaction time between the ELN/COL mixture with that of the citric and lactic acid is increased, the broadness and intensity of O-H stretching were decreased, and from those three experimental results, the matrix which was synthesized at a 2-hour reaction time had a

broader O-H peak and the matrix which was synthesized at a 4-hour reaction time showed a less intense O-H peak than the other matrix's.

However, the intensity of C=O (ester and amide bond) was increased according to the table (4.9) as shown below. As the reaction time was increased, the intensity of both the ester and amide bonds for the synthesized matrix was also increased. Their peak intensity was compared by calculating the peak intensity ratio of the bonds by taking –**CH_3** as a baseline. So from the table (4.10), as shown below the peak intensity ratio of both ester and amide bond for the matrix which was done at the reaction time of 4-hour had 5.74 and 1.32 respectively which is greater than that of both of the matrixes which were done at a reaction time 2 and 3 hours.

This phenomenon was happening since, as the reaction time was increased, the contact time for ELN/COL and that of LA/CA also increased. As a result, it favors the formation of both ester and amide bonds between those of ELN/COL and LA/CA through a condensation reaction with the removal of water (O-H peak decrease). This leads the matrix to have more hydrophobic properties as well as improves the strength of the ELN/COL-LA/CA matrix.

So, from the FTIR result, we conclude that the matrix, which was synthesized at a reaction time of 4-hour, shows less O-H stretching and more intense C=O peaks (amide and ester bonds). As a result, it is a more hydrophobic (i.e., less soluble in water) matrix than others.

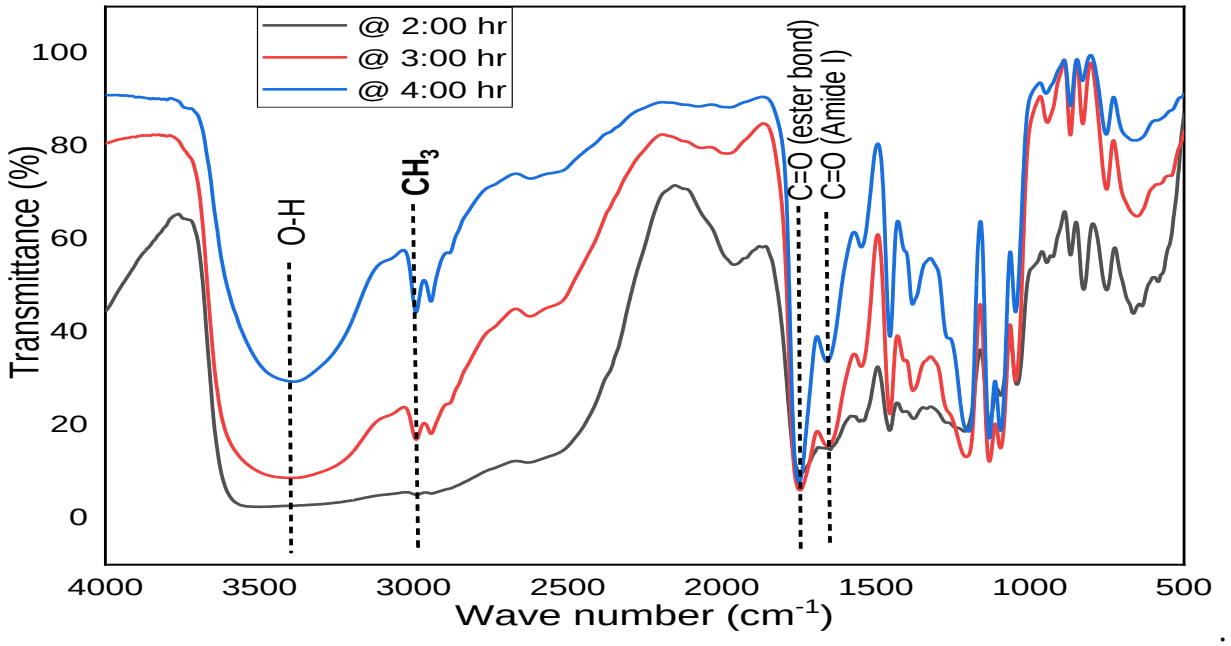

Figure 4.10 FTIR for ELN/COL–LA/CA matrix which was synthesized at different reaction times

Table 4.10 Peak intensity ratio for ester and amide bond for the matrix which was synthesized at different reaction times

Type of matrix	Intensity (%))			peak Intensity ratio = The intensity of CH3 % / The intensity of amide or ester bond	
	-CH_3 (base line)	Ester bond (C=O)	Amide bond (C=O)	Ester bond (C=O)	Amide bond (C=O)
ELN/COL-LA/CA @ 2-hr	5.04	9.81	14.77	0.51	0.34
ELN/COL-LA/CA @ 3-hr	16.87	6.02	15.50	2.80	1.09
ELN/COL-LA/CA @4-hr	44.29	7.72	33.66	5.74	1.32

4.7.2 Effect of temperature on ELN/COL-LA/CA matrix

From the FTIR results, as shown in Figure (4.11) below, there is an O-H stretching within the range of (3500–3300 cm-1 peaks) and C=O (ester bond, amide bond) at a wave number of (1740–1750 cm^{-1}) and (1645–1660 cm^{-1}) respectively.

It shows that as the reaction temperature of the ELN/COL-LA/CA matrix is increased, the broadness and intensity of O-H stretching decrease, and from those three experimental results, the matrix which was synthesized at a temperature of 50 ^{o}c had a broader O-H peak, and the matrix which was done at a reaction temperature of 90 °C shows a less intense O-H peak than the other matrix's. This is because as the reaction temperature increases, the removal of water through condensation reaction also increases (Yoo et al., 2005).

Moreover, the intensity of C=O (ester and amide bond) increases with temperature up to 70 ^{o}c, but further increasing the temperature to 90 °C leads to the decrease of the intensity of both the amide and ester bond. This is due to the breakdown of the C=O bond of both the amide and the ester bond of the matrix. The intensity of both ester and amide bonds for the synthesized matrix was compared according to the table (4.11) shown below by calculating the peak intensity ratio of the bonds by taking –**CH_3** as a baseline. So from the table (4.11), as shown below, the peak intensity ratio of both ester and amide bonds for the matrix which was done at the reaction

temperature of 70 ºC was 5.74 and 1.32, respectively, which is greater than that of both of the matrixes which were done at a reaction temperature of 50 ºC and 90 ºC.

This phenomenon has been happening since, as the reaction temperature was increased, the collusion for the reactants between ELN/COL and that of LA/CA also increased (Tsai et al., 2021). As a result, it favors the formation of both ester and amide bonds between those of ELN/COL and lactic and citric acid through a condensation reaction with the removal of water (O-H peak decrease) up to 70 ºC. This leads the matrix to have more hydrophobic properties as well as improves the strength of the ELN/COL-LA/CA matrix, but further increasing the temperature to 90 ºC may lead to the breakdown of those bonds and make the matrix highly soluble in water.

So, from this result, we conclude that the matrix, which was done at a reaction temperature of 70 ºC, shows moderate O-H stretching and more intense C=O peaks (amide and ester bond). As a result, it is a more hydrophobic (i.e., less soluble in water) matrix than others.

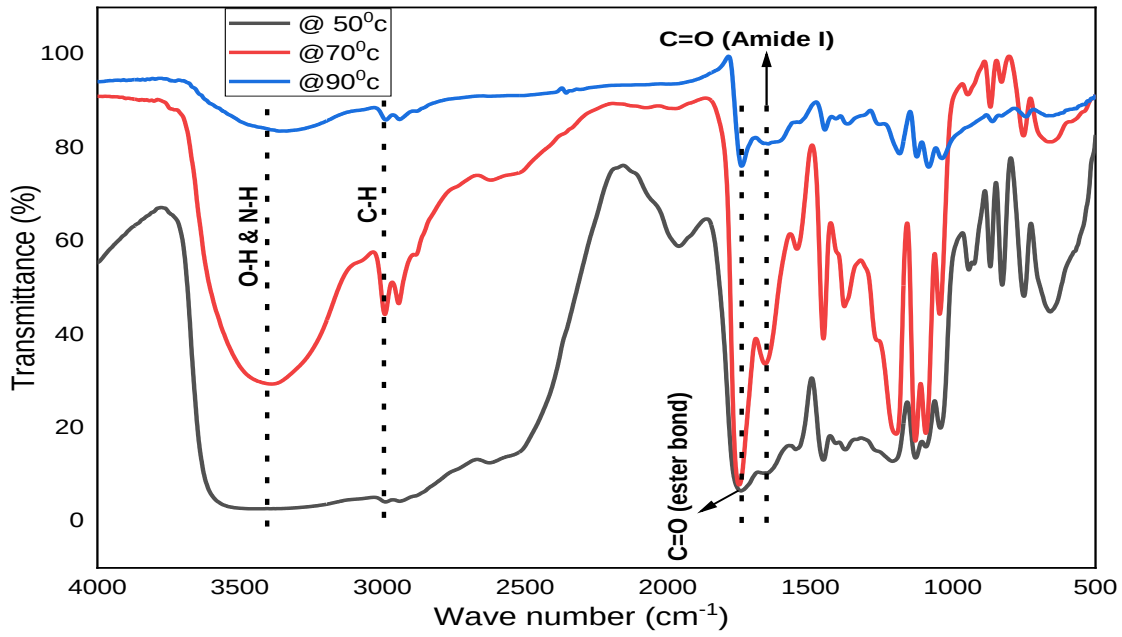

Figure 4.11 FTIR for ELN/COL–LA/CA matrix which was synthesized at a different reaction temperature

Table 4.11 Peak intensity ratio for ester and amide bond for the matrix which was synthesized at different reaction time

Type of matrix	Intensity (%))			peak Intensity ratio = The intensity of CH3 % / The intensity of amide or ester b	
	-CH_3 (base line)	Ester bond (C=O)	Amide bond (C=O)	Ester bond (C=O)	Amide bond (C=O)
ELN/COL-LA/CA @ 50 °c	4.12	6.44	10.32	0.64	0.34
ELN/COL-LA/CA @ 70 °c	44.29	7.72	33.66	5.74	1.32
ELN/COL-LA/CA @ 90 °c	85.92	76.02	80.88	1.13	1.10

4.7.3 Effect of lactic acid (LA) to citric acid (CA) ratio on ELN/COL-LA/CA matrix

From the FTIR results, as shown in Figure (4.12) below, there is an O-H stretching within the range of **(**3500–3300 cm-1 peaks) and C=O (ester bond and amide bond) at a wave number of (1740–1750 cm^{-1}) and (1645–1660 cm^{-1}) respectively, for those three experimental results.

The matrix with lactic acid to a citric acid ratio (LA: CA) of 1:2 shows broader and more intense O-H peaks and less intense C=O peaks than the matrix with a LA: CA ratio of 1:1 and 1:1.5. The intensity of both ester and amide bonds for the synthesized matrix was compared according to the table (4.12) shown below by calculating the peak intensity ratio of the bonds by taking –**CH_3** as a baseline. So from the table (4.12) shown below, the peak intensity ratio of both ester and amide bonds for the matrix which was done at the lactic acid to citric acid ratio of 1:1.5 had 5.74 and 1.32, respectively, which is greater than that of both of the matrix which was synthesized at the lactic acid to citric acid ratio of 1:1 and 1:2.

This was happening since, as the lactic acid to citric acid ratio was increased, the active functional group (carboxylic group) important for the formation of the ester bond with lactic acid grown on the ELN/COL was also increased. As a result, it favors the formation of a highly cross-linked

ELN/COL-LA/CA matrix through a condensation reaction with the removal of water (O-H peak decrease) up to a 1:1.5 ratio. This leads the matrix to have more hydrophobic properties as well as improves the strength of the ELN/COL-LA/CA matrix.

However, further increasing the lactic acid to citric acid ratio may lead to the presence of unreacted/free citric acid within the synthesized ELN/COL-LA/CA matrix. This leads the matrix to have a high hydroxyl group as a result it is easily soluble in water. So from this result, we conclude that the matrix which was synthesized at a 1:1.5 lactic acid to citric acid shows less intense O-H stretching and more intense C=O peaks (amide and ester bond). As a result, it is a more hydrophobic (i.e., less soluble in water) matrix than others.

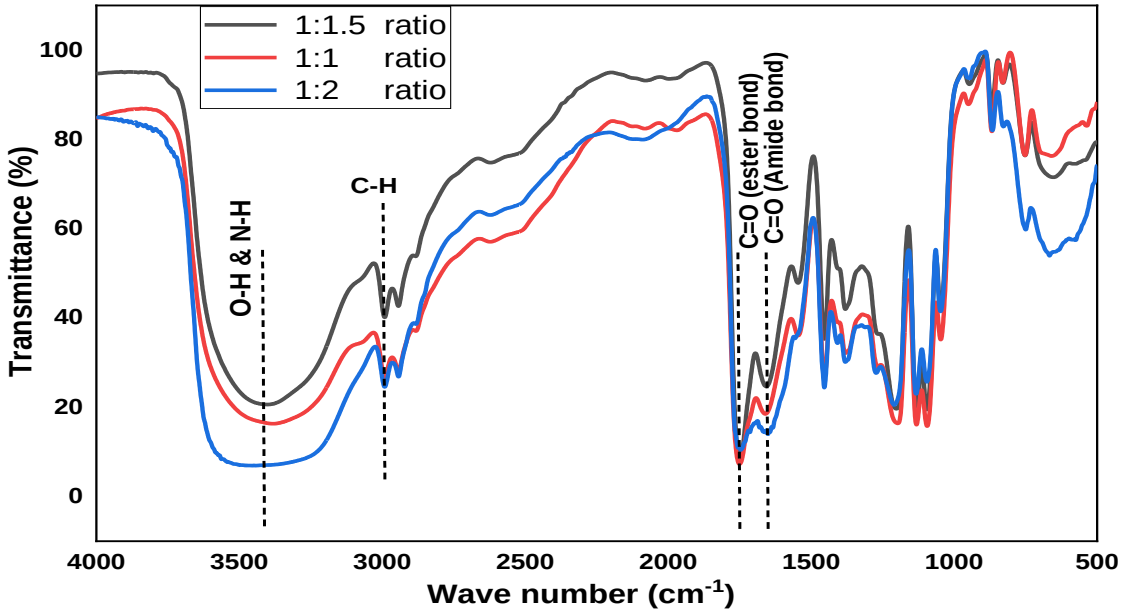

Figure 4.12 FTIR for ELN/COL–LA/CA matrix which was synthesized at a different reaction temperature

Table 4.12 Peak intensity ratio for ester and amide bond for the matrix which was synthesized at different lactic acid to citric acid ratio

Type of matrix	**Intensity (%)**	**peak Intensity ratio =** $\frac{\text{Intensity of CH3 \%}}{\text{Intensity of amide or ester bond}}$

	-CH_3 (base line)	Ester bond (C=O)	Amide bond (C=O)	Ester bond (C=O)	Amide bond (C=O)
ELN/COL-LA/CA @1:1	26.66	7.38	23.87	3.61	1.11
ELN/COL-LA/CA @ 1:1.5	44.29	7.72	33.66	5. 74	1.32
ELN/COL-LA/CA @ 1:2	24.57	10.45	20.13	2.35	1.22

4.8 Water solubility analysis for urea dispersed ELN/COL-LA/CA matrix

Four different samples based on the ratio of ELN/COL-LA/CA matrix to the amount of urea dispersed on it and normal urea were prepared, 1 g of sample from each was added into a beaker containing 200 ml of distilled water. and a sample was taken by syringe with time intervals of (1,6,12,18,24,30,36,42,48,54,60, 66, and 72) hours, so the amount/percentage of nitrogen released from the urea dispersed matrix to water was determined by the Kjeldahl method (S. S. J. F. A. Nielsen, 2010).

From the results as shown in the Figure (4.13) below, the normal urea which has (46% of nitrogen) was released 100% of its nitrogen within 10-minute. The sample S_1 (1:0.5 ratio matrix to urea ratio) which contained 18.88 % of nitrogen within it released around 83.4% of its nitrogen within 72 hours, the sample S_2 (1:1 ratio matrix to urea ratio) which contained 25.66 % of nitrogen within it, released around 90 % of its nitrogen within 54-hour. And also the sample S_3 (1:2 ratio matrix to urea ratio) which contained 32.44 % of nitrogen within it were release around 94% of its nitrogen within 48-hour, further S_4 (1:3 ratio matrix to urea ratio) which has around 35.83 % of nitrogen within it released around 97% of its nitrogen within 18-hour.

So from the result, the solubility of urea dispersed ELN/COL-LA/CA matrix in water was increased as the ratio of ELN/COL–LA/CA and that of urea increased. This is due to the fact that increasing the amount of ELN/COL –LA/CA matrix (cross-linked matrix) was enhancing the polymer's structural integrity against water penetration (Phang et al., 2020). As a whole the release

rate of all the prepared urea dispersed ELN/COL–LA/CA matrix in water was slower than that of the normal urea.

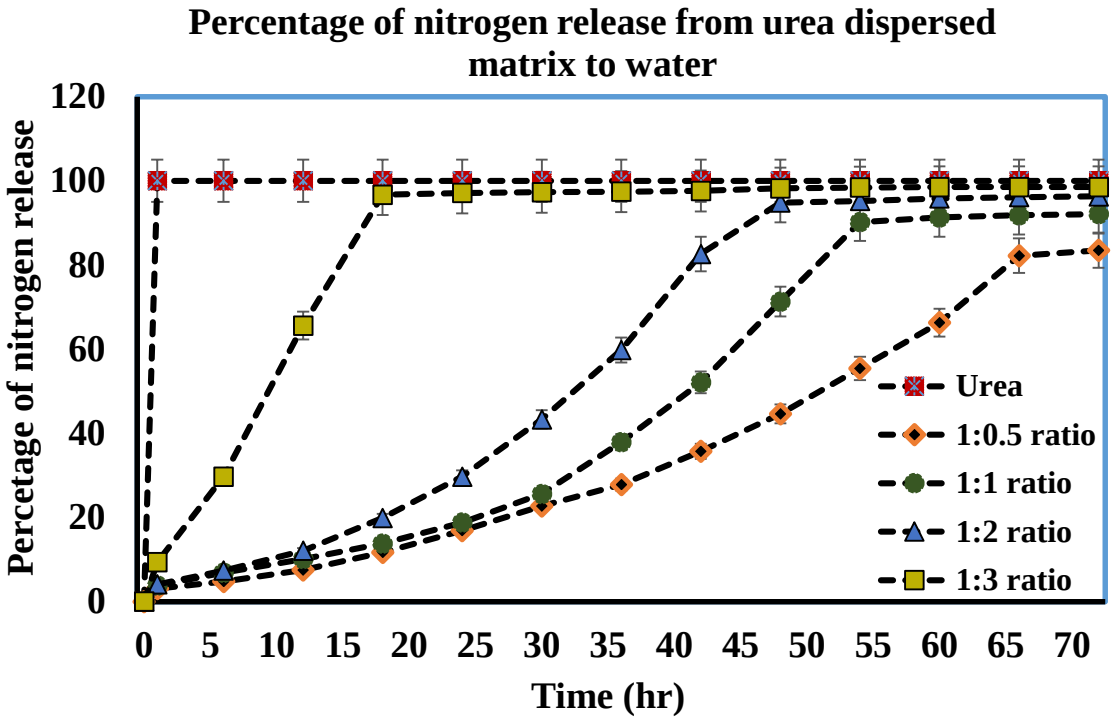

Figure 4.13 Percentage of nitrogen release from urea dispersed ELN/COL–LA/CA matrix and normal urea

4.9 Analysis of the release kinetics/mechanism of nitrogen from urea dispersed ELN/COL –LA/CA matrix

To understand the release behavior /mechanisms of nitrogen for urea dispersed ELN/COL-LA/CA matrix, the Higuchi and the Korsmeyer-Peppas model were applied. The kinetic parameters for all the prepared samples were obtained through a non-linear regression analysis using Microsoft® Excel 2016 Solver Add-in using those models listed in the table (4.13).

Higuchi model equation was developed based on a few hypotheses (Paarakh et al., 2018): i. the diffusion process or pathway is one dimensional; ii. the polymer swelling and dissolution are negligible and iii. the diffusivity is constant. However, the poor ($R^2 < 0.98$) from the non-linear fit of the experimental value obtained from the Higuchi model for all samples, suggests that the release of nitrogen from the urea dispersed ELN/COL–LA/CA matrix should not vary with the square root of time, as with Fickian diffusion indicating the nitrogen release kinetic did not follow

the perfect Fickian's diffusion transportation phenomenon (Xiaoyu et al., 2013). It was clear that the release of nitrogen was governed by other factors such as polymer swelling and dissolution, which, was not reflected in this particular model that was in agreement with the finding from Korsmeyer-Peppas kinetic model (Phang et al., 2020). In all the previous research done by Peppas and his team on drug release behavior by swellable polymer, they stated that the release phenomenon from swellable systems often disagrees with the Higuchi model or the Fickian's behavior, but consists of both diffusions of solute and relaxational swelling of the sample (Peppas & Scott, 1992).

Korsmeyer-Peppas's kinetic model introduced a simple power law model that explained the mixed release mechanism which is linked to multiple factors such as swelling, dissolution, matrix porosity, and erosion of polymeric chain. So from a non-linear regression analysis using Microsoft ®Excel 2016 Solver for the experimental data as shown in table (4.13) for all samples the correlation coefficient (R^2) was ≥ 0.98 for Korsmeyer-Peppas kinetic model. The diffusion exponent (n) for the three samples (S_1, S_2, and S_3) sample was ($n \geq 0.85$) a non-Fickian diffusion, Case II transport mechanism is observed, where the diffusion behavior is dependent on the combination of several factors like matrix dissolution, swelling, with skeleton erosion, decaying of the matrix (Wilmers & Bargmann, 2015). But for the fourth sample (S4) the value of the diffusion exponent was (n=0.75) which follows anomalous transport, and the mechanism of nitrogen release is governed by diffusion and swelling. The diffusion and swelling rates are comparable. The rearrangement of polymeric chains occurring slowly and the diffusion process simultaneously cause the time-dependent anomalous effects (Bruschi, 2015).

Samples with high ELN/COL–LA/CA matrix and lower urea content (S_1), were observed to have a slight law release rate constants (k) for both models as shown in table (4.13) as a result it has longer release period (72 hours) comparing to all other samples. This was attributed to the high cross-linking matrix and hence, enhancing the polymer structural integrity against water penetration (Phang et al., 2020).

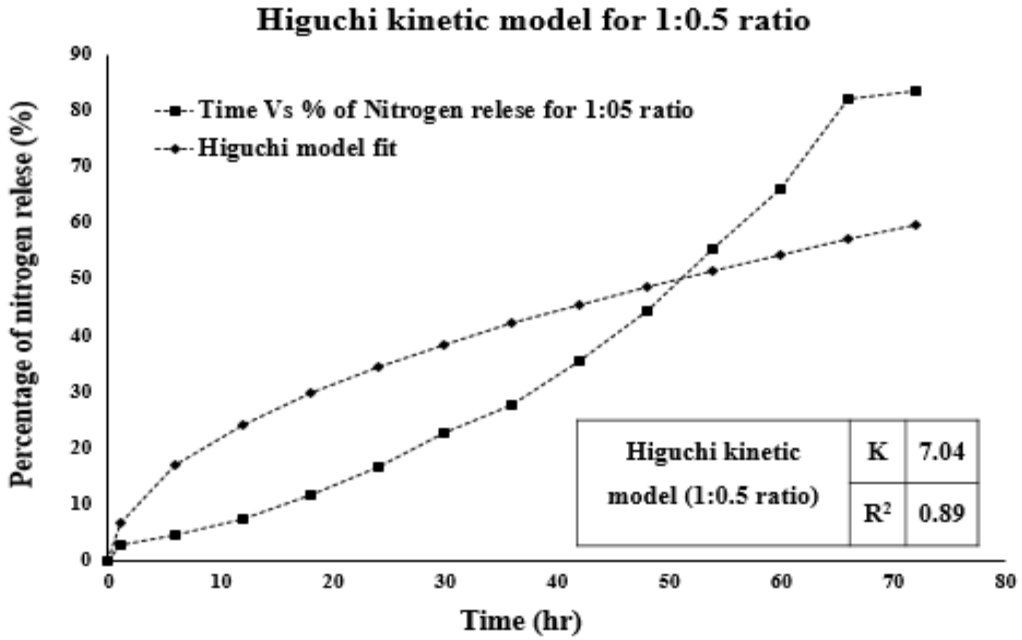

Figure 4.14 Higuchi release kinetic model for a percentage of nitrogen release from S_1 (1:0.5 ratio)

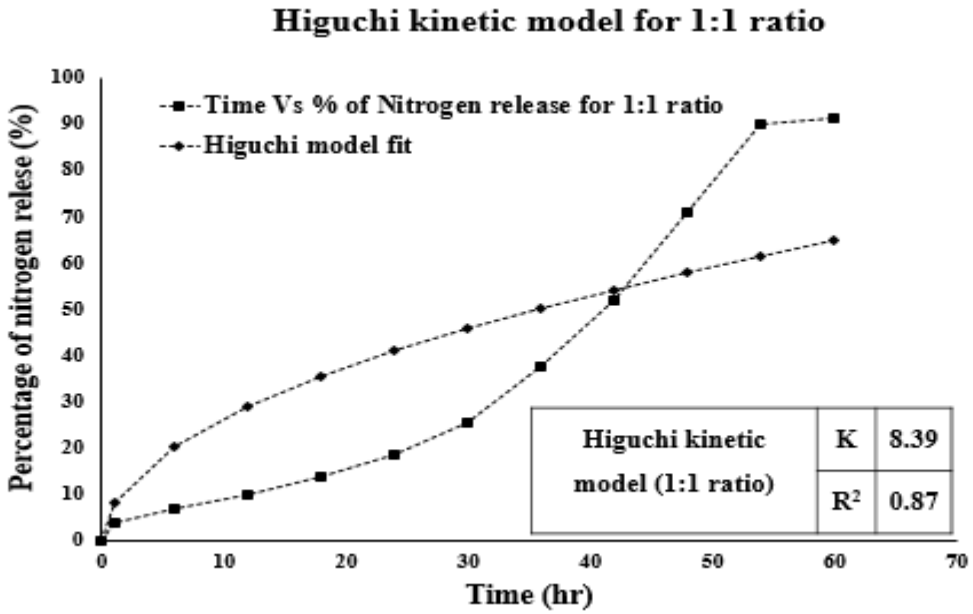

Figure 4.15 Higuchi release kinetic model for a percentage of nitrogen release from S_2 (1:1 ratio)

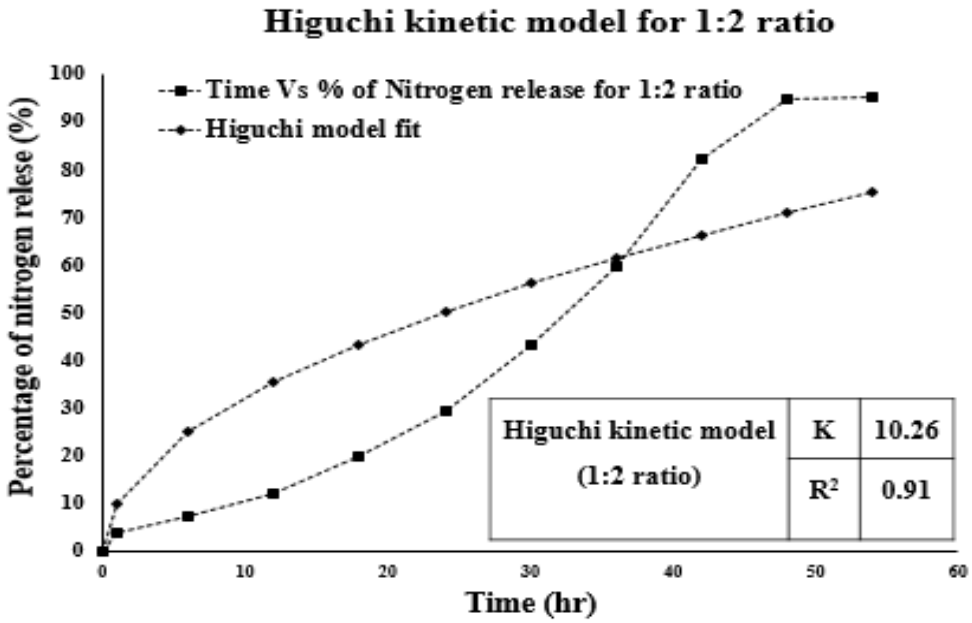

Figure 4.16 Higuchi release kinetic model for a percentage of nitrogen release from S_3 (1:2 ratio)

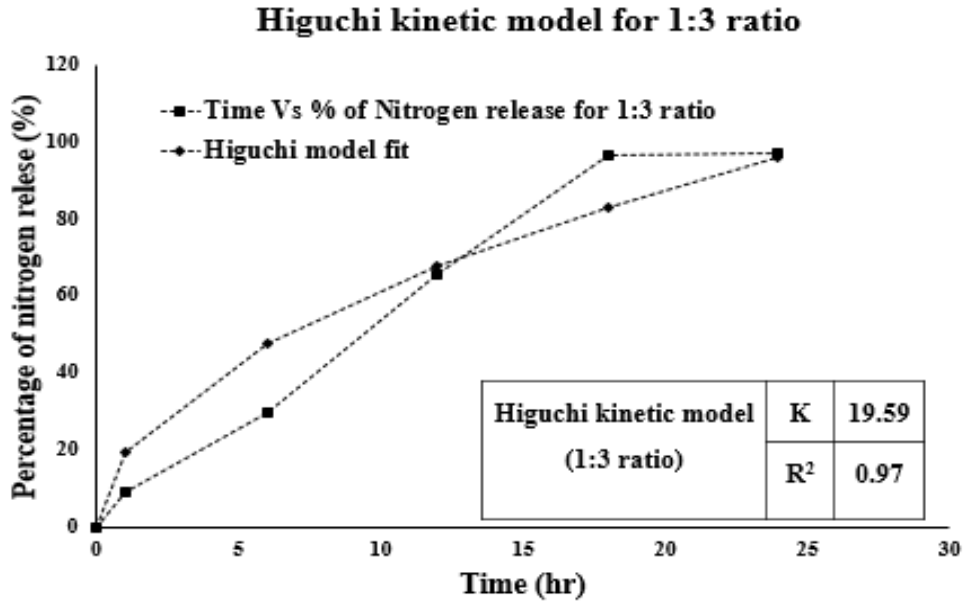

Figure 4.17 Higuchi release kinetic model for a percentage of nitrogen release from S_4 (1:3 ratio)

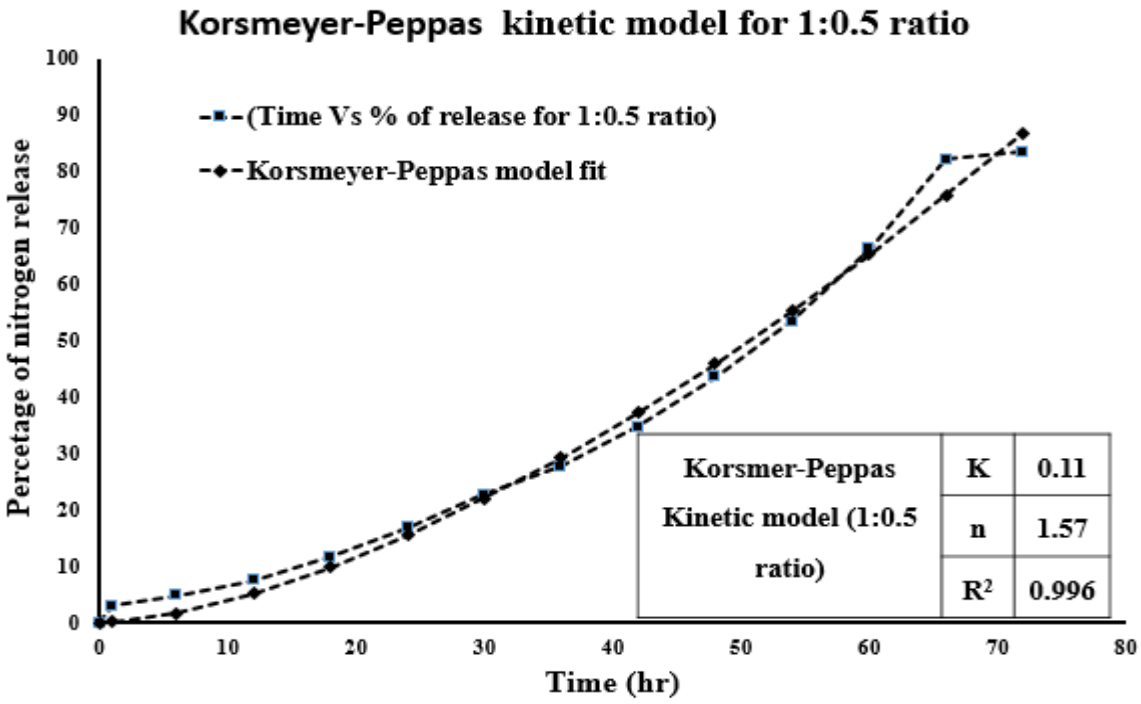

Figure 4.18 Korsmer-Peppas release kinetic model for a percentage of nitrogen release from S_1 (1:0.5 ratio)

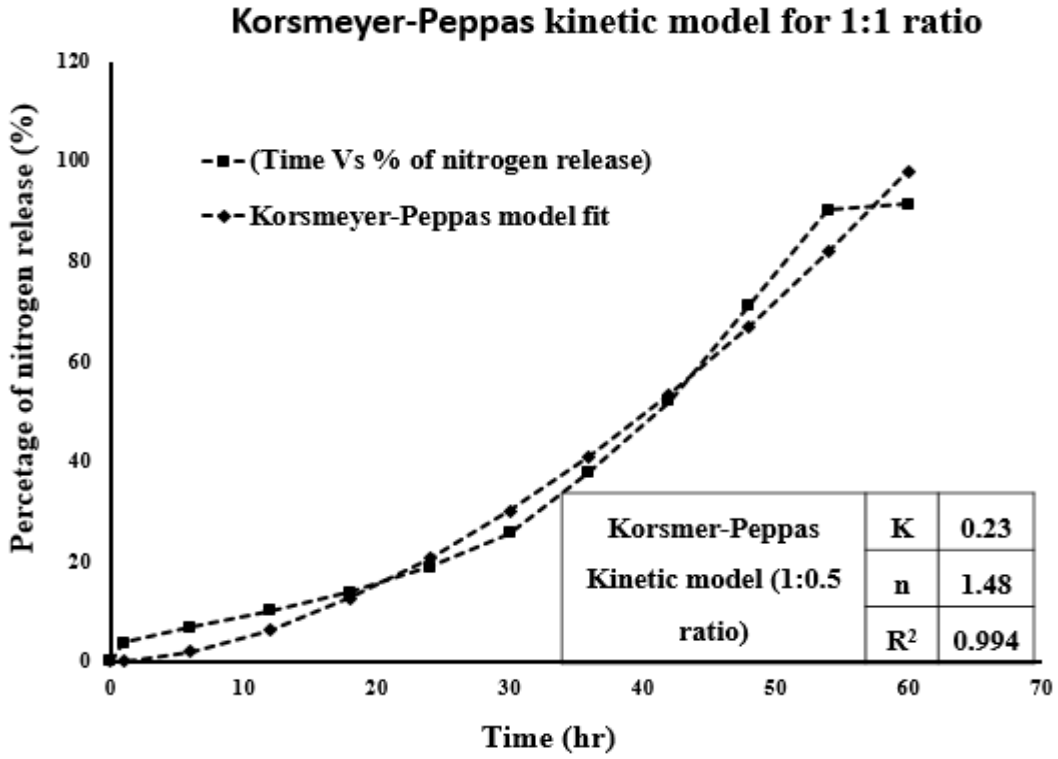

Figure 4.19 Korsmer-Peppas release kinetic model for a percentage of nitrogen release from S_2 (1:1 ratio)

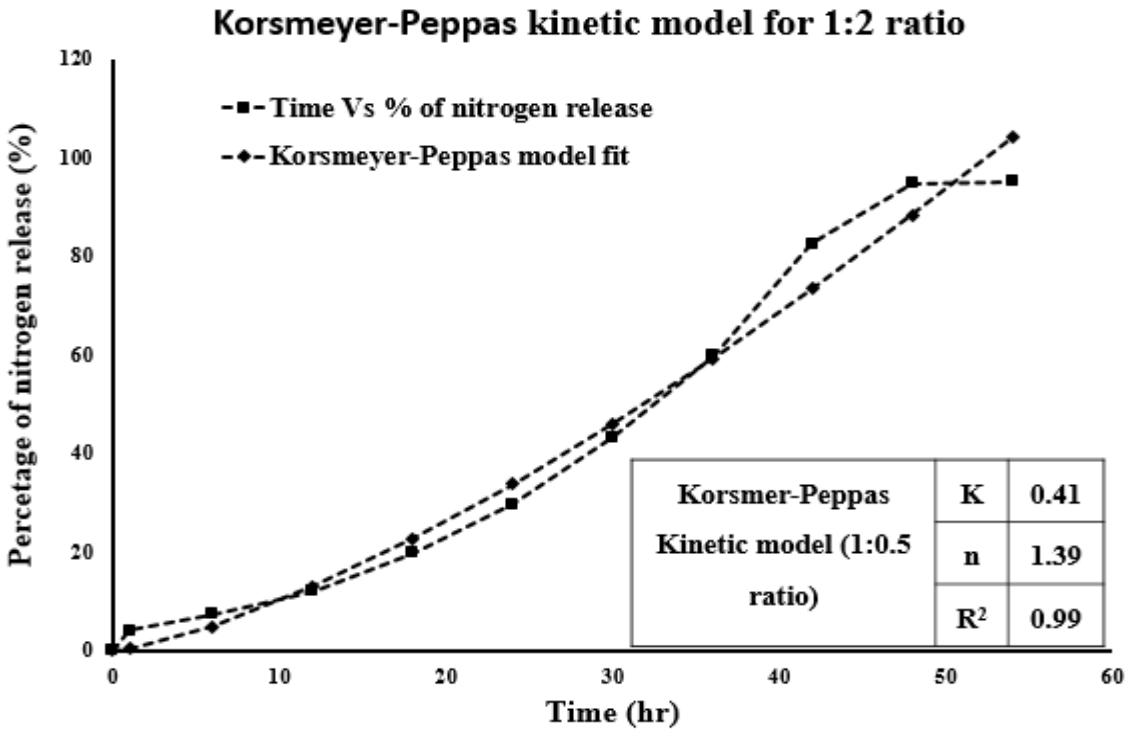

Figure 4.20 Korsmer-Peppas release kinetic model for a percentage of nitrogen release from S_3 (1:2 ratio)

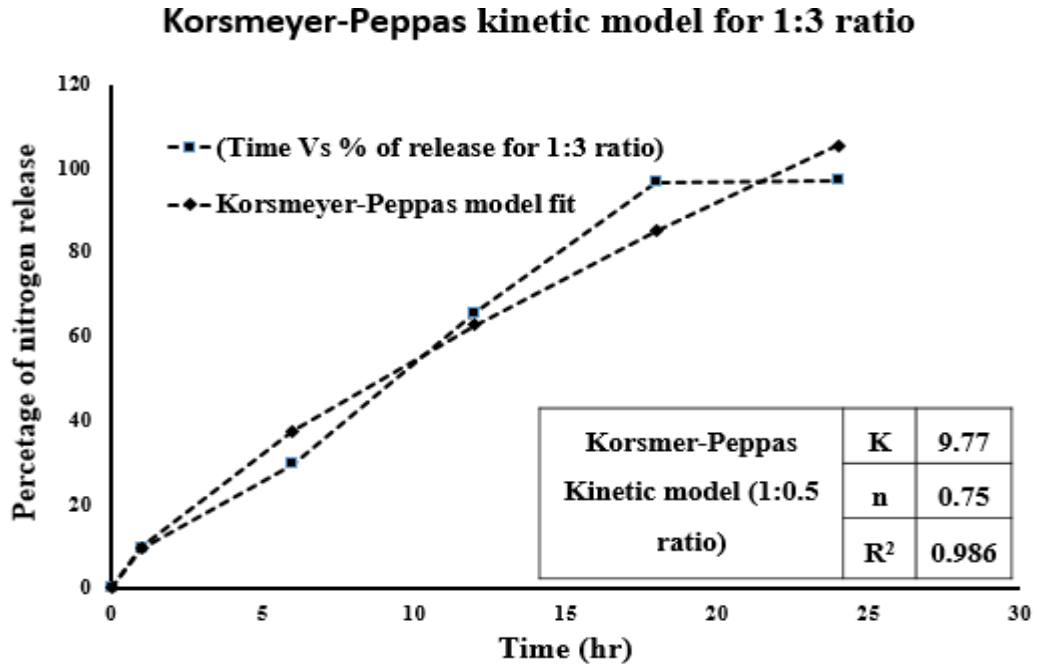

Figure 4.21 Korsmer-Peppas release kinetic model for a percentage of nitrogen release from S_4 (1:3 ratio)

Table 4.13 Kinetic parameters for Higuchi and Korsmeyer-Peppas kinetic model

Type of sample	**Kinetic parameter for Higuchi- model**		**Kinetic parameter for Korsmeyer-Peppas model**		
	K	**R^2**	**k**	**n**	**R^2**
S1 (1:0.5 ratio)	7.04	0.89	0.11	1.57	0.996
S2 (1:1 ratio)	8.39	0.87	0.23	1.48	0.994
S3 (1:2 ratio)	10.26	0.91	0.41	1.39	0.990
S4 (1:3 ratio)	19.59	0.97	9.77	0.75	0.986

5 CONCLUSION AND RECOMMENDATION

5.1 Conclusion

In this research, a least water soluble matrix for urea dispersion was synthesized from elastin/collagen, and that of lactic and citric acid which are bio-based, green, and biocompatible materials was done. Poultry byproducts were used for extracting elastin and collagen mixture. The chemical structure of the extracted ELN/COL mixture was analyzed by FTIR spectroscopy and indicates the amide I, amide II, and amide III groups of elastin and collagen at 1630-1650 cm^{-1}, 1540-1560 cm^{-1}, and 1266-1360 cm^{-1} respectively. To synthesize the least water soluble ELN/COL–LA/CA matrix a condensation reaction of the ELN/COL mixture and that of citric and lactic acid was done by varying the reaction time (2, 3, and 4 hours), the temperature of (50, 70, and 90 ^{o}c), and lactic acid to a citric acid ratio of (1:1, 1:1.5, and 1:2). In order to select the least soluble matrix for urea dispersion, the solubility of the synthesized ELN/COL–LA/CA matrix was performed in distilled water by measuring the percentage of nitrogen release from the matrix to the water with different time interval through Kjeldahl method. So from this result, the matrix which was synthesized at a reaction time of 4 hours, the temperature of 70^{o}c, and lactic acid to citric acid ratio of 1:1.5 released only 10.5 % of its nitrogen within 72 hours, which indicates that the least percentage of nitrogen was released from it to the water than other synthesized matrixes. Moreover, it was further confirmed with FTIR results that the matrix which was synthesized at a reaction time of 4 hours, the temperature of 70^{o}c, and lactic acid to citric acid ratio of 1:1.5 shows less intense O-H peaks and more intense C=O (amide and ester bond), which was formed during the condensation reaction between ELN/COL mixture with that of LA/CA, the formation of this bonds was confirmed with ^{1}H-NMR and ^{13}C-NMR results of ELN/COL– LA/CA matrix. This leads the matrix to have more hydrophobic properties as well as improves the strength of the ELN/COL-LA/CA matrix. Using this least soluble matrix, the urea (which contains 46% of nitrogen) was dispersed on it with ELN/COL–LA/CA matrix to urea ratio of 1:0.5, 1:1, 1:2, and 1:3. Solubility of the urea dispersed ELN/CO–LA/CA matrix for the synthesized sample was performed in distilled water, and its percentage of nitrogen release from the urea dispersed matrix to water was done by Kjeldahl method. From the results of the Kjeldahl method, the percentage of nitrogen release from the urea dispersed matrix to water was 83.5 %, 90%, 95 %, and 97 % for the samples S_1(1:0.5 ratio) within 72 hours, S_2(1:1 ratio) within 54 hours, S_3(1:2 ratio) within 48

hours, and S_4(1:3 ratio) within 18 hours respectively. The solubility of the urea dispersed ELN/COL-LA/CA matrix was increased as the ratio of ELN/COL–LA/CA and that of urea increased. This is due to the fact that increasing the amount of ELN/COL–LA/CA matrix (cross-linked matrix) was enhancing the polymer's structural integrity against water penetration. The percentage of nitrogen release data for the urea dispersed ELN/COL–LA/CA was fitted and compared with two empirical exponential equations models, Higuchi and the Korsmeyer-Peppas to support the interpretation and comprehension of the release mechanisms. The nitrogen release kinetic for urea dispersed ELN/CO–LA/CA matrix was found to have a good Korsmeyer-Peppas model fitting at an R^2 value of more than 0.98. The diffusion exponent (n) for the three samples (S_1, S_2, and S_3) sample was ($n \geq 0.85$) a non-Fickian diffusion, Case II transport mechanism is observed, where the diffusion behavior is dependent on the combination of several factors like matrix dissolution, swelling, with skeleton erosion, decaying of the matrix. But for the fourth sample (S_4) the value of the diffusion exponent was (n=0.75) which follows anomalous transport, and the mechanism of nitrogen release is governed by diffusion and swelling. From the obtained result, it can be concluded that the synthesized ELN/COL–LA/CA matrix can be used for the slow delivery of urea fertilizer.

5.2 Recommendation

For future work, the following recommendations are suggested based on the result obtained from this study.

- ✓ It is recommended that study the nitrogen release mechanism and kinetics for the urea dispersed ELN/COL- LA/CA matrix within the soil.
- ✓ In this work, the solubility study as well as its release mechanism of the urea dispersed ELN/COL–LA/CA matrix was conducted within distilled water (neutral pH). But a further study on the solubility of the urea dispersed ELN/COL–LA/CA matrix at different pH (acidic and basic), and salty conditions will be needed.
- ✓ Moreover, dispersion of NPK fertilizers within the synthesized ELN/COL–LA/CA matrix, and study of its solubility, and release mechanisms within water (neutral pH, acidic pH, basic pH, and salty water) will also be recommended.
- ✓ Furthermore, field test experiments for the synthesized urea dispersed ELN/COL–LA/CA matrix will be recommended for future work.

REFERENCE

Abdel-Basset, M., Mohamed, R., Zaied, A. E.-N. H., Gamal, A., & Smarandache, F. (2020). Solving the supply chain problem using the best-worst method based on a novel Plithogenic model. In *Optimization theory based on neutrosophic and plithogenic sets* (pp. 1-19). Elsevier.

Abdulkhani, A., Hosseinzadeh, J., Ashori, A., Dadashi, S., & Takzare, Z. J. P. t. (2014). Preparation and characterization of modified cellulose nanofibers reinforced polylactic acid nanocomposite. *35*, 73-79.

Ahmad, A., Banat, F., Taher, H. J. E. T., & Innovation. (2020). A review on the lactic acid fermentation from low-cost renewable materials: Recent developments and challenges. *20*, 101138.

Andersen, N. H. (2001). Protein Structure, Stability, and Folding. Methods in Molecular Biology. Volume 168 Edited by Kenneth P. Murphy (University of Iowa College of Medicine). Humana Press: Totowa, New Jersey. 2001. ix+ 252 pp. $89.50. ISBN 0-89603-682-0. In: ACS Publications.

Ariyanti, S., Man, Z., & Bustam, M. A. (2013). Improvement of hydrophobicity of urea modified tapioca starch film with lignin for slow release fertilizer. Advanced Materials Research,

Babadi, F. E., Yunus, R., Rashid, S. A., Salleh, M. A. M., & Ali, S. J. P. (2015). New coating formulation for the slow release of urea using a mixture of gypsum and dolomitic limestone. *23*, 62-67.

Bailey, R. J. T. C. t. c. p.-s.-. (2018). Learn about the 4 types of protein structure.

Beig, B., Niazi, M. B. K., Jahan, Z., Hussain, A., Zia, M. H., & Mehran, M. T. J. J. o. p. n. (2020). Coating materials for slow release of nitrogen from urea fertilizer: A review. *43*(10), 1510-1533.

Beig, B., Niazi, M. B. K., Jahan, Z., Pervaiz, E., Abbas Shah, G., Ul Haq, M., . . . Zia, M. J. S. (2020). Slow-release urea prills developed using organic and inorganic blends in fluidized bed coater and their effect on spinach productivity. *12*(15), 5944.

Bhattarai, N., Ramay, H. R., Chou, S.-H., & Zhang, M. J. I. j. o. n. (2006). Chitosan and lactic acid-grafted chitosan nanoparticles as carriers for prolonged drug delivery. *1*(2), 181.

Bi, S., Barinelli, V., & Sobkowicz, M. J. J. P. (2020). Degradable controlled release fertilizer composite prepared via extrusion: Fabrication, characterization, and release mechanisms. *12*(2), 301.

Bortoletto-Santos, R., Cavigelli, M. A., Montes, S. E., Schomberg, H. H., Le, A., Thompson, A. I., . . . Ribeiro, C. J. J. o. C. P. (2020). Oil-based polyurethane-coated urea reduces nitrous oxide emissions in a corn field in a Maryland loamy sand soil. *249*, 119329.

Bravo-Anaya, L. M., Garbay, B., Nando-Rodríguez, J. L., Ramos, F. C., Ibarboure, E., Bathany, K., . . . science, i. (2019). Nucleic acids complexation with cationic elastin-like polypeptides: Stoichiometry and stability of nano-assemblies. *557*, 777-792.

Brown, J. C., Timpl, R. J. I. a. o. a., & immunology. (1995). The collagen superfamily. *107*(4), 484-490.

Bruschi, M. L. J. S. t. m. t. d. r. f. p. s. (2015). Mathematical models of drug release. In (Vol. 63, pp. 63-86): Woodhead Publishing Cambridge, UK.

Cappello, J., Crissman, J., Crissman, M., Ferrari, F., Textor, G., Wallis, O., . . . Aukerman, L. J. J. o. C. R. (1998). In-situ self-assembling protein polymer gel systems for administration, delivery, and release of drugs. *53*(1-3), 105-117.

Chattopadhyay, S., & Raines, R. T. J. B. (2014). Collagen-based biomaterials for wound healing. *101*(8), 821-833.

Chen, L., Xie, Z., Zhuang, X., Chen, X., & Jing, X. J. C. p. (2008). Controlled release of urea encapsulated by starch-g-poly (L-lactide). *72*(2), 342-348.

Cheng, F.-Y., Hsu, F.-W., Chang, H.-S., Lin, L.-C., & Sakata, R. J. F. C. (2009). Effect of different acids on the extraction of pepsin-solubilised collagen containing melanin from silky fowl feet. *113*(2), 563-567.

Cheon, H. Protein structure and function: A review with application.

Ciriminna, R., Meneguzzo, F., Delisi, R., & Pagliaro, M. J. C. C. J. (2017). Citric acid: emerging applications of key biotechnology industrial product. *11*(1), 1-9.

Coma, V., Sebti, I., Pardon, P., Pichavant, F., & Deschamps, A. J. C. p. (2003). Film properties from crosslinking of cellulosic derivatives with a polyfunctional carboxylic acid. *51*(3), 265-271.

Cozzone, A. J. J. E. o. L. S. N. m. l. J. W., & Ltd, S. (2002). Proteins: Fundamental chemical properties. 1-10.

Cui, Y., Xiang, Y., Xu, Y., Wei, J., Zhang, Z., Li, L., & Li, J. J. I. j. o. b. m. (2020). Poly-acrylic acid grafted natural rubber for multi-coated slow release compound fertilizer: Preparation, properties and slow-release characteristics. *146*, 540-548.

Di Lullo, G. A., Sweeney, S. M., Korkko, J., Ala-Kokko, L., & San Antonio, J. D. J. J. o. B. C. (2002). Mapping the ligand-binding sites and disease-associated mutations on the most abundant protein in the human, type I collagen. *277*(6), 4223-4231.

Dubey, A., Mailapalli, D. R. J. E. T., & Innovation. (2019). Zeolite coated urea fertilizer using different binders: Fabrication, material properties and nitrogen release studies. *16*, 100452.

Dugas, H., & Penney, C. (2013). *Bioorganic chemistry: a chemical approach to enzyme action*. Springer Science & Business Media.

Elavarasan, K., Shamasundar, B. A. J. J. o. f. s., & technology. (2016). Effect of oven drying and freeze drying on the antioxidant and functional properties of protein hydrolysates derived from freshwater fish (Cirrhinus mrigala) using papain enzyme. *53*(2), 1303-1311.

Emami, N., Razmjou, A., Noorisafa, F., Korayem, A. H., Zarrabi, A., Ji, C. J. E. n., monitoring, & management. (2017). Fabrication of smart magnetic nanocomposite asymmetric membrane capsules for the controlled release of nitrate. *8*, 233-243.

Espartero, J., Rashkov, I., Li, S., Manolova, N., & Vert, M. J. M. (1996). NMR analysis of low molecular weight poly (lactic acid) s. *29*(10), 3535-3539.

Exposito, J. Y., Cluzel, C., Garrone, R., & Lethias, C. J. T. A. R. A. O. P. o. t. A. A. o. A. (2002). Evolution of collagens. *268*(3), 302-316.

Faury, G. J. P. B. (2001). Function–structure relationship of elastic arteries in evolution: from microfibrils to elastin and elastic fibres. *49*(4), 310-325.

Feng, C.-X., & Wang, X.-F. J. I. T. (2003). Surface roughness predictive modeling: neural networks versus regression. *35*(1), 11-27.

Fermi, G., Perutz, M. F., Shaanan, B., & Fourme, R. J. J. o. m. b. (1984). The crystal structure of human deoxyhaemoglobin at 1.74 Å resolution. *175*(2), 159-174.

Glusker, J. P. J. A. o. C. R. (1980). Citrate conformation and chelation: enzymic implications. *13*(10), 345-352.

Goldberga, I., Li, R., & Duer, M. J. J. A. o. c. r. (2018). Collagen structure–function relationships from solid-state NMR spectroscopy. *51*(7), 1621-1629.

Hepler, J. R., & Gilman, A. G. J. T. i. b. s. (1992). G proteins. *17*(10), 383-387.

Hermida, L., Agustian, J. J. E. T., & Innovation. (2019). Slow release urea fertilizer synthesized through recrystallization of urea incorporating natural bentonite using various binders. *13*, 113-121.

Hoshide, A. K. (2005). *Re-integrating crops and livestock in Maine: an economic analysis of the potential for and profitability of integrated agricultural production*. The University of Maine.

Kanagaraj, J., Velappan, K., Babu, N., & Sadulla, S. (2006). Solid wastes generation in the leather industry and its utilization for cleaner environment-A review.

Khandey, N. S., Anurag, R., Sengar, S., & Kumar, R. J. I. C. S. (2017). Response of applied neem coated urea (NCU) on yield and yield attributing parameters of rice (Oryza sativa L) in Vertisol. *5*, 1670-1675.

Kibret, M. E., Temesgen, T., & Tesfaye, M. J. H. In-situ oligomerization of lactic acid within broiler skin extracted elastin/collagen matrix for the efficacy of ointment base.

Kurt, A. (2015). Investigation of plant derived substances that promote the biosynthesis of collagen; development of cosmetic and dermatological skin care products.

Lateef, A., Nazir, R., Jamil, N., Alam, S., Shah, R., Khan, M. N., . . . Materials, M. (2016). Synthesis and characterization of zeolite based nano–composite: an environment friendly slow release fertilizer. *232*, 174-183.

Lee, S. H., Md Tahir, P., Lum, W. C., Tan, L. P., Bawon, P., Park, B.-D., . . . Abdullah, U. H. J. P. (2020). A review on citric acid as green modifying agent and binder for wood. *12*(8), 1692.

Leghari, S. J., Wahocho, N. A., Laghari, G. M., HafeezLaghari, A., MustafaBhabhan, G., HussainTalpur, K., . . . Lashari, A. A. J. A. i. E. B. (2016). Role of nitrogen for plant growth and development: A review. *10*(9), 209-219.

Levitt, M., & Chothia, C. J. N. (1976). Structural patterns in globular proteins. *261*(5561), 552-558.

Li, Y., Jia, C., Zhang, X., Jiang, Y., Zhang, M., Lu, P., & Chen, H. J. P. i. O. C. (2018). Synthesis and performance of bio-based epoxy coated urea as controlled release fertilizer. *119*, 50-56.

Liu, B. W., Zhao, H. B., & Wang, Y. Z. J. A. M. (2021). Advanced Flame-Retardant Methods for Polymeric Materials. 2107905.

Lubkowski, K. J. P. J. o. C. T. (2016). Environmental impact of fertilizer use and slow release of mineral nutrients as a response to this challenge. *18*(1).

Mann, M., Kruger, J. E., Andari, F., McErlean, J., Gascooke, J. R., Smith, J. A., . . . chemistry, b. (2019). Sulfur polymer composites as controlled-release fertilisers. *17*(7), 1929-1936.

Mesias, V. S. D., Agu, A. B. S., Benablo, P. J. L., Chen, C.-H., & Penaloza Jr, D. P. J. J. o. E. E. (2019). Coated NPK fertilizer based on citric acid-crosslinked chitosan/alginate encapsulant. *20*(11).

Miskeen, S., An, Y. S., & Kim, J.-Y. J. I. J. o. B. M. (2021). Application of starch nanoparticles as host materials for encapsulation of curcumin: Effect of citric acid modification. *183*, 1-11.

Murray, J., Laurieri, N., Delgoda, R. J. P. F., Applications, & Strategies. (2017). Chapter 24. Proteins. 477-494.

Nadalian, M., Yusop, S. M., Babji, A. S., Mustapha, W. A. W., Najafian, L., & Azman, M. A. J. t. I. C. M. S. T. I.-T.-A. (2013). Extraction and Characterization of Water-soluble Elastin from Spent Hen and Broiler Skin. 1-3.

Nielsen, S. (2010). Food Analysis/edited by S. Suzanne Nielsen. In: New York.

Nielsen, S. S. J. F. A. (2010). Food analysis fourth edition.

Niu, Y., Li, H. J. I., & Research, E. C. (2012). Controlled release of urea encapsulated by starch-g-poly (vinyl acetate). *51*(38), 12173-12177.

Paarakh, M. P., Jose, P. A., Setty, C., & Christoper, G. J. I. J. P. R. T. (2018). Release kinetics–concepts and applications. *8*(1), 12-20.

Patel, N. U., Purser, C. A., Baker, R. C., & Janorkar, A. V. J. B. (2013). Effect of Processing Temperature on the Morphology and Drug-Release Characteristics of Elastin-Like Polypeptide–Collagen Composite Coatings. *14*(8), 2891-2899.

Patwa, R., Saha, N., Sáha, P., & Katiyar, V. J. J. o. A. P. S. (2019). Biocomposites of poly (lactic acid) and lactic acid oligomer-grafted bacterial cellulose: It's preparation and characterization. *136*(35), 47903.

Paul, D. J. I. j. o. p. (2011). Elaborations on the Higuchi model for drug delivery. *418*(1), 13-17.

Peppas, N. A., & Scott, J. E. J. J. o. c. r. (1992). Controlled release from poly (vinyl alcohol) gels prepared by freezing-thawing processes. *18*(2), 95-100.

Phang, S. W., Sin, L. T., Bee, S.-T., & Tee, T.-T. (2020). Release kinetic model of nitrogen released encapsulated in starch-alginate controlled released urea: Diffusion and its decay release. AIP Conference Proceedings,

Poerwono, H., Higashiyama, K., Kubo, H., Achmad Toto Poernomo, N., Sudiana, I. K., Indrayanto, G., & Brittain, H. G. (2001). Citric acid.

Qi, X., Guo, Y., Chen, Q., Zhao, X., & Ao, X. J. J. o. A. P. S. (2022). Preparation and performance of a kitchen waste oil-modified polyvinyl alcohol-grafted urea slow-release fertilizer. *139*(2), 51484.

Ramshaw, J. A., Shah, N. K., & Brodsky, B. J. J. o. s. b. (1998). Gly-XY tripeptide frequencies in collagen: a context for host–guest triple-helical peptides. *122*(1-2), 86-91.

Ravishankara, A., Daniel, J. S., & Portmann, R. W. J. s. (2009). Nitrous oxide (N2O): the dominant ozone-depleting substance emitted in the 21st century. *326*(5949), 123-125.

Rawat, J., Sanwal, P., & Saxena, J. (2016). Potassium and its role in sustainable agriculture. In *Potassium solubilizing microorganisms for sustainable agriculture* (pp. 235-253). Springer.

Reyes-Escobar, J., Zagal, E., Sandoval, M., Navia, R., & Muñoz, C. J. S. (2015). Development of a biochar-plant-extract-based nitrification inhibitor and its application in field conditions. *7*(10), 13585-13596.

Ruszczak, Z., & Friess, W. J. A. d. d. r. (2003). Collagen as a carrier for on-site delivery of antibacterial drugs. *55*(12), 1679-1698.

Salam, A. (2015). *The Synthesis, Characterization, and Application of Polysaccharides-Based Additives to Increase the Dry Strength of Paper*. North Carolina State University.

Sánchez-García, M., Roig, A., Sánchez-Monedero, M. A., & Cayuela, M. L. J. F. i. E. S. (2014). Biochar increases soil N2O emissions produced by nitrification-mediated pathways. *2*, 25.

Savci, S. J. A. P. (2012). Investigation of effect of chemical fertilizers on environment. *1*, 287-292.

Sedano-Castro, G., González-Hernández, V. A., Saucedo-Veloz, C., Soto-Hernández, M., Sandoval-Villa, M., & Carrillo-Salazar, J. A. J. T. L. (2011). Yield and Quality of Zucchini Fruits on High Doses of N and K. *29*(2), 133-142.

Shaviv, A. (2001). Advances in controlled-release fertilizers.

Shoulders, M. D., & Raines, R. T. J. A. r. o. b. (2009a). Collagen structure and stability. *78*, 929-958.

Shoulders, M. D., & Raines, R. T. J. A. r. o. b. (2009b). Collagen structure and stability. *78*, 929.

Skopinska-Wisniewska, J., Bajek, A., Maj, M., & Sionkowska, A. J. P. f. A. T. (2017). PEG-dialdehyde–the new cross-linking agent for collagen/elastin hydrogels. *28*(6), 763-767.

Souri, M. K., Naiji, M., & Kianmehr, M. H. J. J. o. p. n. (2019). Nitrogen release dynamics of a slow release urea pellet and its effect on growth, yield, and nutrient uptake of sweet basil (Ocimum basilicum L.). *42*(6), 604-614.

Tayyab, S., & Boyce, A. N. (2006). *A journey from amino acids to proteins*. University of Malaya press.

Tesfaye, M., Patwa, R., Dhar, P., & Katiyar, V. J. A. o. (2017). Nanosilk-grafted poly (lactic acid) films: influence of cross-linking on rheology and thermal stability. *2*(10), 7071-7084.

Torres-Olivar, V., Villegas-Torres, O. G., Domínguez-Patiño, M. L., Sotelo-Nava, H., Rodríguez-Martínez, A., Melgoza-Alemán, R. M., . . . B, T. (2014). Role of nitrogen and nutrients in crop nutrition. *4*(1B), 29.

Trabbic-Carlson, K., Setton, L. A., & Chilkoti, A. J. B. (2003). Swelling and mechanical behaviors of chemically cross-linked hydrogels of elastin-like polypeptides. *4*(3), 572-580.

Tsai, Y.-T., Huang, C.-W., & Yu, S.-S. J. P. C. C. P. (2021). The effect of temperature on the kinetics of enhanced amide bond formation from lactic acid and valine driven by deep eutectic solvents. *23*(48), 27498-27507.

UN, U. J. P. D. (2017). Department of Economic and Social Affairs.

Varani, J., Dame, M. K., Rittie, L., Fligiel, S. E., Kang, S., Fisher, G. J., & Voorhees, J. J. J. T. A. j. o. p. (2006). Decreased collagen production in chronologically aged skin: roles of age-dependent alteration in fibroblast function and defective mechanical stimulation. *168*(6), 1861-1868.

Versino, F., Urriza, M., & García, M. A. J. I. j. o. b. m. (2019). Eco-compatible cassava starch films for fertilizer controlled-release. *134*, 302-307.

Wang, C.-C., & Chen, C.-C. J. A. C. A. G. (2005). Physical properties of the crosslinked cellulose catalyzed with nanotitanium dioxide under UV irradiation and electronic field. *293*, 171-179.

Wang, Q., He, H., Li, B., Lin, H., Zhang, Y., Zhang, J., & Wang, Z. J. P. o. (2017). UV–Vis and ATR–FTIR spectroscopic investigations of postmortem interval based on the changes in rabbit plasma. *12*(7), e0182161.

Wei, H., Wang, H., Chu, H., & Li, J. J. I. j. o. b. m. (2019). Preparation and characterization of slow-release and water-retention fertilizer based on starch and halloysite. *133*, 1210-1218.

Wen, Q., Mithieux, S. M., & Weiss, A. S. J. T. i. b. (2020). Elastin biomaterials in dermal repair. *38*(3), 280-291.

Wilmers, J., & Bargmann, S. J. E. J. o. M.-A. S. (2015). A continuum mechanical model for the description of solvent induced swelling in polymeric glasses: Thermomechanics coupled with diffusion. *53*, 10-18.

Xiaoyu, N., Yuejin, W., Zhengyan, W., Lin, W., Guannan, Q., & Lixiang, Y. J. B. e. (2013). A novel slow-release urea fertiliser: Physical and chemical analysis of its structure and study of its release mechanism. *115*(3), 274-282.

Xie, J., Yang, Y., Gao, B., Wan, Y., Li, Y. C., Cheng, D., . . . Xu, J. J. A. n. (2019). Magnetic-sensitive nanoparticle self-assembled superhydrophobic biopolymer-coated slow-release fertilizer: fabrication, enhanced performance, and mechanism. *13*(3), 3320-3333.

Xie, X. S., Liu, Q., & Cui, S. W. J. F. R. I. (2006). Studies on the granular structure of resistant starches (type 4) from normal, high amylose and waxy corn starch citrates. *39*(3), 332-341.

Yamamoto, C. F., Pereira, E. I., Mattoso, L. H., Matsunaka, T., & Ribeiro, C. J. C. E. J. (2016). Slow release fertilizers based on urea/urea–formaldehyde polymer nanocomposites. *287*, 390-397.

Yang, C. Q., & Wang, X. J. J. o. a. p. s. (1998). Formation of five-membered cyclic anhydride intermediates by polycarboxylic acids: Thermal analysis and Fourier transform infrared spectroscopy. *70*(13), 2711-2718.

Yang, L., An, D., Wang, T.-J., Kan, C., & Jin, Y. J. P. (2017). Swelling and diffusion model of a hydrophilic film coating on controlled-release urea particles. *30*, 73-82.

Yang, Y.-c., Zhang, M., Li, Y., Fan, X.-h., Geng, Y.-q. J. J. o. a., & chemistry, f. (2012). Improving the quality of polymer-coated urea with recycled plastic, proper additives, and large tablets. *60*(45), 11229-11237.

Yao, F., Bai, Y., Chen, W., An, X., Yao, K., Sun, P., & Lin, H. J. E. p. j. (2004). Synthesis and characterization of functional L-lactic acid/citric acid oligomer. *40*(8), 1895-1901.

Ye, H.-M., Li, H.-F., Wang, C.-S., Yang, J., Huang, G., Meng, X., & Zhou, Q. J. C. E. J. (2020). Degradable polyester/urea inclusion complex applied as a facile and environment-friendly strategy for slow-release fertilizer: Performance and mechanism. *381*, 122704.

Yoo, D. K., Kim, D., & Lee, D. S. J. M. r. (2005). Reaction kinetics for the synthesis of oligomeric poly (lactic acid). *13*(1), 68-72.

Yu, X., & Li, B. J. P. (2019). Release mechanism of a novel slow-release nitrogen fertilizer. *45*, 124-130.

Zhan, X., Wang, D., Tuinstra, M., Bean, S., Seib, P., Sun, X. J. I. C., & Products. (2003). Ethanol and lactic acid production as affected by sorghum genotype and location. *18*(3), 245-255.

Zhang, M., Yang, J. J. I. J. o. P. M., & Biomaterials, P. (2021). Preparation and characterization of multifunctional slow release fertilizer coated with cellulose derivatives. *70*(11), 774-781.

Zhang, X., Liu, Y., Lu, P., Zhang, M. J. G. P., & Synthesis. (2020). Preparation and properties of hydrogel based on sawdust cellulose for environmentally friendly slow release fertilizers. *9*(1), 139-152.

Zhang, Z., Zhu, H., Zheng, Y., Zhang, L., Wang, X., Luo, Z., . . . Biology, P. B. (2020). The effects and mechanism of collagen peptide and elastin peptide on skin aging induced by D-galactose combined with ultraviolet radiation. *210*, 111964.

Zhou, T., Wang, Y., Huang, S., & Zhao, Y. J. S. o. t. T. E. (2018). Synthesis composite hydrogels from inorganic-organic hybrids based on leftover rice for environment-friendly controlled-release urea fertilizers. *615*, 422-430.

Zhou, Y., Luner, P., & Caluwe, P. J. J. o. a. p. s. (1995). Mechanism of crosslinking of papers with polyfunctional carboxylic acids. *58*(9), 1523-1534.

APPENDIXES

Appendix A: Preliminary experimental investigation for the matrix synthesized from ELN/COL and lactic acid

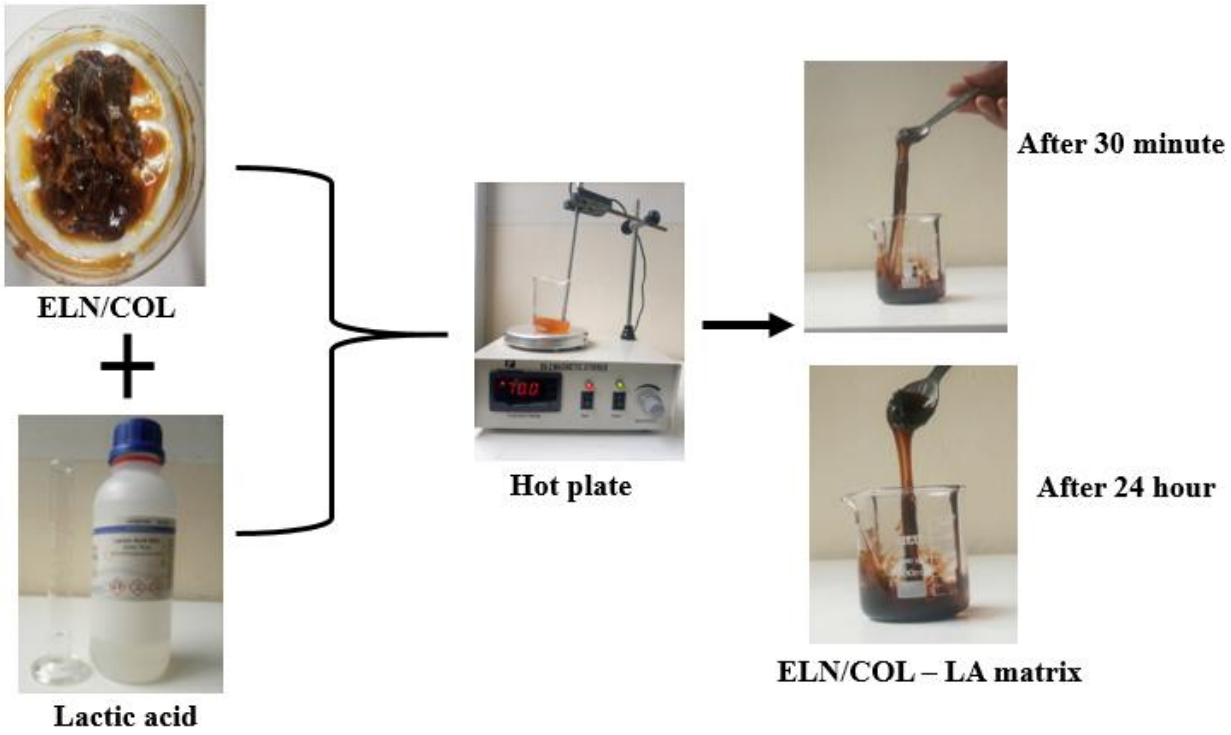

The synthesized matrix was not solidified with time, it was viscous throughout the time.

Appendix B: Preliminary experimental investigation for the matrix synthesized from ELN/COL and citric acid

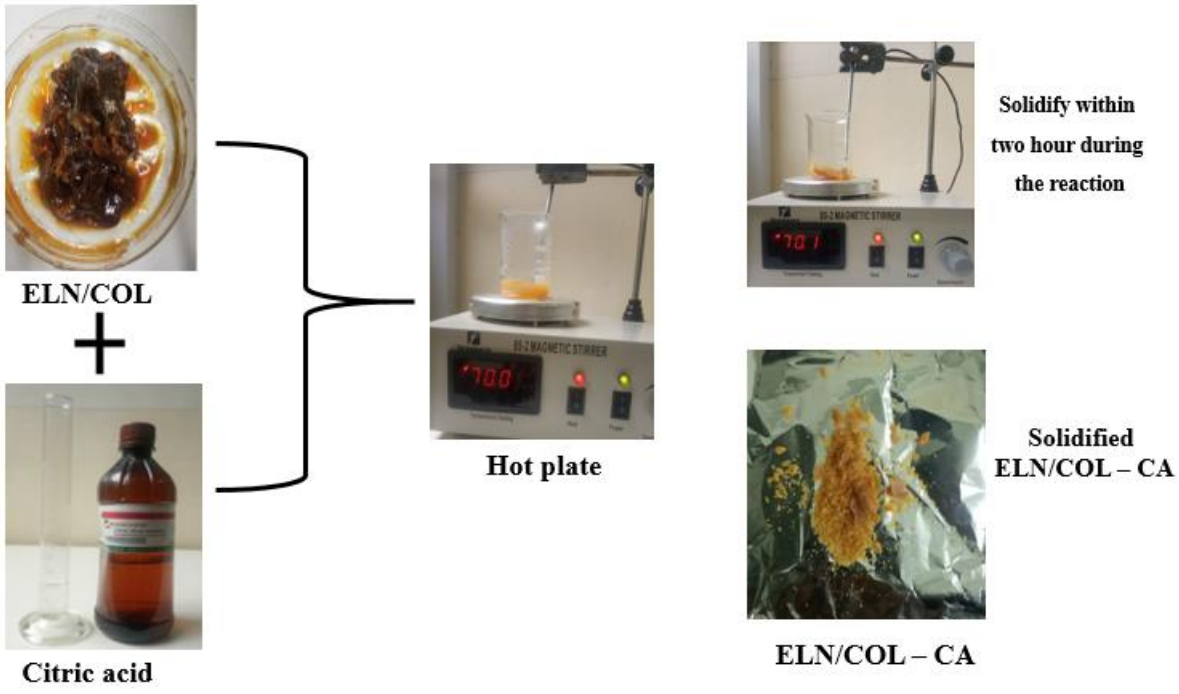

Synthesie of ELN/COL-CA matrix

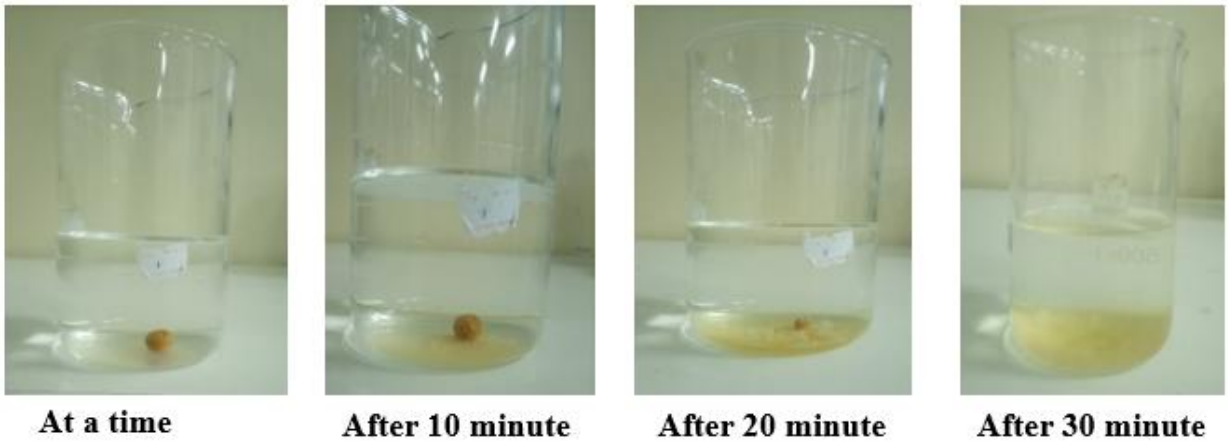

Solubility of ELN/COL-CA matrix in distilled water

The synthesized matrix was solidified within two hours during the reaction, and it was completely solubilized within 30 minutes in distilled water. As a result, it is impossible to disperse urea within the solidified matrix.

Appendix C: Percentage of total nitrogen content analysis for ELN/COL – CA & LA matrix by Kjeldahl method.

Percentage of total nitrogen content analysis for ELN/COL – CA & LA matrix which was extracted at a different reaction time.

Time (min)	% TN within the solution for a 2- hour matrix $*10^{-4}$			% TN within the solution for a 3-hour matrix $*10^{-4}$			% TN within the solution for a 4-hour matrix $*10^{-4}$		
	Trial-1	Trial-2	Avg	Trial-1	Trial-2	Avg	Trial-1	Trial-2	Avg
0	0	0	0	0	0	0	0	0	0
1	3.15	3.17	3.16	2.44	2.42	2.43	2.68	2.66	2.67
12	6.66	6.70	6.68	5.21	5.25	5.23	5.60	5.56	5.58
24	13.04	13.08	13.06	8.94	8.96	8.95	8.61	8.59	8.60
36	21.34	21.38	21.36	13.20	13.22	13.21	12.24	12.22	12.23
48	32.03	32.05	32.04	18.37	18.41	18.39	16.83	16.79	16.81
60	46.01	46.03	46.02	28.86	28.88	28.87	21.58	21.56	21.57
72	69.41	69.45	69.43	43.54	43.56	43.55	27.94	27.90	27.92

Percentage of total nitrogen content analysis for ELN/COL – CA & LA matrix which was synthesized at a different reaction temperature.

Time (min)	% TN within the solution for a 50 ^{o}c matrix $*10^{-4}$			% TN within the solution for a 70 ^{o}c matrix $*10^{-4}$			% TN within the solution for a 90 ^{o}c matrix $*10^{-4}$		
	Trial-1	Trial-2	Avg	Trial-1	Trial-2	Avg	Trial-1	Trial-2	Avg
0	0	0	0	0	0	0	0	0	0
1	4.21	4.24	4.23	2.68	2.66	2.67	3.22	3.20	3.21
12	9.57	9.61	9.59	5.60	5.56	5.58	6.91	6.87	6.89
24	17.17	17.19	17.18	8.61	8.59	8.60	11.82	11.80	11.81
36	26.56	26.58	26.57	12.24	12.22	12.23	17.71	17.69	17.70
48	37.33	37.37	37.35	16.83	16.79	16.81	23.98	24.02	24.00
60	57.34	57.36	57.35	21.58	21.56	21.57	37.78	37.78	37.78

72	85.07	85.11	85.09	27.94	27.90	27.92	58.14	58.12	58.13

Percentage of total nitrogen content analysis for ELN/COL – CA & LA matrix which was synthesized at a different ratio of lactic acid to citric acid.

Time (min)	% TN within the solution for a 1:1 ratio matrix $*10^{-4}$			% TN within the solution for a 1:1.5 ratio matrix $*10^{-4}$			% TN within the solution for a 1:2 ratio matrix $*10^{-4}$		
	Trial-1	Trial-2	Avg	Trial-1	Trial-2	Avg	Trial-1	Trial-2	Avg
0	0	0	0	0	0	0	0	0	0
1	4.13	4.19	4.16	2.68	2.66	2.67	2.43	2.41	2.42
12	8.88	8.92	8.90	5.60	5.56	5.58	4.87	4.85	4.86
24	17.44	17.46	17.45	8.61	8.59	8.60	7.59	7.57	7.58
36	28.01	28.05	28.03	12.24	12.22	12.23	11.60	11.56	11.58
48	42.96	42.98	42.97	16.83	16.79	16.81	16.34	16.32	16.33
60	60.55	60.55	60.55	21.58	21.56	21.57	24.63	24.61	24.62
72	85.73	85.75	85.74	27.94	27.90	27.92	34.76	34.72	34.74

The percentage of nitrogen release from the matrix to the water was calculated using this formula

$$\%\ TN\ release = \frac{\%TN * Total\ mass\ (g)}{mass\ of\ nitrogen\ with\ in\ a\ matrix\ (g)}$$

Where: **%TN** was the percentage of total nitrogen within the solution, Total mass = the sum mass of distilled water and the immersed matrix,

Mass of nitrogen within the matrix =(Mass of matrix immersed in water * Percentage of nitrogen within the matrix)*1/100.

The percentage of nitrogen within each matrix has been fully illustrated in the document table (4.6

Appendix D: Percentage of total nitrogen content analysis of the urea dispersed ELN/COL – CA & LA matrix samples by Kjeldahl method.

	% TN for 1:0.5 ratio	% TN for 1:1 ratio	% TN for 1:2 ratio	% TN for 1:3 ratio

Time (hour)	$*10^{-3}$			$*10^{-3}$			$*10^{-3}$			$*10^{-3}$		
	Trial-1	Trial-2	Avg	Trial-1	Trial-2	Avg	Trial-1	Trial-2	Avg	Trial-1	Trial-2	Avg
0	0	0	0	0	0	0	0	0	0	0	0	0
1	2.89	2.91	2.90	4.84	4.86	4.85	6.64	6.60	6.62	16.74	16.78	16.76
6	4.50	4.48	4.49	8.83	8.79	8.81	11.96	11.92	11.94	52.94	52.66	52.95
12	7.02	7.00	7.01	12.90	12.88	12.89	19.55	19.51	19.53	116.93	116.97	116.95
18	10.96	10.92	10.94	17.64	17.60	17.62	32.14	32.10	32.12	172.39	172.41	172.40
24	15.83	15.79	15.81	24.01	23.99	24.00	47.94	47.92	47.93	173.10	173.12	173.11
30	21.24	21.22	21.23	32.69	32.67	32.68	69.90	69.86	69.88	173.45	173.49	173.47
36	25.98	26.02	26.00	48.39	48.37	48.38	95.53	95.49	95.51	173.62	173.66	173.64
42	33.40	33.38	33.39	66.53	66.49	66.51	139.77	139.75	139.76	173.99	174.01	174.00
48	41.72	41.70	41.71	91.03	91.01	91.02	153.07	153.05	153.06	175.06	175.08	175.07
54	51.83	51.81	51.82	115.17	115.13	115.15	153.66	153.62	153.64	175.40	175.44	175.42
60	62.02	62.00	62.01	116.58	116.52	116.55	154.62	154.60	154.61	175.59	175.61	175.60
72	76.89	76..87	76.88	117.24	117.18	117.20	155.12	155.08	155.10	175.60	175.60	175.60

The percentage of nitrogen release from the matrix to the water was calculated using this formula

$$\%\,TN\ release = \frac{\%TN * Total\ mass\ (g)}{mass\ of\ nitrogen\ with\ in\ a\ sample(g)}$$

Where: **%TN** was the percentage of total nitrogen within the solution,

Total mass = the sum mass of distilled water and the immersed sample, and

Mass of nitrogen within the sample = Mass of nitrogen within the matrix + Mass of nitrogen within the urea

Mass of nitrogen within the matrix =(Mass of matrix immersed in water * Percentage of nitrogen within the matrix)*1/100.

*Mass of nitrogen within one gram matrix =(1 gram * 5.32)*1/100 =* ***0.0532gram ,*** 5.32 was the percentage of nitrogen for the matrix.

*Mass of nitrogen within the 1 gram urea = 0.46 * 1 gram = 0.46 gram, since the commercial as well as laboratory grade urea contains 46 % of nitrogen within it.*

So taking one gram of ELN/COL – CA & LA acid matrix, the mass of urea used for the preparation of urea dispersed matrix with a matrix to urea ratio of 1:0.5,1:1,1:2, and 1:3 were 0.5,1,2, and 3grams respectively.

And the percentage of nitrogen within the sample (urea dispersed ELN/COL – CA & LA) (% Ns) was calculated as follows:

$$\%Ns = \frac{(Mass\ of\ nitrogen\ within\ the\ sample)}{Mass\ of\ matrix(g) + mass\ of\ urea(g)} * 100\%$$

For S_1 (1:0.5 ratio):

$$\%Ns = \frac{0.0532g + (0.5 * 0.46)g}{1g + 0.5g} * 100\% \ = 18.88\ \%$$

For S_2 (1:1 ratio):

$$\%Ns = \frac{0.0532g + (1 * 0.46)g}{1g + 1g} * 100\% \ = 25.66\ \%$$

For S_3 (1:2 ratio):

$$\%Ns = \frac{0.0532g + (2 * 0.46)g}{1g + 2g} * 100\% \ = 32.44\ \%$$

For S_4 (1:3 ratio):

$$\%Ns = \frac{0.0532g + (3 * 0.46)g}{1g + 3g} * 100\% \ = 35.83\ \%$$

Appendix E: Steps for how to use a non-linear regression analysis using Microsoft® Excel 2016 Solver Add-in method

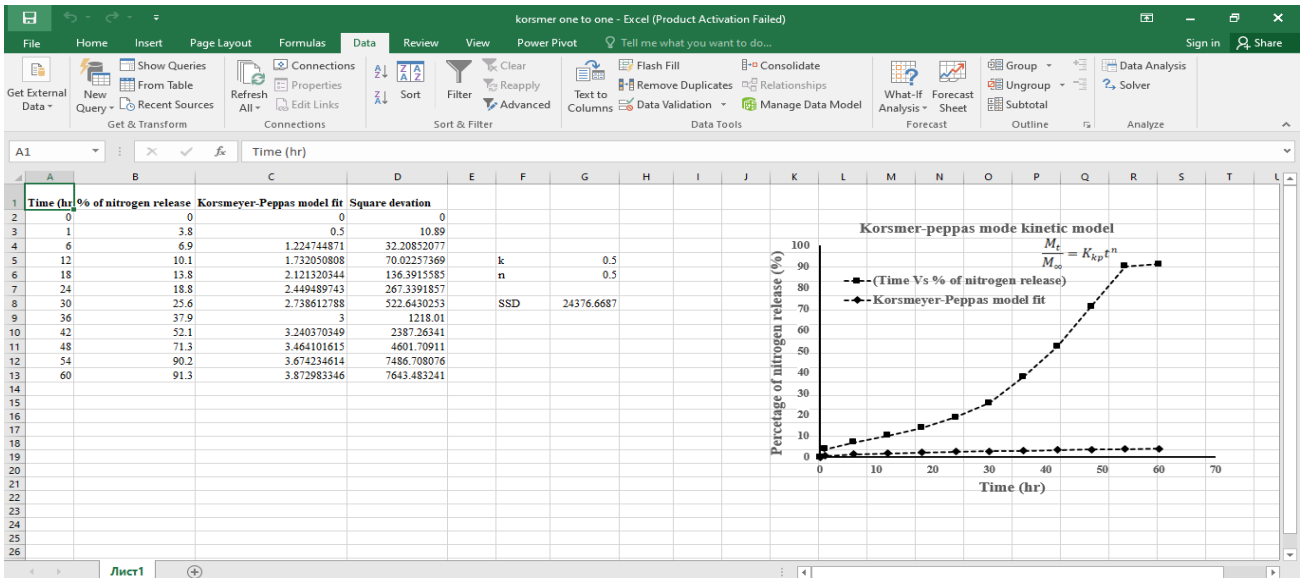

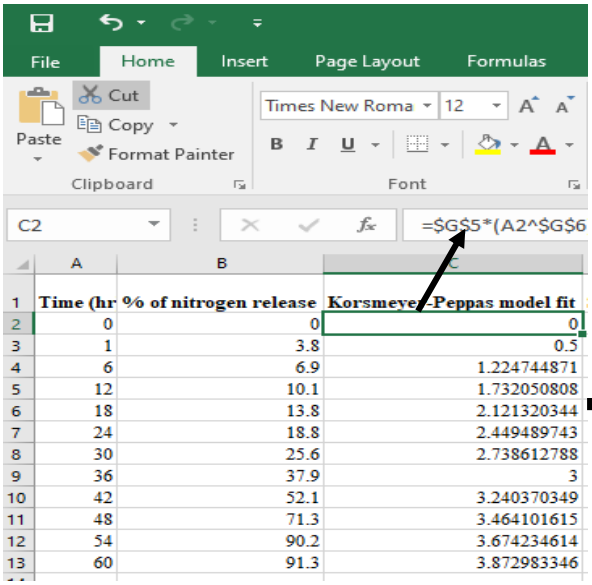

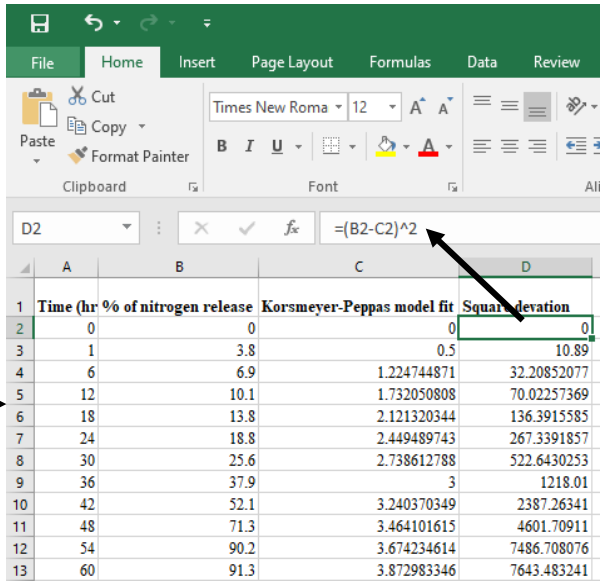

Time (hr	% of nitrogen release	Korsmeyer-Peppas model fit	Square deviation
0	0	0	0
1	3.8	0.5	10.89
6	6.9	1.224744871	32.20852077
12	10.1	1.732050808	70.02257369
18	13.8	2.121320344	136.3915585
24	18.8	2.449489743	267.3391857
30	25.6	2.738612788	522.6430253
36	37.9	3	1218.01
42	52.1	3.240370349	2387.26341
48	71.3	3.464101615	4601.70911
54	90.2	3.674234614	7486.708076
60	91.3	3.872983346	7643.483241

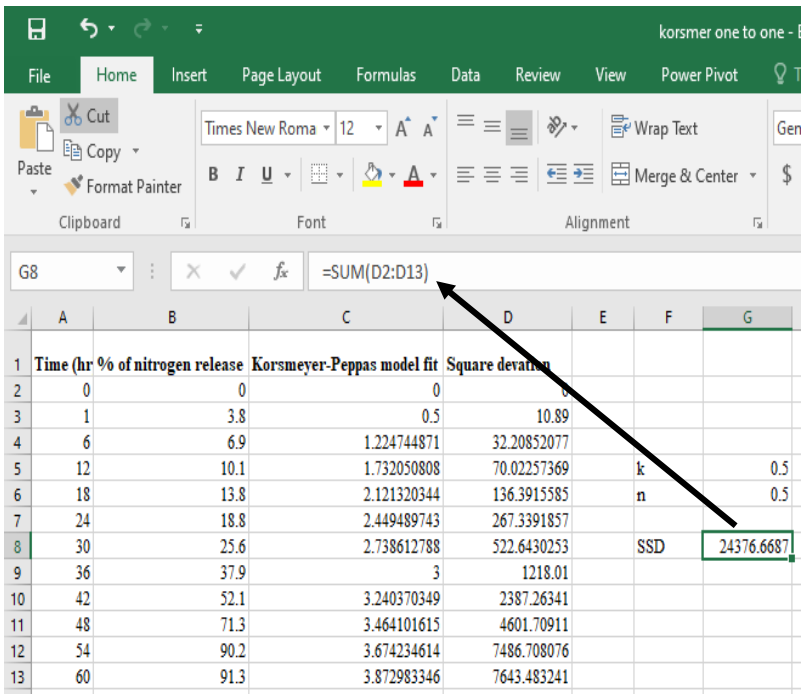

	A	B	C	D	E	F	G
1	Time (hr	% of nitrogen release	Korsmeyer-Peppas model fit	Square deviation			
2	0	0	0	0			
3	1	3.8	0.5	10.89			
4	6	6.9	1.224744871	32.20852077			
5	12	10.1	1.732050808	70.02257369		k	0.5
6	18	13.8	2.121320344	136.3915585		n	0.5
7	24	18.8	2.449489743	267.3391857			
8	30	25.6	2.738612788	522.6430253		SSD	24376.6687
9	36	37.9	3	1218.01			
10	42	52.1	3.240370349	2387.26341			
11	48	71.3	3.464101615	4601.70911			
12	54	90.2	3.674234614	7486.708076			
13	60	91.3	3.872983346	7643.483241			

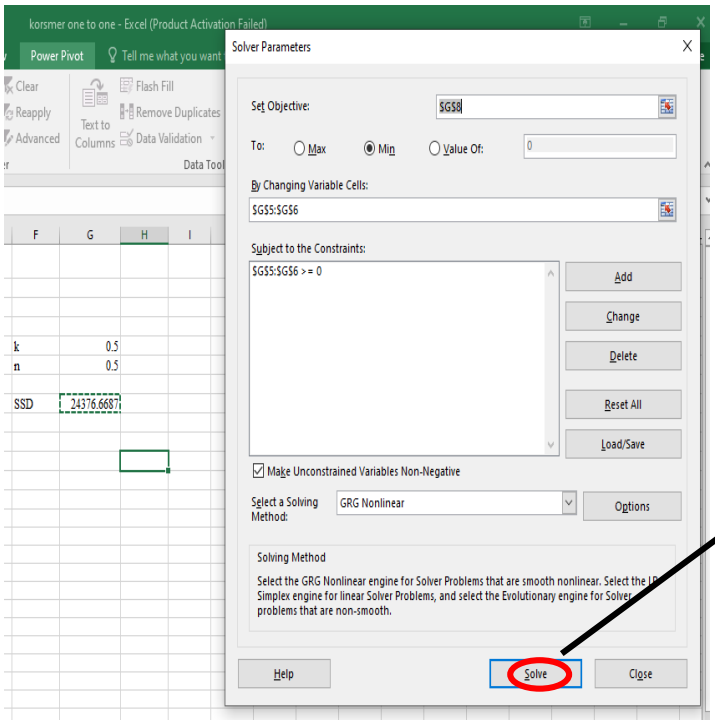

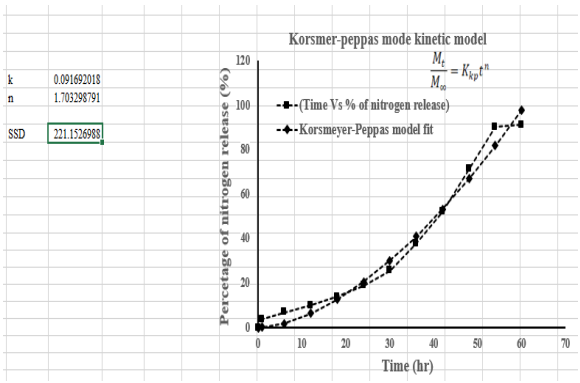

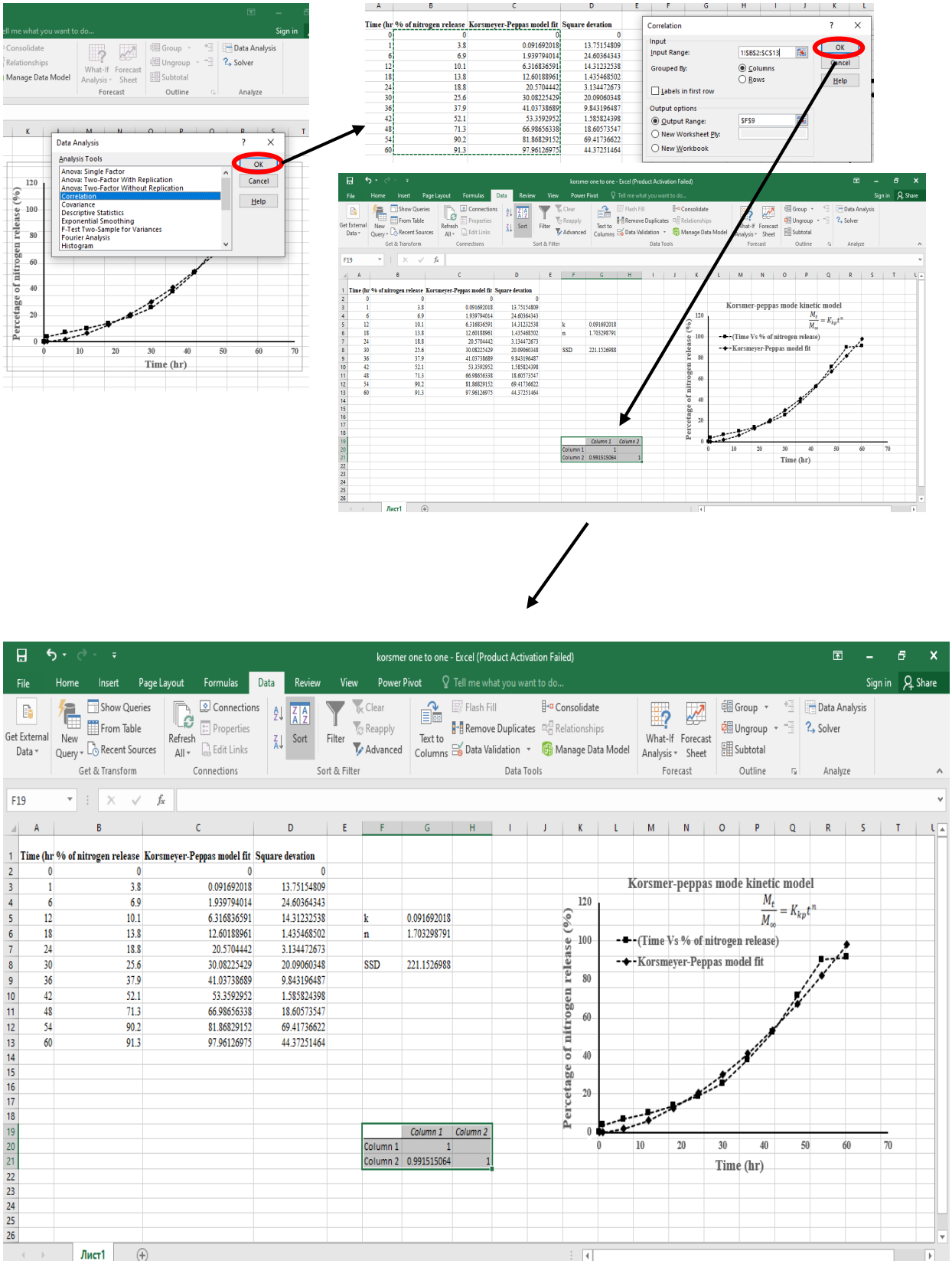

Time (hr	% of nitrogen release	Korsmeyer-Peppas model fit	Square devation
0	0	0	0
1	3.8	0.091692018	13.75154809
6	6.9	1.939794014	24.60364343
12	10.1	6.316836591	14.31232538
18	13.8	12.60188961	1.435468502
24	18.8	20.5704442	3.134472673
30	25.6	30.08225429	20.09060348
36	37.9	41.03738689	9.843196487
42	52.1	53.3592952	1.585824398
48	71.3	66.98656338	18.60573547
54	90.2	81.86829152	69.41736622
60	91.3	97.96126975	44.37251464

k	0.091692018	
n	1.703298791	
SSD	221.1526988	

	Column 1	Column 2
Column 1	1	
Column 2	0.991515064	1